Portfolio Optimization with Transaction Costs and Taxes

Weiwei Shen

Submitted in partial fulfillment of the
requirements for the degree
of Doctor of Philosophy
in the Graduate School of Arts and Sciences

COLUMBIA UNIVERSITY

2014

©2014

Weiwei Shen

All Rights Reserved

ABSTRACT

Portfolio Optimization with Transaction Costs and Taxes

Weiwei Shen

This thesis is concerned with a new computational study of optimal investment decisions with proportional transaction costs or capital gain taxes over multiple periods. The decisions are studied for investors who have access to a risk-free asset and multiple risky assets to maximize the expected utility of terminal wealth. The risky asset returns are modeled by a discrete-time multivariate geometric Brownian motion. As in the model in Davis and Norman (1990) and Lynch and Tan (2010), the transaction cost is modeled to be proportional to the amount of transferred wealth. As in the model in Dammon et al. (2001) and Dammon et al. (2004), the taxation rule is linear, uses the weighted average tax basis price, and allows an immediate tax credit for a capital loss.

For the transaction costs problem, we compute both lower and upper bounds for optimal solutions. We propose three trading strategies to obtain the lower bounds: the hyper-sphere strategy (termed HS); the hyper-cube strategy (termed HC); and the value function optimization strategy (termed VF). The first two strategies parameterize the associated no-trading region by a hyper-sphere and a hyper-cube, respectively. The third strategy relies on approximate value functions used in an approximate dynamic programming algorithm. In order to examine their quality, we compute the upper bounds by a modified gradient-based duality method (termed MG). We apply the new methods across various parameter sets and compare their results with those from the methods in Brown and Smith (2011). We are able to numerically solve problems up to the size of 20 risky assets and a 40-year-long horizon. Compared with their methods, the three novel lower bound methods can achieve higher utilities. HS and HC are about one order of magnitude faster in computation times. The upper bounds from MG are tighter in various examples. The new duality gap is ten times narrower than the one in Brown and Smith (2011) in the best case.

In addition, I illustrate how the no-trading region deforms when it reaches the borrowing constraint boundary in state space. To the best of our knowledge, this is the first study of the deformation in no-trading region shape resulted from the borrowing constraint. In particular, we demonstrate how the rectangular no-trading region generated in uncorrelated risky asset cases (see, e.g., Lynch and Tan, 2010; Goodman and Ostrov, 2010) transforms into a non-convex region due to the binding of the constraint.

For the capital gain taxes problem, we allow wash sales[1] and rule out "shorting against the box" by imposing nonnegativity on portfolio positions. In order to produce accurate results, we sample the risky asset returns from its continuous distribution directly, leading to a dynamic program with continuous decision and state spaces. We provide ingredients of effective error control in an approximate dynamic programming solution method. Accordingly, the relative numerical error in approximating value functions by a polynomial basis function is about 10^{-5} measured by the l_∞ norm and about 10^{-10} by the l_2 norm. Through highly accurate numerical solutions and transformed state variables, we are able to explain the optimal trades through an associated no-trading region. We numerically show in the new state space the no-trading region has a similar shape and parameter sensitivity to that of the transaction costs problem in Muthuraman and Kumar (2006) and Lynch and Tan (2010). Our computational results elucidate the impact on the no-trading region from volatilities, tax rates, risk aversion of investors, and correlations among risky assets. To the best of our knowledge, this is the first time showing no-trading region of the capital gain taxes problem has such similar traits to that of the transaction costs problem.

We also compute lower and upper bounds for the problem. To obtain the lower bounds we propose five novel trading strategies: the value function optimization (VF) strategy from approximate dynamic programming; the myopic optimization and the rolling buy-and-hold heuristic strategies (MO and RBH); and the realized Merton's and hyper-cube strategies (RM and HC) from policy approximation. In order to examine their performance, we develop two upper bound methods (VUB and GUB) based on the duality technique in Brown et al. (2009) and Brown and Smith (2011). Across various sets of parameters, duality

[1] Wash sales mean selling those assets with price falling below their tax basis to get a tax credit and then purchasing the same assets at the current price.

gaps between lower and upper bounds are smaller than 3% in most examples. We are able to solve the problem up to the size of 20 risky assets and a 30-year-long horizon.

Table of Contents

List of Figures

List of Tables

Acknowledgments

Traveling down the road to completion of a Ph.D. degree is a pilgrimage, and to this, I am no exception. A dissertation does not materialize on its own, and it could not have been completed without help of many individuals. To each and every one of them I am forever grateful and indebted. I would like to express my dearly gratitude to my thesis advisor, Professor Mark Broadie. Your patient guidance, ungrudging imparting, and meticulous attitude have shaped my understanding of research per se; your pertinent questions and intuitive teaching have ignited my passion to explore and exploit uncultivated land of computational finance; your amazing dedication and diligence to all your work have shown me the true elixir of success; your philosophy and principle of how to grapple with difficulties coming from all parts of life have perpetually influenced my personal values and beliefs. My highest appreciation to your help, support and enlightenment is not to utter words, but to live by them.

Among many other people who helped me at Columbia, I am especially thankful to Professor David Keyes. You are the first professor I met when I entered the gate of APAM. Your kindness and effort on hosting reunions for students at your home touched me deeply; your irreplaceable support, understanding, and encouragement to me have smoothed and optimized my graduate life; your remarkable skills on language, presentation, and collaboration have enlightened me on the role of communication; your enthusiasm and leadership in computational science have set an example for young scholars like me to fulfill the deepest desires and longings. Thank you - for lack of a more meaningful phrase - for all you have done for me over the ups and downs of my graduate life.

My wholehearted thanks go to my dissertation committee, Professor Guillaume Bal, Professor Tim Leung and Professor Pierre-David Létourneau, for sacrificing time to painstakingly read the draft and attend the defense. Thanks, Professor Bal. In my mind, you represent not only a serious mathematician with deep knowledge but also a liberal friend with affable and humorous personality. Thanks, Professor Leung. If I could talk with you earlier about your invaluable career advice, many parts of my graduate life would be improved tremendously. Thanks, Professor Létourneau, a rising young applied mathematician. Without the timely reply from you, my defense meeting could not be facilitated smoothly. Besides, I appreciate the warm help from many APAMers, Professor Daniel Bienstock, Professor C. K. Chu, Professor Lorenzo Polvani, Professor Michael Weinstein, Professor Liuren Wu, Dina Amin, Montserrat Fernandez-Pinkley and Christina Rohm, among others.

I would also like to thank my dearest friends, near and far, Xin Chen, George Kaladze, Tianhuan Luo, Jian Lv, Sophie Metreveli, Puttisarn Mongkolwisetwara, Kantawat Sriratanaban, Dezheng Sun, Jun Wang, Jonathan Widawsky, Yu You, Yuan Yuan, Xiang Zheng, Xingbo Zhao, who added color to my Ph.D. life. A special thank is due to Jing Zhou, for her extraordinary patience and carefulness in reading my manuscripts of the relevant papers with such exhaustive attention to the details in language. I reserve my last gratitude to my parents for their patience, love, support, and more patience. As I close this chapter of my life and look forward into the future, I am truly excited about the things to come.

To my parents Youming Shen and Zili Qin

Chapter 1

Introduction

Dynamic portfolio optimization problem has received considerable attention in recent years. The seminal papers by Merton (1969, 1971) offer an explicit solution for the portfolio optimization problem in idealized environments without transaction costs or taxes. Merton's optimal strategy for constant relative risk aversion (CRRA) investors is to hold a constant fraction of total wealth in different assets. To implement such a strategy, investors must continually buy and sell assets in order to maintain the target fraction as asset prices fluctuate. However, in a real market with frictions, transactions are costly and continual rebalancing can be expensive. Moreover, due to the presence of transaction costs and taxes, Merton's trading strategy is actually suboptimal, and explicit solutions have not been found yet. Therefore, it is important to consider an optimal solution for dynamic portfolio choice in the presence of market frictions. This dissertation aims to study the optimal strategies for the portfolio optimization problem Merton considered but additionally with either proportional transaction costs or capital gain taxes.

1.1 Portfolio Optimization with Transaction Costs

Portfolio optimization with transaction costs has been studied from different perspectives by a large number of articles. However, research on the problem with more than five assets is rare. This thesis focuses on the problem with more than ten risky assets. Illustrations over a wide range of applications and conclusions involving transaction costs may be found in the review Cvitanic (2001) and Brandt (2010), and the extensive references therein. In this section, we briefly overview the relevant papers.

Magill and Constantinides (1976) pioneer the research about how to incorporate transaction costs into Merton's problem. They conjecture there exists a no-trading region in which investors don't trade, and the optimal strategy is to bring the post-trade position back to the no-trading region via enough trades. The papers by Constantinides (1979, 1986) confirm that there is a no-trading region around Merton's solution in the case of one risky asset. Besides, most of the early papers (see, e.g., Davis and Norman, 1990; Dumas and Luciano, 1991; Shreve and Soner, 1994; Oksendal and Sulem, 2002; Liu and Loewenstein, 2002; Janecek and Shreve, 2004) mainly study the case of a single risky asset. Their studies explicitly provide pathways to solving Merton's problem with proportional transaction costs. In particular, Davis and Norman (1990) first provide a detailed theoretical analysis of the optimal policy for an infinite horizon investment and consumption decision problem. They also calculate the optimal policy by numerically solving the associated Hamilton-Jacobi-Bellman (HJB) partial differential equation. Based on very limited assumptions, Shreve and Soner (1994) conduct an exhaustive and rigorous analysis of the optimal trading strategies in an infinite horizon. They prove existence, uniqueness and regularity of the value function. Janecek and Shreve (2004) derive an asymptotic expansion of the value function and obtain asymptotic results of a single risky asset problem.

Starting with Liu (2004), Muthuraman and Kumar (2006), and Muthuraman and Zha (2008), more research appears for the corresponding multi-asset portfolio optimization problem. This problem is much more challenging to solve. Liu (2004) obtains an almost closed form solution for fixed and proportional costs in continuous time for constant absolute risk aversion (CARA) investors by assuming asset returns are uncorrelated. Muthuraman and Kumar (2006) have developed numerical methods to solve the HJB equation for the case of infinitely-lived CRRA investors who have access to two risky assets. Their method works up to ten risky assets before reaching the bound of their computing power. Muthuraman and Zha (2008) have developed numerical methods based on combining simulation with a boundary update procedure used in solving the HJB equation in the log utility. It scales polynomially in dimension and can solve up to seven risky assets within 72 hours. Dai and

Zhong (2010) solve the similar two risky asset problem as Muthuraman and Kumar (2006) but in a finite horizon. They consider the cases with and without consumption. Their value function is governed by a variational inequality with gradient constraints. They propose a penalty method to deal with the gradient constraints and employ a finite difference discretization. In addition, for the multiple risky-asset case Akian et al. (1996) show the existence of a viscosity solution to the HJB equation and the uniqueness of the long-term expected growth rate. Goodman and Ostrov (2010) carry out asymptotic expansion of the value function and obtain asymptotic results of the no-trading boundaries for the multiple risky-asset problem. For uncorrelated multiple risky assets, Atkinson and Ingpochai (2006) show the no-trading region is a rectangular box for CRRA investors by using asymptotic analysis. However, the fatal difficulty of using partial differential equation approaches in multiple asset problems is the lack of effective techniques to solve curse of dimensionality as the required work grows exponentially with the number of risky assets.

In a discrete time setting Lynch and Tan (2010) and Brown and Smith (2011) conduct a study of the case in which investors are facing a finite horizon, correlated multi-asset returns and nonnegative portfolio constraints. In particular, Lynch and Tan (2010) have considered a similar problem with two risky assets as that in Muthuraman and Kumar (2006) but with a discrete time finite horizon and predictable returns. Their numerical methods are based on a grid approximation of the state space for the associated dynamic program. Brown and Smith (2011) provide heuristic lower bounds via optimizing value functions of Merton's problem and upper bounds by a duality method. They obtain small duality gaps for various examples. Additionally, in a recent series of papers, Kallsen and Muhle-Karbe (2010) and Gerhold et al. (2011) show the transaction costs problem can be solved by the martingale method which was only applicable in a frictionless market (see, e.g., Pliska, 1986; Cox and Huang, 1989). Further, they determine the shadow price process by solving a dual problem in the case of having one risky asset and logarithmic utility. This research extends the application of the martingale method to solving problems with market frictions. Recently, the paper by Choi et al. (2013) further extends the shadow price method to solving the CRRA utility and releases many restrictions of parameters in Kallsen and Muhle-Karbe (2010).

Besides the aforementioned research on proportional transaction costs, there are a variety of papers related to transaction costs. Morton and Pliska (1995) and Schroder (1995) consider the problem with fixed transaction costs and illustrate that there is a particular point to return in the no-trading region. Atkinson, Pliska, and Wilmott (1997) work on a long-term growth model with transaction costs and without consumption. Balduzzi and Lynch (1999) and Lynch and Balduzzi (2000) demonstrate the impact of return predictability and transaction costs on the utility costs and the optimal strategy. Leland (2000) formulates a cost minimal model where he incorporates proportional transaction costs and capital gain taxes. In a single risky asset context, Gerhold et al. (2013) study the relation of transaction costs, liquidity premium, and trading volume.

1.2 Portfolio Optimization with Taxes

Perhaps the most significant friction investors confront in financial markets is taxation, which has a first-order effect on the portfolio optimization. For example, the magnitude of the capital gain taxes is quite large, typically from 20% to 50%. Surprisingly, the literature on the portfolio optimization problem under capital gain taxes is not extensive and is mainly developed in discrete time lattice return models. As taxation is complicated, we review the papers focusing on portfolio optimization problems with capital gain taxes in this section. For comprehensive literature reviews, see Dammon and Spatt (2012) and Brandt (2010).

The challenges of the problem essentially root in the taxation code. In order to calculate capital gains or losses, taxation code needs to specify the basis to which the price of a security has to be compared. The question of whether the problem is strongly or mildly path-dependent depends on how to calculate the basis. The exact tax basis price which is defined as the purchase price of the security in the U.S. leads to a strong path-dependency. This choice requires investors to keep track of the basis price for every single transaction along the investment for tax calculation. As a consequence, the strong path-dependency feature renders the size of the problem to increase exponentially with the number of rebalancng periods, which was known as the curse of dimensionality. Moreover, it leads to a non-Markovian problem to which dynamic programming is inapplicable.

Constantinides (1983) pioneers the research of portfolio optimization with taxes and shows the investment and consumption decisions are separable and the optimal strategy is always to (1) defer gains and (2) realize losses. These conclusions heavily rely on the assumption of allowing costless short selling of risky assets. The strategy of deferring all gains referred to as "shorting against the box" reflects that investors prefer to sell short those assets with embedded capital gains instead of selling them outright. The strategy of realizing all losses known as a "wash sale" rests on selling those assets with price falling below their tax basis to get a tax credit and then rebalancing the portfolio by purchasing the same assets at the current price. However, in practice, short selling is not costless and is prohibited for many classes of investors; and the wash sale of a security with a loss bought within 30 days is disallowed by the U.S. tax code.

By considering capital gain taxes and using the exact tax basis, Dybvig and Koo (1996) formulate the problem as a nonlinear program and numerically solve the problem for four periods and a single stock. DeMiguel and Uppal (2005) extend this model and solve the problem with seven periods and two stocks or with ten periods and a single stock. The strong path-dependency issue makes any further extension of the number of assets and periods intractable.

Dammon et al. (2001) propose employing the weighted average of purchase price as the tax basis to tackle with the strong path-dependency difficulty. In the context of a lattice model with short sale constraints and a linear taxation rule, they present numerical results for a problem with 80 periods and one risky asset and provide extensive characterization of the optimal dynamic consumption and portfolio decisions. The main advantage of the weighted average tax basis lies in that it simplifies the dynamics of the tax basis to be Markovian. This simplification ameliorates the path-dependency of the problem and opens the door to attacking the problem via dynamic programming. Similarly, Dammon et al. (2004) consider how to optimally allocate assets between taxable and tax-deferred accounts. In addition, numerical examples in DeMiguel and Uppal (2005) show that the certainty equivalent loss from choosing the weighted average tax basis rather than the exact tax basis is less than 1% for various parameters in single or two risky asset cases. Using the same lattice model for return dynamics, Garlappi et al. (2001), Dammon et al. (2002), and

Gallmeyer et al. (2006) numerically analyze the problem with two risky assets. Garlappi et al. (2001) analyze the nature of the "no-trading region". Dammon et al. (2002) concentrate on the differences between two risky assets and a single risky asset. They find that the diversification benefit of reducing the exposure to a highly volatile position can overweight the incurred tax cost of selling. Gallmeyer et al. (2006) investigate how short-selling impacts optimal asset allocation when "shorting against the box" is prohibited. They find it possible to short one risky asset when there are no embedded gains in the assets.

Recently, Tahar et al. (2010) formulate the continuous time version of the model in Dammon et al. (2001). In an infinite long horizon, they rigorously derive a first order approximation of the value function as the lower bound according to the strategy of forcing realizing all capital losses or gains. They include a discussion of the characterization of the value function based on the method in Tahar et al. (2007), and numerically show the related value function is not concave. In another series of papers, Constantinides (1984), Dammon et al. (1989), Dammon and Spatt (1996), and Dai et al. (2012) study the optimal consumption and trading strategies with asymmetric long-term/short-term capital gain taxes. Constantinides (1984), Dammon et al. (1989) and Dammon and Spatt (1996) find that when there exists different tax rates for long-term/short-term investment, it is possible to realize long-term capital gains to reset the investors' tax basis, which is known as the restarting option. Dai et al. (2012) illustrate that by assuming the tax rate for long-term capital losses is the same as that for long-term capital gains, it is always optimal to realize all short-term capital losses before they turn into long-term. Besides, by assuming the tax rate for long-term capital losses is the same as the marginal ordinary income tax rate as the law stipulates, they show for low income investors it could be optimal to defer long-term capital losses. Haugh et al. (2014) compute several heuristic strategies for the exact tax basis problem with limited tax loss deduction. Their framework allows them to provide the upper bound through a convex optimization problem.

1.3 Duality Method

On the other hand, a new line of research on the duality techniques developed by Rogers (2007), Brown, Smith, and Sun (2009) and Brown and Smith (2011), which is an extension of the work of Davis and Karatzas (1994), Rogers (2002), Andersen and Broadie (2004) and Haugh and Kogan (2004), can be adopted to evaluate general optimal control problems. Briefly, these techniques root in relaxing decision-maker's information constraints thus providing the upper bounds of optimal control problems. By computing the gaps between lower bounds and upper bounds, one can evaluate the quality of the lower bounds. In particular, the value function-based duality techniques developed in Rogers (2007) and Brown et al. (2009) demand value functions calculated from sub-optimal policies. Alternatively, the gradient-based duality techniques developed in Brown and Smith (2011) has computational cost advantages over the value function-based techniques for high-dimensional problems. More recent applications and developments can be found in Lai et al. (2010), Lai et al. (2011) and Desai et al. (2012).

1.4 Contribution and Outline

In this dissertation, we consider the problem of dynamic multi-asset portfolio optimization in a discrete-time, finite-horizon setting. Our general model considers risk aversion, nonnegativity constraints on portfolio positions, and proportional transaction costs or capital gain taxes. As the model in Davis and Norman (1990) and Lynch and Tan (2010), the transaction cost is modeled to be proportional to the amount of transferred wealth. As the model in Dammon et al. (2001) and Dammon et al. (2004), the taxation rule is linear, adopts the weighted average tax basis price, and allows an immediate tax credit for a capital loss.

We concentrates on the efficient method to compute and understand the optimal investment decisions for investors who have access to multiple investment instruments: a risk-free asset account paying a risk-free rate and several risky assets with stochastic returns. Specifically, the main contributions for the transaction costs problem are as follows:

1. *Propose three novel trading strategies that produce tight lower bounds for the problem*

with not less than ten risky assets

The first trading strategy is value function approximation (VF). This method uses the approximated value functions generated from the associated approximate dynamic programming backward iteration. It has been noticed that the high-dimensional transaction costs problem cannot be solved by a trivial extension of low-dimensional treatments in backward iteration (e.g. Brown and Smith, 2011). Therefore, we carefully design each step in the backward iteration. Specifically, three key ingredients in each step are: (1) using the Sobol low-discrepancy sequence to sample grid points in state space; (2) adopting the complete set of polynomials of state variables as basis functions to approximate certainty equivalents of value functions; (3) applying certainty equivalent transformation to objective functions in optimization to control numerical errors. In particular, across different parameter sets, the l_2 norm of the relative error in approximating certainty equivalent functions is about 10^{-5} and its l_∞ norm is about 10^{-3}. We are able to attain highly accurate results for the problem up to 20 risky assets and 10 periods. To the best of our knowledge, this is the first time obtaining such accurate numerical solutions for the transaction costs problem with this size by approximate dynamic programming.

As VF entails step by step optimization along each simulated return trial, it is relatively expensive. To overcome this limitation, after exploring the optimal policy structure of the problem, we provide two trading strategies motivated from approximating the associated no-trading region by a hyper-sphere (HS) and by a hyper-cube (HC), respectively. Typically, they are about 10 times faster than VF. For multiple assets, numerical examples in Muthuraman and Kumar (2006); Lynch and Tan (2010); Dai and Zhong (2010) and theoretical proofs in Atkinson and Mokkhavesa (2004); Atkinson and Ingpochai (2006); Goodman and Ostrov (2010) show the no-trading region is close to a polyhedron. Thus, to achieve computational cost-effectiveness, we parameterize the no-trading region with one variable. In each time period, HS and HC require a one-dimensional brute-force search for the optimal size of the hyper-sphere and the hyper-cube to maximize the final utility, respectively. By covering the main area of the no-trading region through simple geometries thus approximating closely the trading policy, HS and HC also produce tight lower bounds.

To validate the proposed lower bound strategies, we test across diverse parameter sets and compare the new lower bounds with those from the old methods in Brown and Smith (2011). We find HS and HC are one order of magnitude faster on average and the new low bound provides a 6.5% relative improvement in annualized certainty equivalent return rate in the best case.

2. *Reduce upper bounds by a new gradient-based duality method*

   The gradient-based duality method is originally developed in Brown and Smith (2011) and offers the best upper bounds in many examples in their study. In this paper, we propose a new dual method from the motivation that the most significant trading volume in the transaction costs problem happens in the first period. The critical requirement that ensures the gradient-based duality method to work is to find a modified convex problem that is close to the original primal problem and can be solved to optimality. Our modified problem only incorporates transaction costs in the first period thus satisfying the requirement. As the largest trading costs have been captured, we are able to obtain tight upper bounds in examples. The new duality gap, which is calculated as the relative difference of the annualized certainty equivalent rate between the lower and upper bound, is nine times smaller than the old one on average.

3. *Reveal the distortion of the no-trading region due to the borrowing constraint*

   The no-trading region associated with the transaction costs problem has been studied by many papers (see, e.g., Muthuraman and Kumar, 2006; Lynch and Tan, 2010). However, to the best of our knowledge, this is the first study of the distortion of the no-trading region resulted from the borrowing constraint. Campbell et al. (2001) emphasized that constraints such as nonnegativity of portfolio positions are realistic, and they affect the form of the solution, but relatively little is known about the effects of such constraints on optimal strategies, because the constraints make it hard to find analytical solutions. In the case of two uncorrelated risky assets, the no-trading region forms a rectangle if the constraints on the asset positions are not binding. We demonstrate the course of distortion from a rectangle to a non-convex shape when the no-trading region gradually touches the borrowing constraint boundary. As investors generally confront constraints on portfolio positions, this study provides the insight of the practical shapes of the no-trading region and shines a light on the necessity of an exclusive study of optimal policy structure given those practical constraints.

The main contributions for the capital gain taxes problem are as follows:

1. *Solve the capital gain taxes problem more accurately via approximate dynamic programming*

   By following many other papers for a discrete time setting (see, e.g., Dammon et al., 2001; Garlappi et al., 2001; Gallmeyer et al., 2006), we formulate the portfolio optimization with capital gain taxes problem as a dynamic program with a continuous decision space. However, unlike the other studies in the discrete time setting that build a lattice return model (see, e.g., Dybvig and Koo, 1996; Dammon et al., 2001; Garlappi et al., 2001; DeMiguel and Uppal, 2005; Gallmeyer et al., 2006), we sample returns from a continuous distribution directly to produce more accurate results. This approach results in a dynamic program with continuous decision and state spaces. As is known difficult, a dynamic program with continuous decision and state spaces requires careful error control in approximate dynamic programming solution methods (see, e.g., Rust, 1996). Therefore, in this work we provide detailed ingredients for effective error control in commonly adopted approximate dynamic programming backward iteration. Accordingly, in each step of the iteration, the relative numerical error in approximating transformed value functions by a polynomial basis function is about 10^{-5} measured by the l_∞ norm and about 10^{-10} by the l_2 norm. Our numerical results of lower bounds generated by this method also justify its effectiveness.

2. *Explain the optimal trades through the associated no-trading region and reveal a similar no-trading region shape and parameter sensitivity to that of the transaction costs problem*

   The relevant research by Garlappi et al. (2001) presents a discussion of the no-trading region in a different state space. However, they have not built a link to the no-trading region of the transaction costs problem presented in Muthuraman and Kumar (2006) and Lynch and Tan (2010). In this thesis, through highly accurate numerical solutions and transformed state variables, i.e. relative basis prices and realized risky asset portfolios, we are able to visualize and analyze the no-trading region better. Specifically, for a single risky asset case, besides illustrating and analyzing the optimal trades, we quantitatively characterize the selling and purchasing boundaries of the no-trading region. We obtain mathematical connection between the two boundaries and two Merton's problems with different effective risky returns. For a two risky asset case, we identify the commonalities and differences between the no-trading region of transaction costs problems and that of capital gain taxes problems. In particular, we numerically demonstrate the no-trading region of the capital gain taxes problem with featured optimal trades and show a similar shape and parameter sensitivity to that of the transaction costs problem. To the best of our knowledge, this is the first time (1) explaining optimal trading strategies through the no-trading region of the capital gain taxes problem, and (2) revealing a similar shape and parameter sensitivity of the no-trading region to that of the transaction costs problem.

3. *Develop five lower bound strategies and assess their quality by comparing with upper bounds*

   In most of our numerical examples, the duality gaps, computed as the relative difference between lower and upper bounds, are smaller than 3%. The first strategy, value function optimization (VF), is based on the approximated value functions produced by approximate dynamic programming backward iteration. Since the approximation has a high accuracy, this strategy generates tight lower bounds. Besides, the myopic optimization (MO) and rolling buy-and-hold (RBH) strategies are heuristic, easy to implement and represent close approximation to the original model. The former has been studied by Wang (2008) in single risky asset cases when trading intervals are approaching zero. The latter has served as a robust benchmark that produces tight lower bounds in the transaction costs problem in Brown and Smith (2011) and Broadie and Shen (2013b). However, as these three strategies need step by step optimization along each return trial, they are computationally expensive. Therefore, we propose two strategies motivated from approximating trading policy after exploring solution structures. They are about two to three orders of magnitude faster than VF, MO and RBH, and produce comparable lower bounds. Specifically, the realized Merton's (RM) strategy captures the intuition that the realized wealth as the nominal wealth subtracting liquidation taxes perhaps should be distributed according to the original Merton's solution. The hyper-cube (HC) strategy approximately parameterizes the associated no-trading region by a hyper-cube. As the parameterization only involves one variable, HC is cheap even in high dimensions. In high-dimensional examples, RM and HC are about three orders of magnitude faster on average, and RM takes less than a minute to compute.

To evaluate those lower bounds, we compute upper bounds. We provide two upper bounds based on the duality techniques developed by Brown et al. (2009) and Brown and Smith (2011), the value function-based and gradient-based upper bound methods (VUB and GUB, respectively). Across various parameter sets, most of the duality gaps are smaller than 5%. This result ensures our lower bounds perform well. We are able to solve problems for both lower and upper bounds up to 20 risky assets and 30 periods.

We study the portfolio optimization with transaction costs in Chapter 2 and study the portfolio optimization with capital gain taxes in Chapter 3.

Chapter 2

Portfolio Optimization with Transaction Costs

2.1 Introduction

In presence of transaction costs, Merton's solution for a multi-period portfolio optimization turns to be suboptimal. Therefore, in this chapter, we consider the problem of dynamic multi-asset portfolio optimization in a discrete-time, finite-horizon setting. Our general model considers risk aversion, nonnegativity constraints on portfolio positions, and proportional transaction costs. We are concerned with the efficient method to compute the optimal investment decisions for investors who have access to multiple investment instruments: a risk-free asset account paying a risk-free rate and several risky assets with stochastic returns.

The balance of the chapter is organized as follows: In Section 2.2, we describe the investment model. In Section 2.3, we investigate relevant properties. In Section 2.4, we propose several trading strategies to compute the lower bounds. In Section 2.5 three dual bound methods are given with some discussion. In Section 2.6, we analyze our numerical results and illustrate the borrowing constraint impact. Finally, in Section 2.7, we briefly conclude and discuss some future directions.

2.2 The Portfolio Optimization Model with Transaction Costs

Time is modeled as discrete and indexed as $t_k = k\Delta t$, $k = 0, ..., m$, with $t_0 = 0$ the current period and $t_m = T$ the terminal period. We consider a market that contains one risk-free and multiple n risky assets. The risk-free asset continuously pays a gross risk-free rate R_f. The corresponding net risk-free return rate is denoted by r_f. The returns of the risky assets are stochastic and denoted by $\boldsymbol{R}_{t_k} = (R_{t_k,1}, ..., R_{t_k,n})'$ where $R_{t_k,i}$ is the gross return of asset i from period t_{k-1} to period t_k. The return is modeled by a multivariate geometric Brownian motion:

$$\ln \boldsymbol{R}_{t_k} = \boldsymbol{\mu} - \frac{1}{2}\boldsymbol{\sigma}^2 + \boldsymbol{e}_{t_k} \tag{2.1}$$

with $\boldsymbol{\mu} = (\mu_1, ..., \mu_n)'$ the asset return vector, $\boldsymbol{\sigma} = (\sigma_1, ..., \sigma_n)'$ the return volatility vector, and $\mathbf{e}_{t_k}$ the stochastic increments from the multivariate normal distribution with mean zero, volatility $\boldsymbol{\sigma}$, and correlation Σ_e. All the parameters in the return model are time-independent.

Investors have an initial investment of x_0 dollars invested in a risk-free asset and $\mathbf{y}_0 = (y_{0,1}, ..., y_{0,n})'$ dollars invested in the n risky assets. The positions in the risk-free and risky assets at time t_k are denoted by x_{t_k} and $\mathbf{y}_{t_k} = (y_{t_k,1}, ..., y_{t_k,n})'$, respectively.

In time, investors can either spend money from the risk-free account to buy risky assets or add money to the risk-free account by selling risky assets. To model the transaction we consider buying and selling risky assets separately. Denote $\mathbf{L}_{t_k} = (L_{t_k,1}, ..., L_{t_k,n})'$ as an n-vector whose i-th element represents the amount of money spent from the risk-free account to buy risky asset i before incurring transaction costs. Similarly, denote $\mathbf{U}_{t_k} = (U_{t_k,1}, ..., U_{t_k,n})'$ as an n-vector whose i-th component represents the amount of money obtained from selling risky asset i before incurring transaction costs. Thus, they are both nonnegative. Buying and selling risky assets incur proportional transaction costs. Let $\boldsymbol{\beta} = (\beta_1, ..., \beta_n)' \geq \mathbf{0}$ be the transaction cost factor for buying and selling. More precisely, buying a risky asset i priced at $L_{t_k,i}$ will cost $(1 + \beta_i)L_{t_k,i}$ in risk-free account, and selling a risky asset i priced at $U_{t_k,i}$ will result in $(1 - \beta_i)U_{t_k,i}$ in risk-free account.

The controlled evolution of the positions in the risk-free and risky assets can be described by the system of equations:

$$\begin{pmatrix} x_{t_{k+1}} \\ \mathbf{y}_{t_{k+1}} \end{pmatrix} = \begin{pmatrix} R_f \left(x_{t_k} - \sum_{i=1}^{n} [(1+\beta_i) L_{t_k,i} - (1-\beta_i) U_{t_k,i}] \right) \\ \boldsymbol{R}_{t_{k+1}} \cdot (\mathbf{y}_{t_k} + \mathbf{L}_{t_k} - \mathbf{U}_{t_k}) \end{pmatrix} \tag{2.2}$$

where $\cdot$ denotes the element-wise product of two vectors. To prohibit short selling and borrowing, we assume the trades at time t_k are restricted to a convex set:

$$\mathbb{A}_{t_k} = \left\{ \mathbf{U}_{t_k}, \mathbf{L}_{t_k} \in \mathbb{R}_+^n : x_{t_k} - \sum_{i=1}^{n} [(1+\beta_i) L_{t_k,i} - (1-\beta_i) U_{t_k,i}] \geq 0, \mathbf{y}_{t_k} + \mathbf{L}_{t_k} - \mathbf{U}_{t_k} \geq \mathbf{0} \right\}. \tag{2.3}$$

The wealth W_{t_k} is the sum of the dollar positions across the risk-free and risky assets at time t_k, i.e.,

$$W_{t_k} = x_{t_k} + \sum_{i=1}^{n} y_{t_k,i}. \tag{2.4}$$

The objective is to choose a policy $(\mathbf{U}_{t_k}, \mathbf{L}_{t_k})$ at each period t_k to maximize the expected utility of the final wealth

$$\max_{\substack{(\mathbf{U}_{t_k}, \mathbf{L}_{t_k}) \in \mathbb{A}_{t_k} \\ k=0,\ldots,m-1}} \mathbb{E}[\mathcal{U}(W_T)] \tag{2.5}$$

with the constant relative risk aversion (CRRA) utility function:

$$\mathcal{U}(x) = \begin{cases} \dfrac{x^\gamma}{\gamma} & \gamma < 1, \gamma \neq 0 \\ \ln(x) & \gamma = 0 \end{cases}. \tag{2.6}$$

The CRRA utility function (2.6) has constant relative risk aversion level $1-\gamma$ and thereby a more negative coefficient γ represents a higher risk aversion attitude. The first derivative $\mathcal{U}'(x) > 0$ shows investors prefer more wealth than less and the second derivative $\mathcal{U}''(x) < 0$ exhibits diminishing marginal utility. A very large body of experiment and survey show most individuals have risk aversions between one and 10 (see, e.g., Metrick, 1995; Kimball et al., 2008). Thus, we will use the value of γ between -9 and 0 for the examples in this thesis.

The portfolio optimization problem can be formulated as a stochastic dynamic program with state variables consisting of the current positions in the risk-free and risky assets $(x_{t_k}, \mathbf{y}'_{t_k})$. The terminal value function is the utility of terminal wealth $V_T = \mathcal{U}(W_T)$, and the early value functions V_{t_k} are given recursively as

$$V_{t_k}(x_{t_k}, \mathbf{y}_{t_k}) = \max_{(\mathbf{U}_{t_k}, \mathbf{L}_{t_k}) \in \mathbb{A}_{t_k}} \mathbb{E}_{t_k}[V_{t_{k+1}}(x_{t_{k+1}}(\mathbf{U}_{t_k}, \mathbf{L}_{t_k}), \mathbf{y}_{t_{k+1}}(\mathbf{U}_{t_k}, \mathbf{L}_{t_k}))] \tag{2.7}$$

where the expectations are taken over the stochastic return of risky assets $\boldsymbol{R}_{t_{k+1}}$, and $\mathbb{E}_{t_k}[\cdot]$ denotes the conditional expectation conditioned on the information up to time t_k. Denote the certainty equivalent of the value function $V_{t_k}(\cdot)$ as a strictly monotonic transformation:

$$C_{t_k}(\cdot) = \mathcal{U}^{-1}(V_{t_k}(\cdot)). \tag{2.8}$$

2.3 Model Properties and Approximate Dynamic Programming

Approximate dynamic programming is aiming at developing practical and high-quality approximated solutions when dynamic programming problems are hard to solve exactly. One of the approaches starts with approximating value functions by regression models and then goes backward from the second-to-last period to the first. In each period the solution is found by maximizing the one-step ahead expectation of the approximated value function derived in the previous recursion step. This approach has previously been applied in various areas such as option pricing (see, e.g., Longstaff and Schwartz, 2001), risk estimation (see, e.g., Broadie, Du, and Moallemi, 2011), and portfolio optimization (see, e.g., Brandt, Goyal, Santa-Clara, and Stroud, 2005).

Specifically, the optimization problem (2.7) does not have a closed-form solution for $V_{t_k}(x_{t_k}, \mathbf{y}_{t_k})$. Without the solution, the recursive steps cannot proceed. Thus, a proxy of $V_{t_k}(x_{t_k}, \mathbf{y}_{t_k})$ is required. In each step of the backward iteration, we compute the current-period value function $V_{t_k}(x_{t_k}, \mathbf{y}_{t_k})$ on a grid of the discretized state space of $(x_{t_k}, \mathbf{y}'_{t_k})$ by optimizing the expectation of the next-period value function $V_{t_{k+1}}(x_{t_{k+1}}, \mathbf{y}_{t_{k+1}})$. Then given the optimal values on the grid points, the current-period value function over the entire state space is approximated by regressing on a set of basis functions such as polynomials of state variables. Since the value function at the last step is given by the CRRA utility function (2.6), the iteration can keep going until reach the first period. Approximated value functions are generated in situ with the iteration.

According to this procedure, we will answer three questions in the rest of the section: (1) How to discretize the state space? (2) Which class of basis functions to choose? (3) How to reduce approximation errors when we use basis functions to approximate value functions?

For the first question, by using the homothetic property of the portfolio optimization problem under transaction costs (see, e.g., Davis and Norman, 1990; Shreve and Soner, 1994), we can adopt wealth fractions as state variables rather than wealth holdings. We restate the homothetic property as follows:

Proposition 1. *Suppose $\mathcal{U}(x) = x^\gamma/\gamma$ or $\mathcal{U}(x) = \ln(x)$. Then the certainty equivalent C_{t_k} of the value function V_{t_k} at time t_k defined in the equation* (2.8) *has the homothetic property: for $\theta > 0$*

$$C_{t_k}(\theta x_{t_k}, \theta \mathbf{y}_{t_k}) = \theta C_{t_k}(x_{t_k}, \mathbf{y}_{t_k}) \tag{2.9}$$

Proof. See Appendix A.1. □

Based on the above relation (2.9), by choosing $\theta = W_{t_k}^{-1}$ we can easily compute the value function or its certainty equivalent at time t_k at any positive wealth level by

$$C_{t_k}(x_{t_k}, \mathbf{y}_{t_k}) = W_{t_k} C_{t_k}\left(\frac{x_{t_k}}{W_{t_k}}, \frac{\mathbf{y}_{t_k}}{W_{t_k}}\right). \tag{2.10}$$

In addition, in high dimensions constructing the discretized state space grid by a tensor product of each dimension will confront the curse of dimensionality. Therefore, at time t_k portfolio weights $(x_{t_k}, \mathbf{y}'_{t_k})$ with unit total wealth are sampled according to a uniform distribution on the simplex

$$\mathbb{S}_{t_k} = \left\{(x_{t_k}, \mathbf{y}'_{t_k})' \in \mathbb{R}_+^{n+1} : x_{t_k} + \sum_{i=1}^{n} y_{t_k,i} = 1\right\} \tag{2.11}$$

by the Sobol low-discrepancy sequence (see, e.g., Boyle et al., 1997).

For the second question, we realize that when the dimension of state space is high, the optimal solution cannot be computed fast by using interpolations (see, e.g., Lynch and Tan, 2010), radial basis functions or feedforward neural networks (see, e.g., Garlappi and Skoulakis, 2009, 2010). Moreover, the classic local approximation such as interpolations suffers the curse of dimensionality as the grid is constructed by a tensor product of each dimension. Also, Judd and Solnick (1994) point out that in high dimensions multilinear interpolations and other local approximation methods will not inherit differentiability of value functions. However, the differentiability is typically needed in an optimization routine using gradient methods. Therefore, we choose regressions to globally approximate value functions. Consider a set of K real-valued functions $\phi_{t_k,1}(\cdot), \ldots, \phi_{t_k,K}(\cdot)$ on the state space

$\mathbb{S}_{t_k}$, called basis functions. Then we find a linear combination of the basis functions to approximate the value function at time t_k over the entire state space by

$$V_{t_k}(x_{t_k}, \mathbf{y}_{t_k}) \approx \widetilde{V}_{t_k}(x_{t_k}, \mathbf{y}_{t_k}) = \sum_{l=1}^{K} \phi_{t_k,l}(x_{t_k}, \mathbf{y}_{t_k})\kappa_{t_k,l} \tag{2.12}$$

where the coefficient $\boldsymbol{\kappa}_{t_k} = (\kappa_{t_k,1}, ..., \kappa_{t_k,K})'$ is a column vector and can be computed by ordinary linear regression. In the sequel, denote the certainty equivalent of the approximated value function at time t_k as $\widetilde{C}_{t_k}(\cdot) = \mathcal{U}^{-1}(\widetilde{V}_{t_k}(\cdot))$. Denote $\widetilde{C}_{t_k}(\mathbf{y}_{t_k})$ and $C_{t_k}(\mathbf{y}_{t_k})$ as $\widetilde{C}_{t_k}(x_{t_k}, \mathbf{y}_{t_k})$ and $C_{t_k}(x_{t_k}, \mathbf{y}_{t_k})$ with the total unit wealth condition $x_{t_k} + \sum_{i=1}^{n} y_{t_k,i} = 1$, respectively.

Next, to determine the specific form of the basis functions used in the regression (2.12), we explore the feature of value functions. The analyses about the functional form of the value function show polynomials of state variables would be a good candidate for the basis functions (see, e.g., Shreve and Soner, 1994; Liu and Loewenstein, 2002; Janecek and Shreve, 2004; Goodman and Ostrov, 2010). Using tensor products of low-dimensional polynomials to generate high-dimensional polynomials is a natural idea. However, in high dimensions the tensor product method still suffers the curse of dimensionality. Moreover, the speed of computing basis functions brings concerns, as objective functions in optimization use numerical expectation of approximated value functions, the dominant computational costs come from the computing speed of basis functions.

Combining all the observations, we either use the complete set of polynomials class which grows polynomially as the dimension increases or use the polynomials up to a given order in each dimension that excludes cross terms. We call the second type the principal set of polynomials class. In general, the k-th order expansion of d-dimensional functions using monomials in

$$\mathcal{P}_k^d = \left\{ x_1^{i_1} \cdots x_d^{i_d} : \sum_{l=1}^{n} i_l \leq k, i_1 \geq 0, ..., i_d \geq 0 \right\} \tag{2.13}$$

is called a complete set of polynomials of total order k in n variables (see, e.g., Gaspar and Judd, 1997; Judd, 1998). Compared with tensor products, the complete set of polynomials class retains the asymptotically convergence rate of tensor products, since many of the elements in a tensor product are redundant. For example, the complete set for the total order 3 in 2 variables $(y_{t_k,1}, y_{t_k,2})$ is

$$\mathcal{P}_3^2 = \{1, y_{t_k,1}, y_{t_k,2}, y_{t_k,1}^2, y_{t_k,1}y_{t_k,2}, y_{t_k,2}^2, y_{t_k,1}^3, y_{t_k,1}^2 y_{t_k,2}, y_{t_k,1}y_{t_k,2}^2, y_{t_k,2}^3\} \tag{2.14}$$

and the complete set for the total order 2 in 4 variables $(y_{t_k,1}, y_{t_k,2}, y_{t_k,3}, y_{t_k,4})$ is

$$\begin{aligned}\mathcal{P}_2^4 = \{&1, y_{t_k,1}, y_{t_k,2}, y_{t_k,3}, y_{t_k,4}, y_{t_k,1}^2, y_{t_k,1}y_{t_k,2}, y_{t_k,1}y_{t_k,3}, y_{t_k,1}y_{t_k,4}, \\ &y_{t_k,2}^2, y_{t_k,2}y_{t_k,3}, y_{t_k,2}y_{t_k,4}, y_{t_k,3}^2, y_{t_k,3}y_{t_k,4}, y_{t_k,4}^2\}.\end{aligned} \tag{2.15}$$

For the third question, it is crucial to have an effective control for error accumulation in the backward iteration. The deterioration of value function iteration observed by van Binsbergen and Brandt (2007) can be resolved if we (1) apply certainty equivalent transformation to expected approximated value functions before performing optimization and (2) approximate certainty equivalent functions rather than original value functions. In the transaction costs problem, certainty equivalent functions are much less nonlinear than original value functions, especially for high levels of risk aversion. In addition, original value functions take values close to zero for certain values of state variables, especially for long horizons. In contrast, certainty equivalent functions are stable over time and never get close to zero. Because of these two features, it is much easier to optimize over certainty equivalent functions and approximate them over the entire state space by a set of basis functions. Also, the certainty equivalent transformation is a natural candidate for portfolio choice problems because of its sound economic motivation and its intuitive interpretation. More examples using certainty equivalents in portfolio choice problems can be found in Garlappi and Skoulakis (2009, 2010) and Broadie and Shen (2013a).

As discussed, we express the recursive equation (2.7) in terms of the function $C_{t_k}(\cdot)$:

$$C_{t_k}(\mathbf{y}_{t_k}) = \max_{(\mathbf{U}_{t_k},\mathbf{L}_{t_k})\in\mathbb{A}_{t_k}} \mathcal{U}^{-1}\Big\{\mathbb{E}_{t_k}\left[\mathcal{U}(W_{t_{k+1}}C_{t_{k+1}}(\mathbf{y}_{t_{k+1}}(\mathbf{U}_{t_k},\mathbf{L}_{t_k})))\right]\Big\} \tag{2.16}$$

subject to the wealth dynamics equation (2.2) and the terminal condition $C_T(\mathbf{y}_T) = 1$. Given grid points $(x_{t_k}, \mathbf{y}'_{t_k})$ sampled from (2.11) and the corresponding optimal certainty equivalents calculated by (2.16), the certainty equivalent over the whole state space is approximated by

$$C_{t_k}(\mathbf{y}_{t_k}) \approx \widetilde{C}_{t_k}(\mathbf{y}_{t_k}) = \sum_{l=1}^{K} \phi_{t_k,l}(\mathbf{y}_{t_k})\kappa_{t_k,l}. \tag{2.17}$$

To illustrate the approximation accuracy of different classes of polynomials and the benefit of using certainty equivalent, we provide Table A.1 in Appendix A.2. By comparing different cases, we have seen approximating certainty equivalent functions produces a higher accuracy in terms of fitting and predicting errors than original value functions.

To sum up, at each time step from t_m to t_0, our approximate dynamic programming procedure involves the following steps:

1. Construct state space grid points by uniform randomly sampling on the simplex $\mathbb{S}_{t_k}$ (2.11).

2. Perform optimization as the equation (2.16) and obtain optimal values on grid points over the state space.

3. Approximate the certainty equivalent function over the entire state space $C_{t_k}(\mathbf{y}_{t_k})$ with computed optimal values on grid points by $\widetilde{C}_{t_k}(\mathbf{y}_{t_k})$ as the polynomial regression equation (2.17).

2.4 Forward Trading Strategies for Lower Bounds

For portfolio optimization problems without available closed form solutions, the goal is to search for the near-optimal forward trading strategies. In order to get high quality trading strategies, we can either approximate value functions as we discuss in the previous section or approximate trading policy that we will discuss in Section 2.4.2 and Section 2.4.3. Accordingly, we propose three trading strategies. The first strategy, value function optimization in Section 2.4.1, employs value functions approximated by regressions that we study in Section 2.3 as continuation values. The other two strategies, hyper-sphere and hyper-cube trading strategies in Sections 2.4.2 and 2.4.3, parameterize the no-trading region by simple geometries. For comparison, we also include the formulation of the rolling buy-and-hold heuristic strategy proposed by Brown and Smith (2011) in Section 2.4.5.

2.4.1 Value Function Optimization (VF)

Approximated value functions given by backward iteration could be used as continuation values in forward simulation. Hence, if the approximation of value functions has a high accuracy, we should expect this trading rule to generate a tight lower bound. In each period t_k for each trial VF chooses the trades $\mathbf{U}_{t_k}, \mathbf{L}_{t_k}$ that solve:

$$\max_{(\mathbf{U}_{t_k}, \mathbf{L}_{t_k}) \in \mathbb{A}_{t_k}} \mathcal{U}^{-1}\left\{ \mathbb{E}_{t_k}\left[\mathcal{U}(W_{t_{k+1}} \widetilde{C}_{t_{k+1}}(\mathbf{y}_{t_{k+1}}(\mathbf{U}_{t_k}, \mathbf{L}_{t_k}))) \right] \right\} \tag{2.18}$$

where we will use the CRRA utility in the last period. After following the recommended trades for the current portfolio positions, we generate random returns for risky assets to calculate the portfolio positions for the next period.

Although it is expensive to perform the optimization period by period in high dimensions, this strategy should be near-optimal if value functions have been approximated accurately. Besides, the complexity of the problem grows linearly instead of exponentially with dimensions.

2.4.2 Hyper-sphere Policy Approximation (HS)

In the multiple assets case, the no-trading region is close to a polyhedron, according to numerical examples (see, e.g., Muthuraman and Kumar, 2006; Lynch and Tan, 2010) and theoretical proofs (see, e.g., Atkinson and Mokkhavesa, 2004; Atkinson and Ingpochai, 2006; Goodman and Ostrov, 2010). We attempt to find a hyper-sphere for each trading period to approximate the no-trading region such that the final expected utility is maximized. By parameterizing the policy with one decision variable, the computational costs will be saved considerably. In order to find the optimal radius for this hyper-sphere, we need the following derivation.

In time period t_k the current risk-free and risky assets positions are $(x_{t_k}, \mathbf{y}'_{t_k})$ and the no-trading region approximated by a hyper-sphere $\Omega_{t_k} = \{\mathbf{z}_{t_k} : \|\mathbf{z}_{t_k} - \mathbf{y}^c_{t_k}\|_2 \leq r_{t_k}\}$ is characterized by the center $\mathbf{y}^c_{t_k} = (y^c_{t_k,1}, y^c_{t_k,2}, ..., y^c_{t_k,n})'$ and the radius r_{t_k}, where $\|\cdot\|_2$ is the ℓ_2 norm. The center is obtained from the optimal solution of the Merton's problem and the radius will be determined according to an optimization algorithm in the end of this section. We approximate the trading policy of the problem as follows: if the risky asset position

$\mathbf{y}_{t_k} \notin \Omega_{t_k}$, the optimal trade is the minimal distance from the current position $\mathbf{y}_{t_k}$ to Ω_{t_k}; if the current position $\mathbf{y}_{t_k} \in \Omega_{t_k}$, the optimal trade is to keep it unchanged. Denote the post-trade positions of the risk-free and risky assets as $x^*_{t_k}$ and $\mathbf{y}^*_{t_k}$, respectively. We define the distance from the pre-trade risky asset position to the center of the hyper-sphere as

$$d_{t_k} = \sqrt{\sum_{i=1}^{n}(y_{t_k,i} - y^c_{t_k,i})^2}. \tag{2.19}$$

From geometric properties of the hyper-sphere, the post-trade position of the i-th risky asset is

$$y^*_{t_k,i} = \begin{cases} y^c_{t_k,i} + (y_{t_k,i} - y^c_{t_k,i})\dfrac{r_{t_k}}{R_{t_k}} & d_{t_k} \geq r_{t_k} \\ y_{t_k,i} & d_{t_k} < r_{t_k} \end{cases} \tag{2.20}$$

or in a compact form

$$y^*_{t_k,i} = y_{t_k,i} + \max(1 - \frac{r_{t_k}}{d_{t_k}}, 0)(y^c_{t_k,i} - y_{t_k,i}). \tag{2.21}$$

The corresponding risk-free asset position is

$$x^*_{t_k} = x_{t_k} + \sum_{i=1}^{n}(y_{t_k,i} - y^c_{t_k,i} - \beta_i|y^c_{t_k,i} - y_{t_k,i}|)\max(1 - \frac{r_{t_k}}{d_{t_k}}, 0). \tag{2.22}$$

Integrating this formula with the transaction costs model gives the controlled dynamics from time t_k to t_{k+1} as,

$$\begin{pmatrix} x_{t_k} \\ y_{t_k,1} \\ \vdots \\ y_{t_k,n} \end{pmatrix} \rightarrow \begin{pmatrix} x^*_{t_k} \\ y^*_{t_k,1} \\ \vdots \\ y^*_{t_k,n} \end{pmatrix} \rightarrow \begin{pmatrix} x^*_{t_k} R_f \\ y^*_{t_k,1} R_{t_k,1} \\ \vdots \\ y^*_{t_k,n} R_{t_k,n} \end{pmatrix} = \begin{pmatrix} x_{t_{k+1}} \\ y_{t_{k+1},1} \\ \vdots \\ y_{t_{k+1},n} \end{pmatrix} \tag{2.23}$$

where

$$\begin{pmatrix} x^*_{t_k} \\ y^*_{t_k,1} \\ \vdots \\ y^*_{t_k,n} \end{pmatrix} = \begin{pmatrix} x_{t_k} + \max(1 - \frac{r_{t_k}}{d_{t_k}}, 0)\sum_{i=1}^{n}\left(y_{t_k,i} - y^c_{t_k,i} - \beta_i|y_{t_k,i} - y^c_{t_k,i}|\right) \\ y_{t_k,1} + \max(1 - \frac{r_{t_k}}{d_{t_k}}, 0)(y^c_{t_k,1} - y_{t_k,1}) \\ \vdots \\ y_{t_k,n} + \max(1 - \frac{r_{t_k}}{d_{t_k}}, 0)(y^c_{t_k,n} - y_{t_k,n}) \end{pmatrix}. \tag{2.24}$$

To determine a series of optimal radius r_{t_k} required in the trading strategy, we implement a two track policy approximation algorithm. First, by following a predetermined naive strategy to simulate the controlled dynamics step by step, we get the controlled asset position distribution in each step. Second, by using backward iteration, we determine the best radius of the hyper-sphere that maximizes the expected final utility from the last step to the initial step. For example, in the last step we find the best radius for the one period problem by following the trading rule given in (2.23), and in the step before the last step we carry out the same search for the best radius for that period but we will use the radius found in the last step when we simulate one step forward to reach the final period. The process is similar to a backward bootstrap procedure. To summarize, the algorithm can be described as:

1. Decide a naive strategy to simulate to the step before the last step. The controlled asset positions at time $t_{(m-1)\Delta t}$ serve as the distribution of starting positions for the last period. The naive strategy can be a hyper-sphere strategy with a fixed size of radius. The radius is calculated by the distance between the Merton's solution and the post-trade position given by VF.

2. Take a search to get the optimal radius at time $t_{(m-1)\Delta t}$. We set up the search bound of the radius from the Merton's solution to the furthest vertices of the simplex $\mathbb{S}_{t_k}$. This is a nonsmooth optimization with only one decision variable. Thus, we can perform a brute-force search, which is similar to the policy search for Bermudan swaption by Andersen (2000).

3. Go back to $t_{(m-2)\Delta t}$. Use the simulated paths in step 1 to $t_{(m-2)\Delta t}$. Find the best radius at time $t_{(m-2)\Delta t}$ that maximizes the final expected utility function by following the policy given by step 2.

4. Iterate until reaching the first time step t_0.

5. Forward simulate according to the series of radius found in the previous steps.

2.4.3 Hyper-cube Policy Approximation (HC)

The motivation behind of the hyper-cube policy is to approximate the no-trading region by a hyper-cube instead of a hyper-sphere. Since the shape of the no-trading region varies with different parameters, the hyper-cube approximation might work better than the hyper-sphere. In order to derive the formulation, we only need to replace the hyper-sphere by the hyper-cube in the algorithm given in Section 2.4.2 and calculate the post-trade positions.

To get the post-trade positions for time period t_k, we assume the current risk-free and risky assets positions $(x_{t_k}, \mathbf{y}'_{t_k})$ and the no-trading region that is approximated by a hyper-cube $\Omega_{t_k} = \{\mathbf{z}_{t_k} : \|\mathbf{z}_{t_k} - \mathbf{y}^c_{t_k}\|_\infty \leq r_{t_k}\}$, which is characterized by the half of its side length r_{t_k} and by the center from the Merton's model $\mathbf{y}^c_{t_k}$, where $\|\cdot\|_\infty$ is the ℓ_∞ norm. Accordingly, we approximate the trading rule as follows: if $\mathbf{y}_{t_k} \notin \Omega_{t_k}$, the optimal trade is the minimal distance from the current portfolio $\mathbf{y}_{t_k}$ to Ω_{t_k}; if the current risky asset position $\mathbf{y}_{t_k} \in \Omega_{t_k}$, the optimal trade is to keep the current positions unchanged. From geometric properties of the hyper-cube, the post-trade position of the i-th risky asset is

$$y^*_{t_k,i} = \begin{cases} r_{t_k} + y^c_{t_k,i} & y_{t_k,i} > r_{t_k} + y^c_{t_k,i} \\ y_{t_k,i} & -r_{t_k} + y^c_{t_k,i} \leq y_{t_k,i} \leq r_{t_k} + y^c_{t_k,i} \\ -r_{t_k} + y^c_{t_k,i} & y_{t_k,i} < -r_{t_k} + y^c_{t_k,i} \end{cases} \tag{2.25}$$

or in a compact form

$$y^*_{t_k,i} = \max(y_{t_k,i}, -r_{t_k} + y^c_{t_k,i}) + \min(y_{t_k,i}, r_{t_k} + y^c_{t_k,i}) - y_{t_k,i}. \tag{2.26}$$

The corresponding risk-free asset position is

$$x^*_{t_k} = x_{t_k} + \sum_{i=1}^{n} (y_{t_k,i} - y^*_{t_k,i} - \beta_i |y_{t_k,i} - y^*_{t_k,i}|). \tag{2.27}$$

The series of optimal side length of the hyper-cube in the HC strategy is determined by the same method in Section 2.4.2.

Further, in order to understand how the hyper-sphere and the hyper-cube approximate the no-trading region, Figure 2.1 illustrates the approximation of the no-trading region for a two risky asset problem. From left to right, the correlation between the two risky assets is increasing. In the first case, when they are uncorrelated, the no-trading region is a square.

The HC method approximates the region better than the HS method. When the correlation is non-zero, in the second case, the HS method is more conservative in terms of covering more area of the no-trading region than the HC method. In the third case, the difference between them is larger, but they both cover the main part of the no-trading region. Although the approximation looks crude, in the process of forward trading, controlled portfolio positions may only concentrate around a particular area of the no-trading region rather than be uniformly distributed in the state space.

Both HS and HC follow the trades given by VF in the first trading period, and maximize the expected CRRA utility function in the last period. In the first period optimization can be taken only once as all simulation trials start from the same initial positions, while in the last period optimizing the expected CRRA utility function is not expensive and produces accurate solutions.

2.4.4 Handle Borrowing

We need to formulate a rule when a forward trading strategy needs to finance a purchase by borrowing cash from the risk-free account. Mathematically, we have to ensure the post-trade risk-free position $x^*_{t_k}$ nonnegative. Since HS and HC derived by the corresponding geometric properties do not implicitly prohibit borrowing, we have to explicitly set up the rule to meet the borrowing constraint. Heuristically, we can either sell more or buy less risky assets. More precisely, purchase-less rule means that investors will buy λ percentage of the originally suggested purchase $\mathbf{L}_{t_k}$ to guarantee exhausting the new post-trade risk-free asset position, i.e.

$$0 = x^*_{t_k} = x_{t_k} + \sum_{i=1}^{n}(1-\beta_i)U_{t_k,i} - \sum_{i=1}^{n}(1+\beta_i)\lambda L_{t_k,i} \tag{2.28}$$

which yields the scaling factor

$$\lambda = \frac{x_{t_k} + \sum_{i=1}^{n}(1-\beta_i)U_{t_k,i}}{\sum_{i=1}^{n}(1+\beta_i)L_{t_k,i}} \tag{2.29}$$

Figure 2.1: Illustration of approximation of the no-trading region by a hyper-sphere and a hyper-cube.

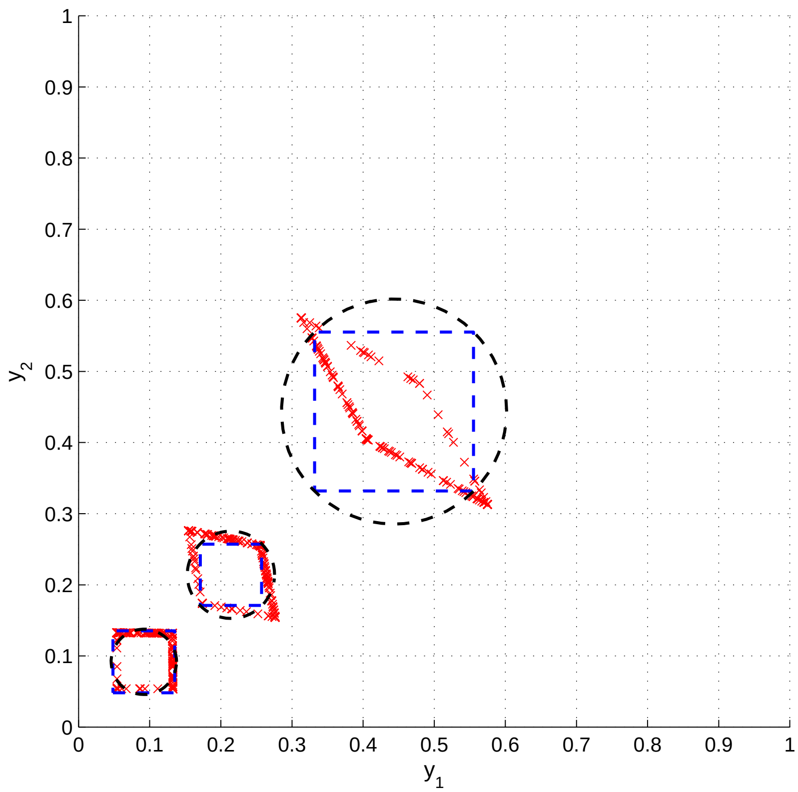

Note: y_1 and y_2 represent risky asset one and two, respectively. The red dots computed from three different parameter sets represent three types of the no-trading region. The blue dash line is the approximation result from the hyper-cube method. The black dash line is the result from the hyper-sphere method. The parameters we use to generate the three types of no-trading region for the one period problem, from left to right, are: $R_f = 110\%$, $R_1 = R_2 = 115\%$, $\sigma_1 = \sigma_2 = 50\%$, $\rho = 0.0$, $\beta_1 = \beta_2 = 2\%$, $\gamma = -1$, $T = 1$ year; $R_f = 106.5\%$, $R_1 = R_2 = 115\%$, $\sigma_1 = \sigma_2 = 40.2\%$, $\rho = 0.20$, $T = 1$ year, $\beta_1 = \beta_2 = 1.5\%$, $\gamma = -1$; $R_f = 103.5\%$, $R_1 = R_2 = 115\%$, $\sigma_1 = \sigma_2 = 29.1\%$, $\rho = 0.53$, $T = 1$ year, $\beta_1 = \beta_2 = 1\%$, $\gamma = -1$.

and the corresponding post-trade i-th risky asset position

$$y^*_{t_k,i} = y_{t_k,i} - U_{t_k,i} + \lambda L_{t_k,i} = y_{t_k,i} - U_{t_k,i} + \frac{x_{t_k} + \sum_{i=1}^{n}(1-\beta_i)U_{t_k,i}}{\sum_{i=1}^{n}(1+\beta_i)L_{t_k,i}} L_{t_k,i}. \tag{2.30}$$

Alternatively, sell-more rule means investors will sell λ percentage of the original suggested selling $\mathbf{U}_{t_k}$ to use up the risk-free asset. Similarly, the scaling factor is

$$\lambda = \frac{-x_{t_k} + \sum_{i=1}^{n}(1+\beta_i)L_{t_k,i}}{\sum_{i=1}^{n}(1-\beta_i)U_{t_k,i}} \tag{2.31}$$

and the rebalanced position is

$$y^*_{t_k,i} = y_{t_k,i} - \lambda U_{t_k,i} + L_{t_k,i} = y_{t_k,i} + L_{t_k,i} + \frac{x_{t_k} - \sum_{i=1}^{n}(1+\beta_i)L_{t_k,i}}{\sum_{i=1}^{n}(1-\beta_i)U_{t_k,i}} U_{t_k,i}. \tag{2.32}$$

Note due to the homothetic property of the transaction costs model, tuning buying and selling simultaneously by the same factor will not resolve the issue. According to our numerical results, there is no significant difference between the two rules regarding to the final utility. In the sequel, we adopt purchase-less rule in calculation.

2.4.5 Rolling Buy-and-Hold Optimization (RBH)

The idea of the RBH strategy is that in each period investors choose trades in the current period to maximize the expected utility of wealth at some h horizon period in the future. It incorporates transaction costs in the current period and the portfolio will follow its dynamics without any control in the future periods. Its continuation values are approximated by value functions from the Merton's model. In each period t_k for each trial RBH chooses the trades $\mathbf{U}_{t_k}, \mathbf{L}_{t_k}$ that solve:

$$\max_{(\mathbf{U}_{t_k},\mathbf{L}_{t_k})\in\mathbb{A}_{t_k}} \mathcal{U}^{-1}\Big\{\mathbb{E}_{t_k}[\mathcal{U}(C^f_{t_{k+1}}(x_{t_{k+h}}(\mathbf{U}_{t_k},\mathbf{L}_{t_k}), \mathbf{y}_{t_{k+h}}(\mathbf{U}_{t_k},\mathbf{L}_{t_k})))]\Big\} \tag{2.33}$$

where $C^f_{t_k}$ denotes the certainty equivalent of the Merton's model and the CRRA utility function replaces the value function from the Merton's problem whenever $k+h > m$. For comparison, we will use $h = \frac{m}{2}$ as Brown and Smith (2011). RBH has the same order of magnitude of computational costs as VF. Besides, RBH is advantageous because it is intuitive, it does not require approximating value functions, and it can explicitly incorporate constraints. However, given the same amount of computing costs it will not converge to the true optimal solution as the value function optimization strategy.

2.5 Duality Methods for Upper Bounds

After implementing a lower bound strategy, to evaluate how much better we could possibly reach, we need an upper bound, which is given by the duality methods in Brown et al. (2009) and Brown and Smith (2011). Briefly, the duality method is based on two elements: (1) relax the nonanticipativity constraints that require the trading decisions to depend on the information available when the decision is made and (2) impose penalty that punishes violations of nonanticipativity constraints. While it is easy to relax constraints, it is not easy to impose valid penalty. However, it is still crucial to impose penalty, otherwise the bound is too loose to serve as an informative benchmark.

We now briefly describe the dual formulation by Brown et al. (2009) and Brown and Smith (2011) which should be consulted for further details and proofs of the results given below. Between the proposed two types of penalty functions, value function-based penalties and gradient-based penalties, for high-dimensional problems we will adopt gradient-based penalties instead of the former. The reason is that penalties are used in objective functions of optimization, and value function-based penalties require taking expectation in each period for a proxy of the true value function, which is typically expensive. In contrast, the gradient-based penalties do not require taking any expectations in each simulation trial. Therefore, as a guideline, for low-dimensional problems the former might be preferred, whereas in high dimensions gradient-based penalties are superior in computational costs.

Denote $(\mathbf{U}, \mathbf{L}) = (\mathbf{U}_0, ..., \mathbf{U}_{t_{m-1}}, \mathbf{L}_0, ..., \mathbf{L}_{t_{m-1}})$ as a path of trades and $\mathbf{R} = (\boldsymbol{R}_0, ..., \boldsymbol{R}_{t_{m-1}})$ as the path of returns from time 0 to t_{m-1}. Denote $\mathbb{A}$ as the set of feasible trade sequences in which each entity of $(\mathbf{U}, \mathbf{L})$ is feasible, and denote $\pi(\mathbf{U}, \mathbf{L}, \mathbf{R})$ as the penalty function that depends upon the sequence of trades and returns in a given simulation trial. A penalty function π is dual feasible if $\mathbb{E}\left[\pi(\mathbf{U},\mathbf{L},\mathbf{R})\right] \leq 0$ for any feasible trading strategy. The following proposition plays a central role in the dual bound computation.

Proposition 2. *For any feasible trading strategy* $(\mathbf{U},\mathbf{L})$ *and any dual feasible penalty* π*,*

$$\mathbb{E}\left[\mathcal{U}(W_T)\right] \leq \mathbb{E}\left[\max_{(\mathbf{U},\mathbf{L})\in\mathbb{A}} \{\mathcal{U}(W_T(\mathbf{U},\mathbf{L},\mathbf{R})) - \pi(\mathbf{U},\mathbf{L},\mathbf{R})\}\right]. \tag{2.34}$$

Proof. See Brown et al. (2009). □

Notice that the right hand side of the inequality (2.34) gives the dual bound

$$\mathbb{E}\left[\max_{(\mathbf{U},\mathbf{L})\in\mathbb{A}} \{\mathcal{U}(W_T(\mathbf{U},\mathbf{L},\mathbf{R}) - \pi(\mathbf{U},\mathbf{L},\mathbf{R})\}\right]. \tag{2.35}$$

The outer expectation is computed by simulation, while the inner problem is a deterministic problem along each simulation path of asset returns. In each trial of the simulation, we will generate a sequence of asset returns, and then solve the inner problem for this particular trial by optimizing over the whole trades decision set $(\mathbf{U},\mathbf{L})$. Thus, the size of the decision variables is $2nm$, growing linearly with the number of periods.

In order to compute the equation (2.35), the details of how the penalty function π is computed need to be specified in advance. We choose the gradient-based penalty function as

$$\pi = \nabla_a \mathcal{U}(W_T(\mathbf{U},\mathbf{L})^*)[(\mathbf{U},\mathbf{L}) - (\mathbf{U},\mathbf{L})^*] = \mathcal{U}'(W_T(\mathbf{U},\mathbf{L})^*)(\nabla_a W_T)'[(\mathbf{U},\mathbf{L}) - (\mathbf{U},\mathbf{L})^*]. \tag{2.36}$$

where ∇_a denotes the gradient on the decision variables for simplicity.

The gradient-based penalty exploits the convex structure of primal optimization problems. Its motivation lies in the fact that for any feasible strategy a convex primal problem has the first-order optimal condition as

$$\mathbb{E}[\pi] = \mathbb{E}\Big[\nabla_a \mathcal{U}(W_T(\mathbf{U},\mathbf{L})^*)[(\mathbf{U},\mathbf{L}) - (\mathbf{U},\mathbf{L})^*]\Big] \leq 0. \tag{2.37}$$

This implies the yield gradient-based penalty is dual feasible. After incorporating this penalty term, the dual bound is given by

$$\mathbb{E}\left[\max_{(\mathbf{U},\mathbf{L})\in\mathbb{A}} \Big\{\mathcal{U}(W_T(\mathbf{U},\mathbf{L},\mathbf{R}) - \nabla_a \mathcal{U}(W_T(\mathbf{U},\mathbf{L})^*)[(\mathbf{U},\mathbf{L}) - (\mathbf{U},\mathbf{L})^*]\Big\}\right]. \tag{2.38}$$

Following (2.16) to reduce numerical errors, we take the certainty equivalent transformation of the objective function as

$$\mathbb{E}\left[\max_{(\mathbf{U},\mathbf{L})\in\mathbb{A}} \mathcal{U}^{-1}\Big\{\mathcal{U}(W_T(\mathbf{U},\mathbf{L},\mathbf{R}) - \nabla_a \mathcal{U}(W_T(\mathbf{U},\mathbf{L})^*)[(\mathbf{U},\mathbf{L}) - (\mathbf{U},\mathbf{L})^*]\Big\}\right]. \tag{2.39}$$

Notice that if the trade sequence has been selected as the optimal strategy, the penalty term vanishes so that the duality gap turns out to be zero. In other words, the optimal trades for the primal problem could be reached if the dual trades are optimal.

Unfortunately, the optimal trades $(\mathbf{U},\mathbf{L})^*$ are generally unknown, otherwise the problem would have been solved. However, in order to construct penalty functions, we can seek an approximation of the primal problem, called a modified problem, and use the modified problem to compute penalty functions. Theoretically, to come up with a valid modified problem, we need to meet three requirements. First, the modified problem needs to be solved to optimality, because this offers the dual feasibility of the associated penalty functions. Second, if the set of feasible trades for the modified model includes those from the original model, then the dual feasibility in the feasible set for the modified model will lead to the feasibility of the original problem. Third, the modified model should be a convex optimization problem. The corresponding theorems and proofs can be found in Brown and Smith (2011).

We will consider two types of gradient-based penalty dual method. In order to compute upper bounds, we need to calculate the controlled positions of risk-free and risky assets at each time period. Assume all the assets face the same transaction costs factor β. By the asset dynamics (2.2), at time t_k the risk-free and risky asset positions x_{t_k} and $\mathbf{y}_{t_k}$ are

$$x_{t_k} = R_f^k x_0 + \sum_{\tau=0}^{k-1} R_f^{k-\tau}[\mathbf{1}'(\mathbf{U}_{t_\tau} - \mathbf{L}_{t_\tau}) - \beta\mathbf{1}'(\mathbf{U}_{t_\tau} + \mathbf{L}_{t_\tau})] \tag{2.40}$$

and

$$\mathbf{y}_{t_k} = (\boldsymbol{R}_{t_k} \cdot \dots \cdot \boldsymbol{R}_1)\cdot \mathbf{y}_0 + \sum_{\tau=0}^{k-1} \boldsymbol{R}_{t_k} \cdot \dots \cdot \boldsymbol{R}_{t_{\tau+1}}(\mathbf{L}_{t_\tau} - \mathbf{U}_{t_\tau}) \tag{2.41}$$

with the final wealth $W_T = x_T + \sum_{i=1}^n y_{T,i}$, where $\mathbf{1}$ denotes a column vector of n ones.

1. Frictionless gradient method (FL)

The frictionless model as a well-studied convex optimization problem is the natural consideration for the modified model. In addition, it can be solved optimally and includes the feasible set of the original problem.

In order to compute the derivatives used in the penalty function (2.36), since $\nabla_a \mathcal{U}(W_T) = \mathcal{U}'(W_T)\nabla_a W_T$ and $W_T = x_T + \sum_{i=1}^{n} y_{T,i}$, we only need to calculate the following gradient:

$$\nabla_a W_T = \nabla_a \left(\sum_{\tau=0}^{m-1} [R_f^{m-\tau}[\mathbf{1}'(\mathbf{U}_{t_\tau} - \mathbf{L}_{t_\tau}) + \mathbf{L}_{t_\tau})] + \boldsymbol{R}_T \cdot \cdots \cdot \boldsymbol{R}_{t_{\tau+1}} \mathbf{1}'(\mathbf{L}_{t_\tau} - \mathbf{U}_{t_\tau})] \right). \tag{2.42}$$

To get the explicitly form of this penalty, we need

$$\begin{aligned} \nabla_{\mathbf{L}_{t_k}} W_T &= -R_f^{m-k}\mathbf{1}' + \boldsymbol{R}_T \cdot \cdots \cdot \boldsymbol{R}_{t_{k+1}} \mathbf{1}', \quad 0 \le k \le m-1 \\ \nabla_{\mathbf{U}_{t_k}} W_T &= R_f^{m-k}\mathbf{1}' - \boldsymbol{R}_T \cdot \cdots \cdot \boldsymbol{R}_{t_{k+1}} \mathbf{1}', \quad 0 \le k \le m-1. \end{aligned} \tag{2.43}$$

2. Modified gradient method (BS and MG)

The frictionless gradient-based penalty does not take transaction costs into account. In order to incorporate the effect of transaction costs and satisfy the three requirements for a valid gradient-based penalty, we consider two methods as follows. The first method is proposed in Brown and Smith (2011), termed BS. Instead of imposing transaction costs on trades, it imposes proportional transaction costs on post-trade positions and adjusts the transaction costs factor β to β/m. We propose the second modified gradient method, termed MG. Our method focuses on the effect of transaction costs in the first trading period. In later periods it adopts the frictionless model. In addition, this convex model can be solved to optimality and we use the feasible set of the frictionless model to ensure the second requirement.

The formula for the risk-free asset dynamics in the MG method is

$$x_T = R_f^m x_0 - R_f^m \beta \mathbf{1}'(\mathbf{U}_0 + \mathbf{L}_0) + \sum_{\tau=0}^{m-1} R_f^{m-\tau}\mathbf{1}'(\mathbf{U}_{t_\tau} - \mathbf{L}_{t_\tau}). \tag{2.44}$$

The corresponding derivatives of the final wealth are expressed by

$$\nabla_a W_T = \nabla_a \left(-R_f^m \beta \mathbf{1}'(\mathbf{U}_0 + \mathbf{L}_0) + \sum_{\tau=0}^{m-1} R_f^{m-\tau}\mathbf{1}'(\mathbf{U}_{t_\tau} - \mathbf{L}_{t_\tau}) + \boldsymbol{R}_T \cdot \cdots \cdot \boldsymbol{R}_{t_{\tau+1}} \mathbf{1}'(\mathbf{L}_{t_\tau} - \mathbf{U}_{t_\tau}) \right)$$

namely,

$$\begin{aligned}
\nabla_{\mathbf{L}_0} W_T &= -R_f^m(1+\beta)\mathbf{1}' + \boldsymbol{\alpha}_T \cdot \cdots \cdot \boldsymbol{R}_0\mathbf{1}', \quad k=0 \\
\nabla_{\mathbf{U}_0} W_T &= R_f^m(1-\beta)\mathbf{1}' - \boldsymbol{R}_T \cdot \cdots \cdot \boldsymbol{R}_0\mathbf{1}', \quad k=0 \\
\nabla_{\mathbf{L}_{t_k}} W_T &= -R_f^{m-k}\mathbf{1}' + \boldsymbol{R}_T \cdot \cdots \cdot \boldsymbol{R}_{t_k}\mathbf{1}', \quad 1 \le k \le m-1 \\
\nabla_{\mathbf{U}_{t_k}} W_T &= R_f^{m-k}\mathbf{1}' - \boldsymbol{R}_T \cdot \cdots \cdot \boldsymbol{R}_{t_k}\mathbf{1}', \quad 1 \le k \le m-1.
\end{aligned} \tag{2.45}$$

We include the formula for the risk-free asset dynamics and derivatives used in the BS model:

$$x_T = R_f^m x_0 + \sum_{\tau=0}^{m-1} R_f^{m-\tau}[(1+\beta/m)\mathbf{1}'(\mathbf{U}_{t_\tau} - \mathbf{L}_{t_\tau}) - \beta/m\mathbf{1}'\mathbf{y}_{t_\tau}]. \tag{2.46}$$

The corresponding derivatives of the final wealth are

$$\nabla_a W_T = \nabla_a \left(\sum_{\tau=0}^{m-1} [R_f^{m-\tau}(1+\beta/m) - \boldsymbol{R}_T \cdot \cdots \cdot \boldsymbol{R}_{t_{\tau+1}}]\mathbf{1}'(\mathbf{U}_{t_\tau} - \mathbf{L}_{t_\tau}) - R_f^{m-\tau}\beta/m\mathbf{1}'\mathbf{y}_{t_\tau} \right)$$

namely,

$$\begin{aligned}
\nabla_{\mathbf{L}_{t_k}} W_T &= -R_f^{m-k}(1+\beta/m)\mathbf{1}' + \prod_{i=t_{k+1}}^{m} \boldsymbol{R}_{t_i}\mathbf{1}' - \beta/m \sum_{\tau=0}^{m-1} R_f^{m-\tau} \prod_{i=t_{k+1}}^{t_\tau} \boldsymbol{\alpha}_{t_i}\mathbf{1}', 0 \le k \le m-1 \\
\nabla_{\mathbf{U}_{t_k}} W_T &= R_f^{m-k}(1+\beta/m)\mathbf{1}' - \prod_{i=t_{k+1}}^{m} \boldsymbol{R}_{t_i}\mathbf{1}' + \beta/m \sum_{\tau=0}^{m-1} R_f^{m-\tau} \prod_{i=t_{k+1}}^{t_\tau} \boldsymbol{R}_{t_i}\mathbf{1}', 0 \le k \le m-1.
\end{aligned}$$

2.6 Numerical Results

In this section, we assess the quality of proposed three lower bounds and upper bounds by (i) comparing their solutions to the results of a ten risky asset case in Brown and Smith (2011), (ii) illustrating the solutions of twenty risky asset cases, and (iii) discussing the impact of the borrowing constraint on the no-trading region. All the results are converted to annualized certainty equivalent rates of return (termed CER).[1]

[1] The optimal certainty equivalent rate of return decreases with risk aversion. This is because a more risk averse investor allocates less wealth to risky assets and therefore has a lower expected portfolio return and because even for the same expected portfolio return, a more risk averse investor requires a smaller incentive to abstain from risky instruments. It is a dual impact from the larger risk averse coefficient (see, e.g., Brandt, 2010).

For the CRRA utility and a T year long horizon, the annualized certainty equivalent rate is defined by

$$\mathrm{CER} = \left(\frac{\mathcal{U}^{-1}(\mathbb{E}[\mathcal{U}(W_T)])}{W_{t_0}}\right)^{1/T} - 1 \tag{2.47}$$

as the risk-free rate that makes investors indifferent between holding the optimal portfolio and earning the annual certainty equivalent rate over the next T years.

The results are reported in a 95% confidence interval. All the simulations use the control variate from the Merton's model. Our numerical results show that the utilities obtained by the lower bound strategies or the upper bound methods have a over 90% correlation with those by the Merton's model. Forward simulations start with one unit of wealth in risk-free asset. The duality gap is computed by "$(\mathrm{CER}_{\mathrm{upper}} - \mathrm{CER}_{\mathrm{lower}})/\mathrm{CER}_{\mathrm{lower}}$", where $\mathrm{CER}_{\mathrm{upper}}$ represents the annualized certainty equivalent rate computed for an upper bound and $\mathrm{CER}_{\mathrm{lower}}$ represents for a lower bound. In the following examples, we choose the same transaction costs factor β for all the risky assets; denote CER to represent annualized certainty equivalent rates of portfolio return, CI to represent 95% confidence intervals of annualized certainty equivalent rates, and NT to represent results of the Merton's model with corresponding parameters. The computations are based on the Matlab implementation and the general purpose nonlinear optimization routine in the NAG library.

2.6.1 Model with Ten Risky Assets

In the ten asset case, for the purpose of comparison we take the return model, the approach to compute the numerical expectation, and the parameters from Brown and Smith (2011). Their return model for risky assets is written as $\ln \boldsymbol{R}_{t_k} = \mathbf{a_r} + \mathbf{e}_{t_k}$, where $\mathbf{a_r} = \boldsymbol{\mu} - \frac{1}{2}\boldsymbol{\sigma}^2$ represents a vector of log return means. The data for parameter estimation is at a monthly frequency and span a period from 1981 to 2006. All parameters can be found in Appendix A.7. The monthly net risk-free rate $r_f = 0.48\%$. The expectations in this model are computed by a non-product quadrature rule in Stroud (1971) that includes $2^n + 2n$ points, which exactly matches the first five moments of a normal distribution. This rule is obligated to reduce computational costs in the ten asset case.

Table 2.1 illustrates the lower and upper bounds from both new and old methods. The results of RBH, FL and BS are consistent with those in Brown and Smith (2011). VF, HS and HC consistently outperform RBH. Specifically, when the level of risk aversion is low, $\gamma = -0.5$, or the transaction costs factor is small, $\beta = 0.5\%$, the differences of those strategies are tiny. When the transaction costs factor is larger, the differences tend to be wider. Using the BS method as the upper bound benchmark, when $\gamma = -2$, -7, -13 and $\beta = 2\%$, the new methods about cut the duality gap by a factor of 9. Also, by examining dual bounds, we realize that the FL upper bound method gives looser upper bounds than the BS method, but it is better than that by Merton's model.

To compare the run time for different methods, we normalize the CPU time according to results of HS. RBH typically takes less time than VF, as the associated optimization problem is easier. HS and HC perform comparably and are both on average five times faster than VF and RBH. The dominance is a result of considerable computational saving from replacing step by step multivariate optimization by a one-dimensional brute-force search. We note that if the exact utility function optimization in the last step, both HS and HC work roughly two orders of magnitude faster than RBH. Typically the no-trading region becomes wider when the investment approaches maturity. Given a short rebalance time, e.g. monthly rebalance, in many of our examples we find the optimal solutions in the last period suggests no trades. Thus, we could adopt the approximated HC or HS policy in the last step to accelerate the computing more by sacrificing some utility. On the other hand, upper bounds take longer time to compute, as the yield optimization problems are more difficult when the number of decision variables grows linearly with time periods.

Table 2.1: Results of the ten risky asset model for a 12-month-long horizon.

Parameters				Forward Strategies				Dual Bounds				Best Performance		
m	β	γ		VF	HS	HC	RBH	FL	BS	MG	NT	Strategy	Dual Bound	Gap
12	0.5%	-0.5	CER(%)	13.06	13.05	13.05	13.06	13.36	13.08	13.06	13.62	13.06	13.06	0.0%
			CI(%)	±0.00	±0.00	±0.01	±0.00	±0.01	±0.01	±0.00		VF	MG	
12	1%	-0.5	CER(%)	12.50	12.50	12.50	12.49	13.15	12.55	12.96	13.62	12.50	12.55	0.4%
			CI(%)	±0.00	±0.02	±0.01	±0.01	±0.02	±0.01	±0.03		VF	BS	
12	2%	-0.5	CER(%)	11.39	11.39	11.39	11.39	12.82	11.47	12.96	13.62	11.39	11.47	0.7%
			CI(%)	±0.01	±0.01	±0.01	±0.01	±0.04	±0.01	±0.03		VF	BS	
12	0.5%	-2	CER(%)	11.36	11.35	11.35	11.36	11.71	11.38	11.45	11.91	11.36	11.38	0.2%
			CI(%)	±0.01	±0.01	±0.01	±0.01	±0.02	±0.00	±0.02		VF	BS	
12	1%	-2	CER(%)	10.80	10.80	10.81	10.79	11.53	10.84	11.41	11.91	10.81	10.84	0.3%
			CI(%)	±0.01	±0.01	±0.01	±0.02	±0.02	±0.01	±0.02		HC	BS	
12	2%	-2	CER(%)	9.71	9.71	9.72	9.22	11.19	9.79	11.40	11.91	9.72	9.79	0.7%
			CI(%)	±0.02	±0.01	±0.01	±0.01	±0.03	±0.01	±0.02		HC	BS	
12	0.5%	-7	CER(%)	9.18	9.18	9.19	9.17	9.60	9.20	9.43	9.74	9.19	9.20	0.1%
			CI(%)	±0.02	±0.01	±0.01	±0.03	±0.01	±0.01	±0.01		HC	BS	
12	1%	-7	CER(%)	8.64	8.65	8.65	8.52	9.47	8.68	9.42	9.74	8.65	8.68	0.3%
			CI(%)	±0.02	±0.01	±0.01	±0.02	±0.01	±0.01	±0.01		HS	BS	
12	2%	-7	CER(%)	7.63	7.64	7.65	7.18	9.24	7.71	9.41	9.74	7.65	7.71	0.8%
			CI(%)	±0.03	±0.02	±0.02	±0.02	±0.02	±0.03	±0.01		HC	BS	
12	0.5%	-13	CER(%)	7.89	7.88	7.88	7.85	8.33	7.90	8.23	8.43	7.89	7.90	0.1%
			CI(%)	±0.02	±0.01	±0.01	±0.03	±0.01	±0.01	±0.01		VF	BS	
12	1%	-13	CER(%)	7.46	7.48	7.48	7.41	8.23	7.52	8.22	8.43	7.48	7.52	0.5%
			CI(%)	±0.02	±0.02	±0.01	±0.04	±0.01	±0.02	±0.01		HC	BS	
12	2%	-13	CER(%)	6.89	6.90	6.91	6.64	8.05	6.97	8.21	8.43	6.91	6.97	0.9%
			CI(%)	±0.03	±0.02	±0.02	±0.04	±0.02	±0.03	±0.01		HC	BS	
Average CPU Time				10.3	1.0	0.8	5.3	19.7	20.3	19.5				

Note: Lower bounds by VF and RBH are computed over 2^{12} trials and those of HS and HC are over 2^{14} trials, respectively; dual bounds are computed over 2^{11} trials. When $\gamma = -0.5$, we use fifth order principal polynomials. When $\gamma = -2$, -7 and -13, we use polynomials with cross terms up to the second order and add third order polynomials without cross terms.

2.6.2 Model with Twenty Risky Assets

In the twenty asset case, we assume annual adjustment of the portfolio and give two examples of twenty stocks and two examples of twenty ETFs in a 10-year-long and a 40-year-long horizon, respectively.

We estimate the return parameter $\boldsymbol{\mu}$ for individual stocks by the Fama-French three factor model and compute market implied returns used as the return parameter $\boldsymbol{\mu}$ for ETFs (see, e.g., Merton, 1980; Broadie, 1993). While using an appropriate factor model could improve the estimation accuracy of high-dimensional covariance matrices (see, e.g., Fan et al., 2008), in our examples we use the sample covariance matrices without imposing any models for simplicity. In particular, we choose the monthly data from 2001 to 2011 of twenty stocks among the top fifty selected stocks by hedge funds according to the Goldman Sachs VIP list, and the monthly data from 2009 to 2011 of the twenty ETFs that widely spread across different asset classes for testing. See Appendix A.8 for parameter details. The annual net risk-free rate $r_f = 0.00\%$. On the other hand, we use the results calculated by Monte Carlo simulation as a benchmark and compare the results of expected CRRA utility computed by non-product quadrature rules in Stroud (1971) with those by Sobol low-discrepancy sequences. Due to the nonlinearity of the CRRA utility function, our numerical examination indicates that the accuracy of the non-product quadrature rules deteriorates when risk aversion is large; and Sobol low-discrepancy sequences produce higher approximation accuracy than the non-product quadrature rules. Thus, the expectations are computed numerically by the Sobol low-discrepancy sequences.

In general, the new lower bounds strategies consistently outperform RBH; meanwhile MG outperforms BS in all the examples. In Table 2.2, in the example of a small risk aversion coefficient and a large transaction costs factor, $\gamma = -0.5$ and $\beta = 2\%$, the duality gap calculated from VF and MG is about 1.8%; whereas it is about 4.6% when we use RBH and BS. The gap has been cut by a factor of 2.5. In the example of a medium level risk aversion and a large transaction costs factor, $\gamma = -2$ and $\beta = 2\%$, combining VF and MG generates a duality gap of 2.8%; whereas combining RBH and BS gives a duality gap of 8.2%. The gap has been cut by a factor of 3.0. In Table 2.3, we evaluate those methods across more parameter sets. When $\gamma = -2$ and $\beta = 2\%$, the duality gap from combining

HS and MG is about 9.5%; whereas that from combining RBH and BS is about 14.5%. The gap has been cut by a factor of 1.5. When $\gamma = -7$ and $\beta = 2\%$, the duality gap from combining HC and MG is about 2.1%; whereas that from combing RBH and BS is about 6.9%. The gap has been cut by a factor of 3.3. From Tables 2.2 and 2.3, we find that the high level risk aversion and high transaction costs examples are most difficult, the VF method still provides the best results, and the HS and the HC methods work better in the ETF examples.

On the other hand, duality gaps calculated from the long term investment are larger than those from the short term investment in general. In Tables 2.4 and 2.5, we compute the results for a 40-year-long horizon with the same set of parameters used for Tables 2.2 and 2.3. The new forward strategies still consistently outperform RBH; meanwhile MG outperforms BS in all the cases. Both tables show when $\gamma = -0.5$, -2, -7 and $\beta = 2\%$, the new methods about cut the duality gap by a factor of 2.5.

The superior new lower bound results come from the fact that HS and HC account for the effect from transaction costs in each period, whereas RBH only considers the effect in the current period. For various examples in Tables 2.4 and 2.5, BS even gives looser upper bounds than those from Merton. The crux is that choosing the number of rebalance times as the transaction costs factor divisor to incorporate impacts from transaction costs may not generate the model close to the original one. In particular, in the post-trade model, increasing the divisor to infinity results in the Merton's portfolio, while deceasing it to zero leads to the full investment in the risk-free asset. By choosing the rebalance times as the divisor, we essentially select a modified model with an optimal solution somewhere between the aforementioned two extreme portfolios. If this optimal solution is close to the true optimal solution, we would expect a tight upper bound. Otherwise, the chosen model may yield worse results than those by the frictionless model. One possible improvement is tuning the divisor. In Table 2.6, we illustrate the idea of how tuning the transaction costs factor divisor improves the performance of BS. In upper panel, we see a decrease in the upper bounds when we increase the size of the divisor. For example, when $\beta = 1\%$, the best upper bound given by the BS method has improved from 1.23 to 1.19, which is the same as the result from the MG method; when $\beta = 0.5\%$ and $\beta = 2\%$, the best upper bounds given by

BS have improved from 1.21 to 1.20, from 1.26 to 1.19, respectively, which are still slightly worse than those by MG. In lower panel, we see an increase in upper bounds following a trend of decrease while continuously increasing the size of the divisor. For example, when $\beta = 2\%$, the result by the BS method decreases from 3.04 to 3.01 and then increases from 3.01 to 3.03. The best result 3.01 is still worse than that by MG, 2.94. This study shows the possibility of the improvement, the trend of the improvement, and the extent of the improvement, via tuning the transaction costs factor divisor for BS.

In previous examples, MG gives tighter bounds than BS. The MG model is similar to the frictionless model and in addition captures the most significant impact from the transaction costs. To justify this, in Table 2.7, we illustrate the results from five different initial positions. Except for the last example where the initial position is the optimal portfolio of the frictionless model, MG still works better than BS. We note the difference in the last example is small. The trading volume has been dramatically reduced, as the Merton's solution lies inside the no-trading region thus suggesting no trade.

Table 2.2: Results of the twenty stock model for a 10-year-long horizon.

Parameters				Forward Strategies				Dual Bounds				Best Performance		
m	β	γ		VF	HS	HC	RBH	FL	BS	MG	NT	Strategy	Dual Bound	Gap
10	0.5%	-0.5	CER(%)	4.49	4.49	4.48	4.48	4.58	4.54	4.53	4.59	4.49	4.53	0.9%
			CI(%)	±0.03	±0.02	±0.02	±0.01	±0.00	±0.01	±0.00		VF	MG	
10	1%	-0.5	CER(%)	4.42	4.42	4.42	4.40	4.57	4.49	4.48	4.59	4.42	4.48	1.4%
			CI(%)	±0.02	±0.01	±0.02	±0.01	±0.00	±0.01	±0.00		VF	MG	
10	2%	-0.5	CER(%)	4.30	4.29	4.30	4.27	4.55	4.47	4.38	4.59	4.30	4.38	1.8%
			CI(%)	±0.02	±0.02	±0.03	±0.02	±0.01	±0.01	±0.00		VF	MG	
10	0.5%	-2	CER(%)	3.05	3.05	3.03	3.02	3.13	3.11	3.10	3.15	3.05	3.10	1.6%
			CI(%)	±0.02	±0.01	±0.01	±0.01	±0.00	±0.02	±0.00		HS	MG	
10	1%	-2	CER(%)	2.99	2.98	2.98	2.94	3.12	3.08	3.05	3.15	2.99	3.05	2.0%
			CI(%)	±0.01	±0.01	±0.01	±0.02	±0.01	±0.01	±0.01		VF	MG	
10	2%	-2	CER(%)	2.86	2.85	2.83	2.81	3.10	3.04	2.94	3.15	2.86	2.94	2.8%
			CI(%)	±0.02	±0.01	±0.01	±0.02	±0.00	±0.01	±0.01		VF	MG	
10	0.5%	-7	CER(%)	1.16	1.14	1.15	1.14	1.19	1.19	1.17	1.20	1.16	1.17	0.8%
			CI(%)	±0.01	±0.01	±0.01	±0.01	±0.00	±0.01	±0.01		VF	MG	
10	1%	-7	CER(%)	1.13	1.10	1.12	1.11	1.19	1.19	1.15	1.20	1.13	1.15	1.7%
			CI(%)	±0.01	±0.01	±0.01	±0.01	±0.01	±0.01	±0.00		VF	MG	
10	2%	-7	CER(%)	1.07	1.04	1.06	1.04	1.18	1.18	1.12	1.20	1.07	1.12	4.7%
			CI(%)	±0.01	±0.01	±0.01	±0.01	±0.01	±0.01	±0.01		VF	MG	
			Average CPU Time	19.4	1.0	1.1	8.5	1.1	8.3	8.5				

Note: Lower bounds by the VF method are computed over 2^{11} trials and those of HS and HC are computed over 2^{12} trials; dual bounds are computed over 2^{8} trials for FL, and 2^{10} for BS and MG, respectively. We use the fifth order principal polynomial as basis functions.

Table 2.3: Results of the twenty ETF model for a 10-year-long horizon.

Parameters				Forward Strategies				Dual Bounds				Best Performance		
m	β	γ		VF	HS	HC	RBH	FL	BS	MG	NT	Strategy	Dual Bound	Gap
10	0.5%	-0.5	CER(%)	1.90	1.91	1.89	1.90	1.97	1.95	1.95	1.99	1.91	1.95	2.1%
			CI(%)	±0.02	±0.01	±0.02	±0.01	±0.00	±0.01	±0.00		HS	MG	
10	1%	-0.5	CER(%)	1.84	1.85	1.84	1.85	1.96	1.92	1.92	1.99	1.85	1.92	3.8%
			CI(%)	±0.03	±0.02	±0.02	±0.01	±0.01	±0.01	±0.01		HS	MG	
10	2%	-0.5	CER(%)	1.73	1.75	1.75	1.75	1.94	1.87	1.86	1.99	1.75	1.86	6.3%
			CI(%)	±0.03	±0.03	±0.03	±0.01	±0.01	±0.01	±0.01		HS	MG	
10	0.5%	-2	CER(%)	0.93	0.93	0.92	0.93	0.98	0.97	0.96	0.99	0.93	0.96	3.2%
			CI(%)	±0.01	±0.02	±0.01	±0.02	±0.00	±0.01	±0.01		HS	MG	
10	1%	-2	CER(%)	0.88	0.90	0.89	0.89	0.97	0.96	0.95	0.99	0.90	0.95	5.6%
			CI(%)	±0.02	±0.01	±0.02	±0.01	±0.00	±0.01	±0.00		HS	MG	
10	2%	-2	CER(%)	0.81	0.84	0.84	0.83	0.95	0.95	0.92	0.99	0.84	0.92	9.5%
			CI(%)	±0.03	±0.02	±0.03	±0.01	±0.01	±0.01	±0.01		HS	MG	
10	0.5%	-7	CER(%)	0.34	0.34	0.34	0.34	0.36	0.37	0.36	0.37	0.34	0.36	5.8%
			CI(%)	±0.01	±0.01	±0.01	±0.00	±0.00	±0.00	±0.00		HS	MG	
10	1%	-7	CER(%)	0.32	0.33	0.32	0.33	0.36	0.37	0.35	0.37	0.33	0.35	6.0%
			CI(%)	±0.01	±0.01	±0.01	±0.01	±0.00	±0.00	±0.01		HS	MG	
10	2%	-7	CER(%)	0.30	0.30	0.31	0.30	0.35	0.36	0.34	0.37	0.31	0.34	9.6%
			CI(%)	±0.01	±0.01	±0.01	±0.01	±0.01	±0.00	±0.01		HC	MG	
			Average CPU Time	14.3	1.0	1.1	10.3	1.1	7.0	8.5				

Note: Lower bounds by VF are computed over 2^{11} trials; those of HS, HC and RBH are computed over 2^{12} trials; dual bounds are computed over 2^8 trials for FL, 2^{10} for BS and MG, respectively. We use the fifth order principal polynomial as basis functions.

Table 2.4: Results of the twenty stock model for a 40-year-long horizon.

Parameters				Forward Strategies			Dual Bounds				Best Performance		
m	β	γ		HS	HC	RBH	FL	BS	MG	NT	Strategy	Dual Bound	Gap
40	0.5%	-0.5	CER(%)	4.52	4.51	4.51	4.58	4.59	4.57	4.59	4.52	4.57	1.1%
			CI(%)	±0.01	±0.01	±0.00	±0.00	±0.00	±0.00		HS	MG	
40	1%	-0.5	CER(%)	4.48	4.46	4.45	4.58	4.59	4.56	4.59	4.48	4.56	1.8%
			CI(%)	±0.01	±0.00	±0.00	±0.00	±0.00	±0.00		HS	MG	
40	2%	-0.5	CER(%)	4.42	4.39	4.37	4.58	4.59	4.53	4.59	4.42	4.53	2.5%
			CI(%)	±0.01	±0.00	±0.00	±0.00	±0.00	±0.00		HS	MG	
40	0.5%	-2	CER(%)	3.06	3.08	3.04	3.14	3.15	3.13	3.15	3.08	3.13	1.6%
			CI(%)	±0.02	±0.02	±0.02	±0.00	±0.00	±0.00		HC	MG	
40	1%	-2	CER(%)	3.02	3.03	2.98	3.14	3.15	3.12	3.15	3.03	3.12	2.9%
			CI(%)	±0.02	±0.03	±0.02	±0.00	±0.00	±0.00		HC	MG	
40	2%	-2	CER(%)	2.98	2.97	2.91	3.14	3.17	3.09	3.15	2.98	3.09	3.7%
			CI(%)	±0.02	±0.02	±0.01	±0.00	±0.00	±0.02		HS	MG	
40	0.5%	-7	CER(%)	1.15	1.17	1.15	1.20	1.21	1.19	1.20	1.17	1.19	1.7%
			CI(%)	±0.03	±0.03	±0.02	±0.00	±0.00	±0.00		HC	MG	
40	1%	-7	CER(%)	1.12	1.15	1.12	1.20	1.23	1.19	1.20	1.15	1.19	3.5%
			CI(%)	±0.03	±0.03	±0.02	±0.00	±0.00	±0.00		HC	MG	
40	2%	-7	CER(%)	1.09	1.12	1.07	1.19	1.26	1.18	1.20	1.12	1.18	5.3%
			CI(%)	±0.04	±0.03	±0.02	±0.00	±0.03	±0.01		HC	MG	
Average CPU Time				1.0	0.8	2.6	1.7	4.2	5.0				

Note: Lower bound for RBH are computed over 2^{11} trials; those of HS and HC are computed over 2^{12} trials; dual bounds are computed over 2^8 trials. We use the fifth order principal polynomial as basis functions.

Table 2.5: Results of the twenty ETF model for a 40-year-long horizon.

Parameters				Forward Strategies			Dual Bounds				Best Performance		
m	β	γ		HS	HC	RBH	FL	BS	MG	NT	Strategy	Dual Bound	Gap
40	0.5%	-0.5	CER(%)	1.93	1.93	1.86	1.98	1.99	1.98	1.99	1.93	1.98	2.6%
			CI(%)	±0.01	±0.02	±0.02	±0.01	±0.00	±0.01		HC	MG	
40	1%	-0.5	CER(%)	1.90	1.89	1.83	1.98	1.99	1.97	1.99	1.90	1.97	3.7%
			CI(%)	±0.01	±0.01	±0.02	±0.01	±0.01	±0.00		HS	MG	
40	2%	-0.5	CER(%)	1.84	1.81	1.79	1.97	1.99	1.96	1.99	1.84	1.96	6.5%
			CI(%)	±0.02	±0.02	±0.02	±0.02	±0.01	±0.00		HS	MG	
40	0.5%	-2	CER(%)	0.92	0.95	0.91	0.98	0.99	0.98	0.99	0.95	0.98	3.2%
			CI(%)	±0.02	±0.02	±0.02	±0.00	±0.01	±0.00		HC	MG	
40	1%	-2	CER(%)	0.91	0.93	0.86	0.98	0.99	0.98	0.99	0.93	0.98	5.3%
			CI(%)	±0.02	±0.02	±0.01	±0.01	±0.01	±0.01		HC	MG	
40	2%	-2	CER(%)	0.86	0.89	0.83	0.97	1.01	0.97	0.99	0.89	0.97	8.9%
			CI(%)	±0.02	±0.03	±0.03	±0.01	±0.02	±0.00		HC	MG	
40	0.5%	-7	CER(%)	0.34	0.35	0.33	0.36	0.37	0.36	0.37	0.35	0.36	2.8%
			CI(%)	±0.01	±0.01	±0.01	±0.00	±0.00	±0.01		HC	MG	
40	1%	-7	CER(%)	0.33	0.34	0.32	0.36	0.38	0.36	0.37	0.34	0.36	5.8%
			CI(%)	±0.01	±0.01	±0.01	±0.00	±0.01	±0.01		HC	MG	
40	2%	-7	CER(%)	0.32	0.32	0.30	0.36	0.40	0.36	0.37	0.32	0.36	12.5%
			CI(%)	±0.01	±0.02	±0.01	±0.00	±0.01	±0.00		HC	MG	
Average CPU Time				1.0	1.1	3.6	2.9	4.8	6.0				

Note: Lower bounds by RBH are computed over 2^{11} trials; those of HS and HC are computed over 2^{12} trials; dual bounds are computed over 2^8 trials. We use the fifth order principal polynomial as basis functions.

Table 2.6: Results for the change of divisor in the BS method for a 40-year-long investment horizon example and a 10-year-long investment horizon example.

Parameters				Dual Bound	BS Dual Bound Divisor							
m	β	γ		MG	30	40	60	80	100	120	140	160
40	0.5%	-7	CER(%)	1.19	1.23	1.21	1.20	1.20	1.20	1.20	1.20	1.20
			CI(%)	±0.00	±0.00	±0.00	±0.01	±0.00	±0.00	±0.00	±0.00	±0.00
40	1%	-7	CER(%)	1.19	1.26	1.23	1.21	1.20	1.20	1.20	1.19	1.19
			CI(%)	±0.00	±0.00	±0.00	±0.00	±0.00	±0.00	±0.01	±0.01	±0.00
40	2%	-7	CER(%)	1.18	1.34	1.26	1.23	1.21	1.20	1.19	1.19	1.19
			CI(%)	±0.00	±0.02	±0.00	±0.01	±0.00	±0.00	±0.01	±0.00	±0.00
Parameters				Dual Bound	BS Dual Bound Divisor							
m	β	γ		MG	5	10	15	20				
10	0.5%	-2	CER(%)	3.10	3.13	3.11	3.11	3.11				
			CI(%)	±0.00	±0.01	±0.02	±0.00	±0.01				
10	1%	-2	CER(%)	3.05	3.12	3.08	3.08	3.09				
			CI(%)	±0.01	±0.01	±0.01	±0.00	±0.01				
10	2%	-2	CER(%)	2.94	3.11	3.04	3.01	3.03				
			CI(%)	±0.01	±0.02	±0.01	±0.01	±0.01				

Note: We use the same parameters for the return dynamics as Table 2.4 and Table 2.2 respectively for the above two examples. The results of the BS dual bound method are computed over 2^8 trials.

2.6.3 Impact From Borrowing Constraint

The borrowing constraint is usually imposed on the portfolio model with transaction costs to prohibit a negative risk-free asset position. However, its influence cannot be completely revealed until the no-trading region touches the borrowing constraint boundary. To visualize the impact on the no-trading region from the borrowing constraint, we demonstrate this phenomenon by the no-trading region of two risky asset examples with uncorrelated returns and numerical examples of twenty risky assets.

Table 2.7: Results for the change of initial position for a 10-year-long horizon.

Parameters					Forward Strategies			Dual Bounds			
m	β	γ	$\mathbf{x}_0$		HS	HC	RBH	FL	BS	MG	NT
10	2%	-2	$\mathbf{x}_{0,1}$	CER(%)	2.84	2.85	2.81	3.10	3.04	2.94	3.15
				CI(%)	±0.03	±0.03	±0.02	±0.00	±0.01	±0.01	
10	2%	-2	$\mathbf{x}_{0,2}$	CER(%)	2.77	2.80	2.74	3.11	3.11	2.98	3.15
				CI(%)	±0.02	±0.03	±0.02	±0.01	±0.01	±0.01	
10	2%	-2	$\mathbf{x}_{0,3}$	CER(%)	2.73	2.75	2.70	3.11	3.11	2.96	3.15
				CI(%)	±0.02	±0.02	±0.02	±0.00	±0.01	±0.01	
10	2%	-2	$\mathbf{x}_{0,4}$	CER(%)	2.71	2.72	2.66	3.10	3.09	2.91	3.15
				CI(%)	±0.02	±0.03	±0.02	±0.00	±0.01	±0.01	
10	2%	-2	$\mathbf{x}_{0,5}$	CER(%)	3.06	3.07	3.01	3.13	3.13	3.14	3.15
				CI(%)	±0.02	±0.02	±0.02	±0.01	±0.01	±0.00	

Note: We use the same parameters for the return dynamics as Table 2.2. The five different initial positions are $\mathbf{x}_{0,1} = (1, 0, ..., 0)$, $\mathbf{x}_{0,2} = (0, 1/20, 1/20, ..., 1/20)$, $\mathbf{x}_{0,3} = (0, 0, 1/10, 0, 1/10, ..., 0, 1/10)$, $\mathbf{x}_{0,4} = (0, 0, 0, 0, 1/5, 0, 0, 0, 1/5, ..., 0, 0, 0, 1/5)$, $\mathbf{x}_{0,5} = \mathbf{x}_{0,0}$, where $\mathbf{x}_{0,0}$ represents the optimal solution from the Merton's model. All the simulations are based on the same trials as previous examples.

In Figure 2.2, we illustrate the no-trading region and the optimal trades of a two risky asset problem. The optimal trades bring the initial portfolio positions to the boundary of the no-trading region. There are nine regions split by the no-trading region. The north and east boundaries are selling boundaries. Investors need to sell risky assets to reach them from the outside. Meanwhile the south and west boundaries are buying boundaries. Investors need to purchase risky assets to reach the no-trading region from the outside. This is the generalization of the one risky asset result, which has been studied (see, e.g., Muthuraman and Kumar, 2006; Lynch and Tan, 2010; Dai and Zhong, 2010).

In Figure 2.3, we illustrate the change of the no-trading region of risky assets by tuning parameters. As the arrow shows, for example, the lower risk-free rate is, the more investors tend to invest in the risky assets. However, the borrowing constraint prohibits investors

Figure 2.2: Illustration of the shape of no-trading region in the uncorrelated two risky asset case and the corresponding optimal trades.

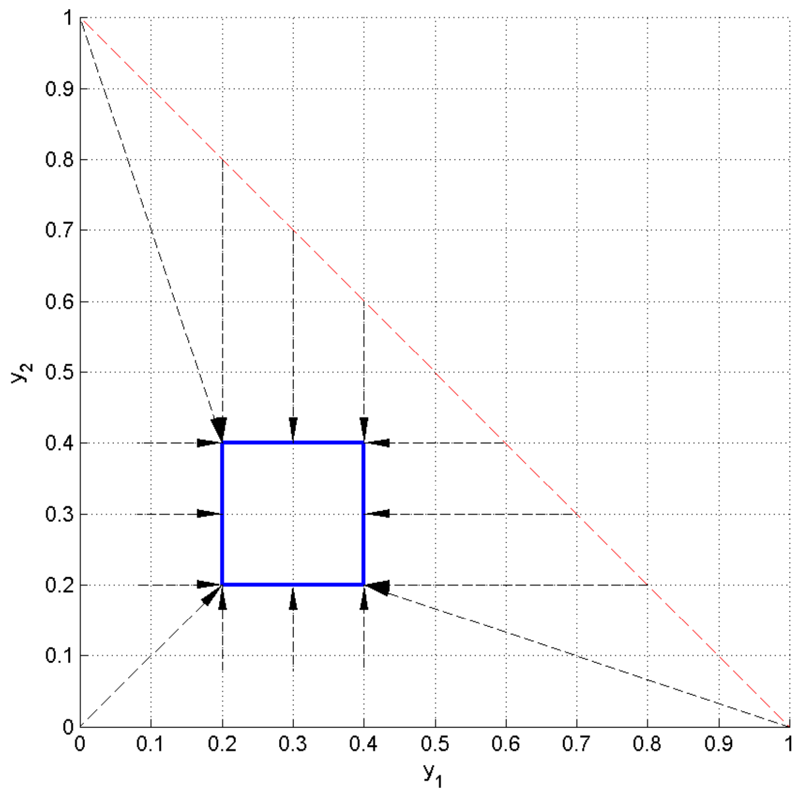

Note: y_1 and y_2 represent risky asset one and two, respectively. The red dash line represents the borrowing constraint where the portfolio only invests in risky assets and has zero cash. The region surrounded by solid blue line represents the no-trading region. The arrows represent the optimal trade from initial portfolio positions to the rebalanced positions.

from leveraging positions, which renders the distortion of the no-trading region. When the no-trading region touches the borrowing constraint boundary, it cannot drift further to northeast. The whole region tends to collapse on the borrowing constraint boundary as the arrow shows in the figure. Particularly, the selling boundary will only be cut off by the borrowing constraint boundary, while the purchasing boundary will however extend along it. This change of the no-trading region, from a normal rectangle to a non-convex "tent", has not been studied in other papers. We will discuss three relevant cases below.

Figure 2.3: Illustration of the change of no-trading region.

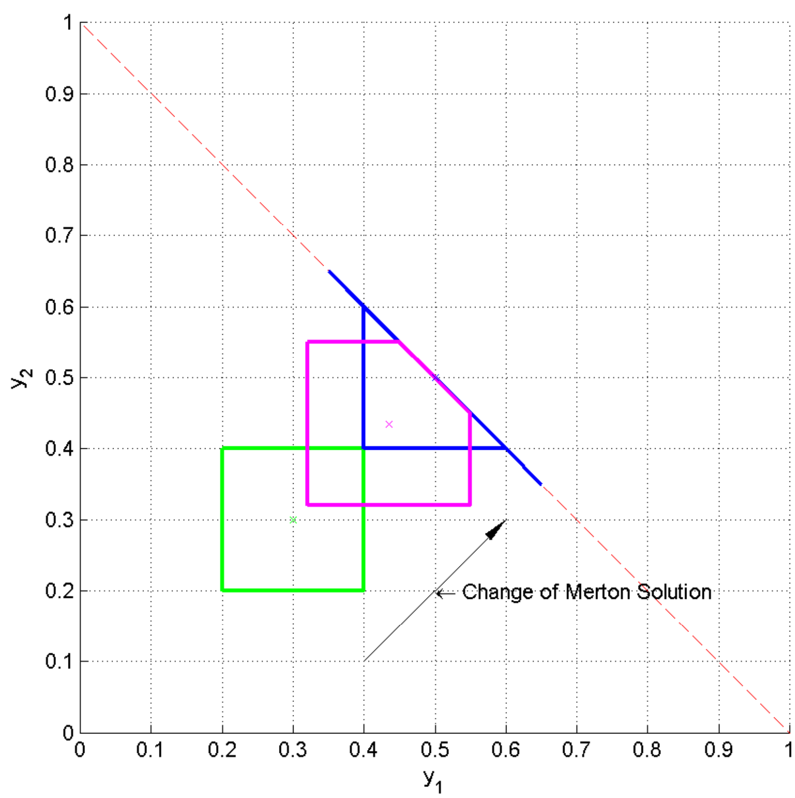

Note: y_1 and y_2 represent risky asset one and two, respectively. The red dash line represents the borrowing constraint where the portfolio only invests in risky assets and has zero cash. The region surrounded by blue line represents the no trading region. The arrow directs the drift of the no-trading region when some parameters are changed, e.g., a reduction of the volatilities, a reduction of the risk-free rate or an increase of the risk averse coefficient.

In Figures 2.4 and 2.5, we illustrate the optimal trades in the cases that the selling and buying boundaries of the no-trading region have been cut off due to the borrowing constraint, respectively. Different types of boundaries of the no-trading region touch the borrowing boundary causes different types of distortion. As shown in Figure 2.4, when the selling boundaries reach the borrowing constraint boundary, the trades could still be implemented without borrowing since the recommended trades are to sell more risky assets; whereas as shown in Figure 2.5, if the buying boundaries reach the borrowing constraint boundary and the recommended trades are to buy more risky assets, the trades need to be financed by the risk-free asset account. Once investors are "cash-strapped" and no borrowing is allowed, the no-trading region has to be enlarged along the borrowing constraint boundary to reduce costs.

In addition, if the return rate of different risky assets is different, the no-trading region turns out to form a rectangle. In this case, if the borrowing constraint is binding, it is possible that one buying boundary and one selling boundary are reaching the constraint boundary simultaneously. We plot the optimal trades and no-trading region of this case in Figure 2.6 that shows its deformation.

In general multiple risky asset case, investors in principle cannot easily recognize the deformation of the no-trading region. However, if the optimal portfolio from the relevant Merton's model suggests retaining no wealth in the risk-free asset, the no-trading region is similar to that in Figure 2.5 or 2.4. Therefore, we can conclude that the no-trading region indeed touches the borrowing constraint boundary.

Table 2.8 shows the results from the case of triggering the borrowing constraint. In the first three examples parameters are chosen to guarantee the relevant no-trading region is indeed a hyper-cube. Accordingly, HS and HC perform even slightly better than VF. For example, when $\gamma = -7$, $\beta = 2\%$, they are 2 basis points higher in CER than VF; when $\gamma = -7$, $\beta = 5\%$, they are 4 basis points higher in CER than VF. In the next six examples parameters are chosen to make the no-trading region distort. Therefore, HS and HC work worse than VF but they are still better than RBH. For example, when $\gamma = -2$, $\beta = 1\%$, HS and HC are 2 basis points higher in CER than RBH.

Figure 2.4: Illustration of the optimal trades when the selling boundaries reach the borrowing constraint.

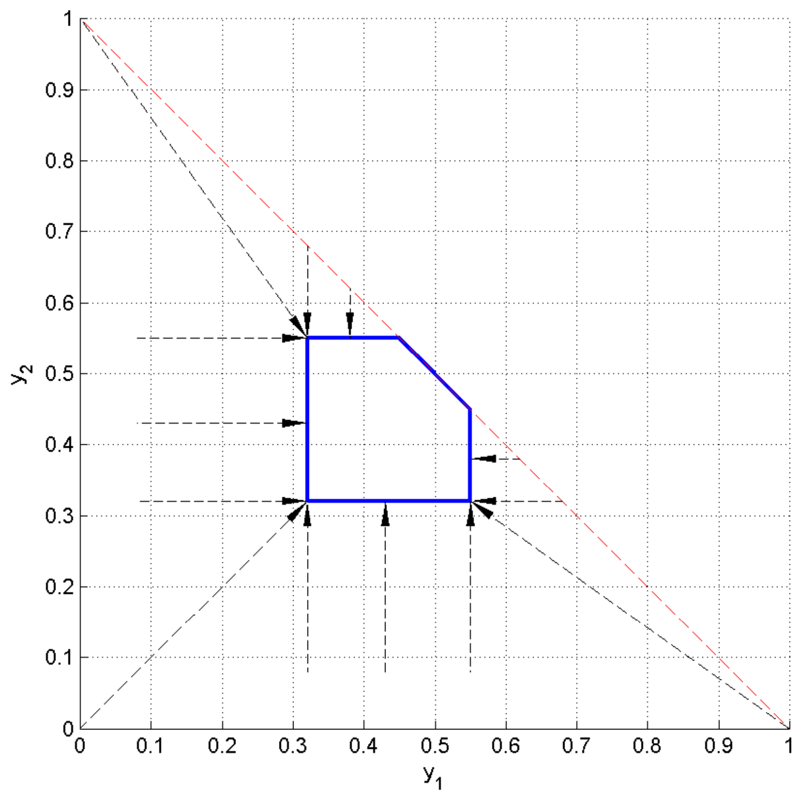

Note: y_1 and y_2 represent risky asset one and two, respectively. The red dash line represents the borrowing constraint where the portfolio only invests in risky assets and has zero cash. The region surrounded by blue line represents the no-trading region.

Figure 2.5: Illustration of the optimal trades when the purchasing boundaries reach the borrowing constraint.

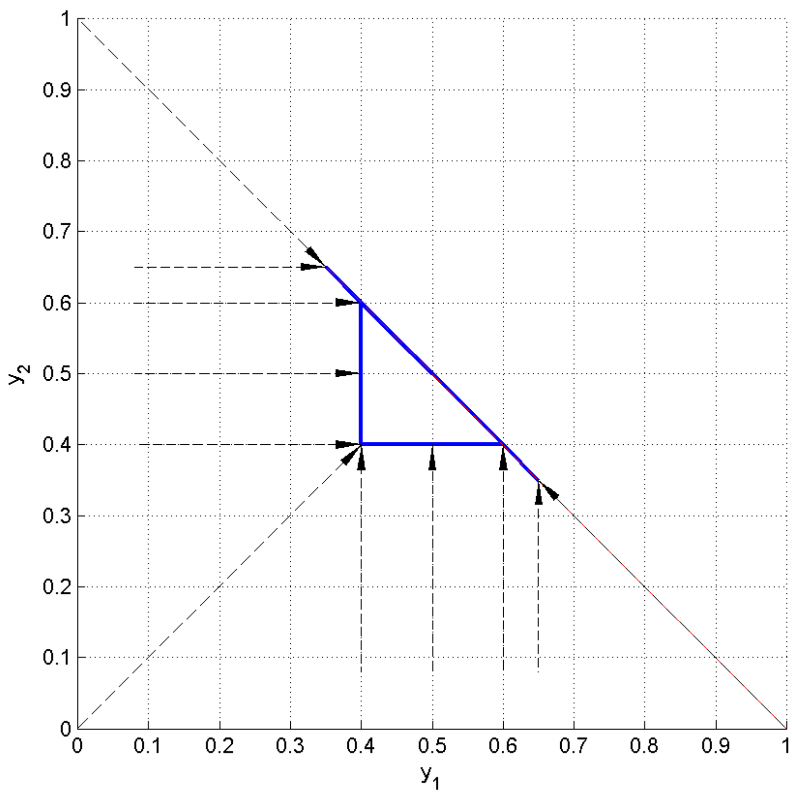

Note: y_1 and y_2 represent risky asset one and two, respectively. The red dash line represents the borrowing constraint where the portfolio only invests in risky assets and has zero cash. The region surrounded by blue line represents the no-trading region.

Figure 2.6: Illustration of the optimal trades when one selling boundary and one buying boundary reaches the borrowing constraint.

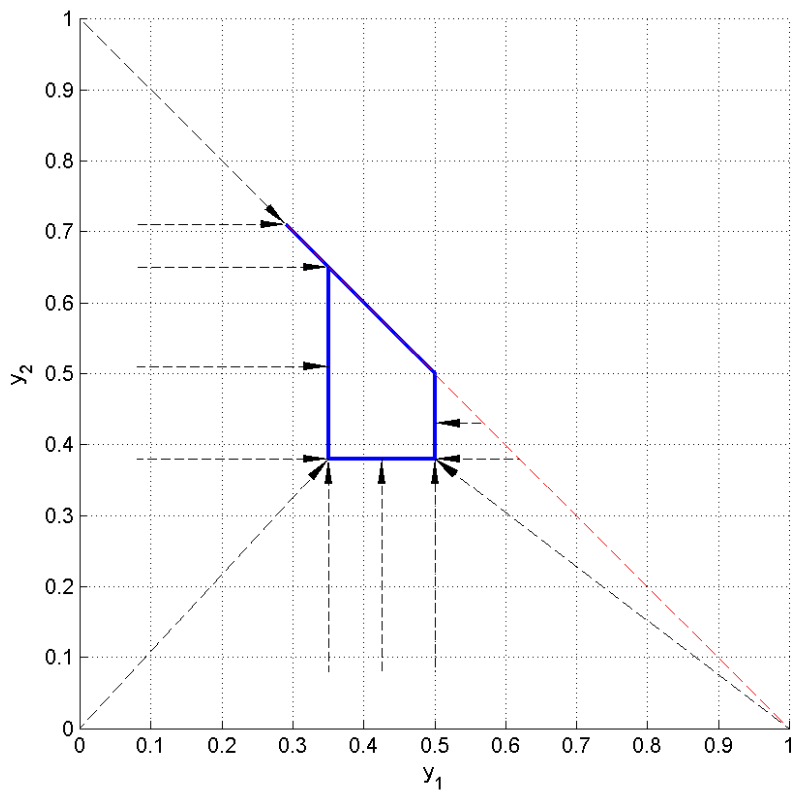

Note: y_1 and y_2 represent risky asset one and two, respectively. The red dash line represents the borrowing constraint where the portfolio only invests in risky assets and has zero cash. The region surrounded by blue line represents the no-trading region.

Table 2.8: Results of the twenty risky assets model in three different cases.

Parameters				Forward Strategies				Dual Bounds				Best Performance		
m	β	γ		VF	HS	HC	RBH	FL	BS	MG	NT	Strategy	Dual Bound	Gap
5	1%	-7	CER(%)	8.27	8.26	8.27	8.22	8.49	8.47	8.37	8.49	8.27	8.37	1.2%
			CI(%)	±0.01	±0.00	±0.01	±0.01	±0.00	±0.01	±0.01		HC	MG	
5	2%	-7	CER(%)	8.10	8.10	8.12	8.06	8.47	8.45	8.30	8.49	8.12	8.30	2.2%
			CI(%)	±0.01	±0.01	±0.01	±0.01	±0.01	±0.01	±0.01		HC	MG	
5	5%	-7	CER(%)	7.74	7.76	7.78	7.73	8.42	8.54	8.24	8.49	7.78	8.24	5.9%
			CI(%)	±0.01	±0.01	±0.01	±0.01	±0.01	±0.02	±0.01		HC	MG	
5	1%	-2	CER(%)	14.27	14.25	14.21	14.16	14.66	14.57	14.44	14.68	14.27	14.44	1.2%
			CI(%)	±0.05	±0.01	±0.02	±0.03	±0.00	±0.01	±0.00		VF	MG	
5	2%	-2	CER(%)	13.91	13.86	13.91	13.75	14.64	14.49	14.22	14.68	13.91	14.22	2.2%
			CI(%)	±0.04	±0.01	±0.01	±0.04	±0.01	±0.01	±0.00		HC	MG	
5	5%	-2	CER(%)	13.16	13.15	13.12	12.82	14.60	14.22	13.56	14.68	13.16	13.56	3.0%
			CI(%)	±0.10	±0.04	±0.05	±0.05	±0.00	±0.02	±0.00		VF	MG	
10	1%	-2	CER(%)	14.36	14.26	14.32	14.26	14.64	14.66	14.56	14.67	14.36	14.56	1.4%
			CI(%)	±0.02	±0.02	±0.02	±0.01	±0.01	±0.00	±0.00		VF	MG	
10	2%	-2	CER(%)	14.10	13.93	13.91	13.87	14.64	14.65	14.44	14.67	14.10	14.44	2.4%
			CI(%)	±0.05	±0.01	±0.01	±0.02	±0.01	±0.01	±0.00		VF	MG	
10	5%	-2	CER(%)	13.55	13.31	13.47	13.16	14.65	14.56	14.11	14.67	13.55	14.11	4.1%
			CI(%)	±0.06	±0.05	±0.05	±0.02	±0.00	±0.01	±0.00		VF	MG	

Note: In the first case, $\gamma = -7$, $r_f = 7\%$, $\mu_i = 11\%$ and $\sigma_i = 40\%$ and all the assets are uncorrelated.

In the second and third cases, $\gamma = -2$, $r_f = 7\%$, $\mu_i = 15\%$ and $\sigma_i = 40\%$ and all the assets are uncorrelated.

The parameters are taken from examples in Muthuraman and Kumar (2006). The difference between the second and the third case is that the third case uses a ten year long time horizon. The results of VF and RBH are computed over 2^{12} trials; those of HS and HC are computed over 2^{14} trials; dual bounds are over 2^{10} trials.

2.7 Concluding Remarks

In this work, we have provided three lower bound and one upper bound strategies for the dynamic portfolio optimization problem in the presence of transaction costs in high dimensions. The first and second lower bound strategies (HS and HC) parameterize the no-trading region by simple geometries. The third lower bound strategy (VF) uses accurately approximated value functions from an approximate dynamic programming algorithm. In order to evaluate the lower bounds, we propose a modification of the gradient-based dual method (MG) to compute upper bounds. We test them across various input parameters and compare their results with those from old methods in Brown and Smith (2011).

We are able to solve the problems up to the size of 20 risky assets and a 40-year-long horizon. Compared with the old methods, the three novel lower bound methods can achieve higher utilities, HS and HC are about one order of magnitude faster, and the upper bounds from MG are tighter in various examples. The new duality gap is ten times narrower than the old one in the best case.

Campbell et al. (2001) emphasized that constraints such as nonnegativity of portfolio positions are realistic, and they affect the form of the solution, but relatively little is known about the effects of such constraints on optimal strategies, because the constraints make it hard to find analytical solutions. In this work, we demonstrate the distortion of the no-trading region when it reaches the borrowing constraint boundary. We show how the rectangular no-trading region generated in uncorrelated risky asset cases transforms into a non-convex region due to the binding of the constraint. This study expands the scope of understanding the shape of the no-trading region. To the best of our knowledge, this is the first study of the deformation in no-trading region shape resulted from the borrowing constraint.

The future research direction includes but not restricts to exploring other approximation approaches for value functions, adding consumption and other realistic ingredients to the portfolio model (Mulvey and Vladimirou, 1992), testing the impact from different return models, e.g. return models with return predictability (Brandt et al., 2005), with stochastic volatility (Heston, 1993), and with jump processes (Merton, 1976). For those extensions, we would expect to encounter a larger state space due to the extra randomness of the parameters. The discrete time framework will accommodate the jumps that happen between the rebalance interval, unless the interval is narrow, such as in a high frequency trading framework. When the state space is expanded, HS and HC need some refinements such as interpolation or regression of the optimal radius and center on extra state variables, as Merton's solution will change with respect to different return parameters. VF needs exploiting the shape of the new value functions to choose appropriate basis functions to control errors. Further, the duality methods developed in Brown et al. (2009) that are taking path-wise optimization inherently accommodate those extra randomness from the state variables.

Chapter 3

Portfolio Optimization with Taxes

3.1 Introduction

In presence of capital gain taxes, Merton's solution for a multi-period portfolio optimization becomes suboptimal. Compared with the transaction cost problem, portfolio optimization with capital gain taxes may be even more important and perhaps plays the first order role in practice (Dammon and Spatt, 2012). In this chapter, we consider the problem of dynamic multi-asset portfolio optimization in a discrete-time, finite-horizon setting. Our general model underlines risk aversion, nonnegativity constraints on portfolio positions and capital gain taxes. The taxation rule is linear, adopts the weighted average tax basis price, and allows an immediate tax credit for a loss. We allow wash sales, rule out "shorting against the box", and prohibit tax forgiveness upon maturity. We are concerned with the efficient method to compute and understand the optimal investment decisions for investors who have access to multiple investment instruments: a risk-free asset account paying a risk-free rate and several risky assets with stochastic returns.

The rest of the chapter is organized as follows: In Section 3.2, we describe the investment model. In Section 3.3, we discuss the model properties and how we solve the problem via approximate dynamic programming. In Section 3.4, we investigate the no-trading region for single and two risky asset cases. In Section 3.5, we propose several trading strategies. In Section 3.6, we provide two dual methods to complement the lower bounds from Section 3.5. In Section 3.7, we analyze our numerical results. Finally, in Section 3.8, we conclude.

3.2 The Portfolio Optimization Model with Taxes

Time is modeled as discrete and indexed as $t_k = k\Delta t$, $k = 0, ..., m$, where $t_0 = 0$ represents the current period and $t_m = T$ represents the terminal period. Also, t_k^+ denotes the post-trade time of t_k. We consider a market contains one risk-free and multiple n risky assets. We adopt the assumption in Constantinides (1983) that the risk-free asset continuously pays a gross risk-free return R_f and behaves as a tax exempt bond. The corresponding net risk-free return rate is denoted by r_f. The returns of the risky assets are stochastic and denoted by $\mathbf{R}_{t_k} = (R_{t_k,1}, ..., R_{t_k,n})'$ where $R_{t_k,i}$ is the gross return of asset i from t_{k-1} to t_k. The return is modeled by a multivariate geometric Brownian motion:

$$\ln \mathbf{R}_{t_k} = \boldsymbol{\mu} - \frac{1}{2}\boldsymbol{\sigma}^2 + \boldsymbol{e}_{t_k} \tag{3.1}$$

with $\boldsymbol{\mu} = (\mu_1, ..., \mu_n)'$ the asset return vector, $\boldsymbol{\sigma} = (\sigma_1, ..., \sigma_n)'$ the return volatility vector, and $\mathbf{e}_{t_k}$ the stochastic increments from the multivariate normal distribution with mean zero, volatility $\boldsymbol{\sigma}$, and correlation Σ_e. All the parameters in the return model are time-independent. We sample the asset returns from the continuous distribution instead of a lattice model. The prices of the risky assets are denoted by $\mathbf{S}_{t_k} = (S_{t_k,1}, ..., S_{t_k,n})'$. Without loss of generality, we set their initial prices to one, i.e., $\mathbf{S}_0 = (1, ..., 1)'$. Investors have an initial investment of x_0 dollars invested in the risk-free asset account and $\mathbf{y}_0 = (y_{0,1}, ..., y_{0,n})'$ dollars in the n risky assets. The positions in risk-free and risky assets at time t_k are denoted by x_{t_k} and $\mathbf{y}_{t_k} = (y_{t_k,1}, ..., y_{t_k,n})'$, respectively.

In time, investors can choose to either spend money from the risk-free account to buy risky assets or add money to the risk-free account by selling risky assets. To model capital gain taxes, we consider buying and selling risky assets separately. Denote $\mathbf{L}_{t_k} = (L_{t_k,1}, ..., L_{t_k,n})'$ as an n-vector whose i-th element represents the amount of money spent from the risk-free account to buy risky asset i. Similarly, denote $\mathbf{U}_{t_k} = (U_{t_k,1}, ..., U_{t_k,n})'$ as an n-vector whose i-th component represents the amount of money obtained from selling risky asset i before incurring capital gain taxes if there is any. Thus, they are both nonnegative.

In order to compute the tax for a transaction we need to introduce a model to compute the tax basis price. We adopt the weighted average basis price to reduce path-dependency and a linear taxation model allowing immediate tax credit realization without any limit (Dammon et al., 2001, see, e.g.,).[1] Let $\boldsymbol{\tau} = (\tau_1, ..., \tau_n)' \geq \mathbf{0}$ be the tax rate vector for the risky assets and $\mathbf{B}_{t_k} = (B_{t_k,1}, ..., B_{t_k,n})'$ be the corresponding tax basis price vector. The dynamics of the weighted average tax basis for the i-th risky asset is modeled by

$$B_{t_{k+1},i} = \frac{B_{t_k,i}(y_{t_k,i} - U_{t_k,i}) + S_{t_k,i} L_{t_k,i}}{y_{t_k,i} + L_{t_k,i} - U_{t_k,i}}, \tag{3.2}$$

and the linear taxation rule of selling $U_{t_k,i}$ dollar amount i-th risky asset is formulated as

$$\text{Capital Gain Tax} = \tau_i \frac{U_{t_k,i}}{S_{t_k,i}}(S_{t_k,i} - B_{t_k,i}). \tag{3.3}$$

The tax model implies several useful properties. First, selling a risky asset does not change its tax basis. Second, when the current asset price is lower than its basis price there exists a tax credit. Third, the basis price after any trades will keep unchanged until the next rebalancing time, i.e., $B_{t_k^+,i} = B_{t_{k+1},i}$.[2] Fourth, if investors liquidate the entire position for a risky asset, i.e., $U_{t_k,i} = y_{t_k,i}$, the current tax basis price will not affect the basis price when the same risky asset is bought in the later period. Hence, in this case we can freely choose the basis price as $B_{t_{k+1},i} = S_{t_k,i}$. Without loss of generality, we set initial basis prices to one, i.e., $\mathbf{B}_0 = (1, ..., 1)'$.

For convenience, let us define the realized cash from the sale of one share i-th risky asset:

$$b(S_{t_k,i}, B_{t_k,i}) = S_{t_k,i} - \tau_i(S_{t_k,i} - B_{t_k,i}). \tag{3.4}$$

The controlled evolution of the positions in risk-free and risky assets can be described by the system of equations:

$$\begin{pmatrix} x_{t_{k+1}} \\ \mathbf{y}_{t_{k+1}} \end{pmatrix} = \begin{pmatrix} R_f \left(x_{t_k} + \sum_{i=1}^{n} \left[\frac{U_{t_k,i}}{S_{t_k,i}} b(S_{t_k,i}, B_{t_k,i}) - L_{t_k,i} \right] \right) \\ \mathbf{R}_{t_{k+1}} \cdot (\mathbf{y}_{t_k} + \mathbf{L}_{t_k} - \mathbf{U}_{t_k}) \end{pmatrix} \tag{3.5}$$

[1] The current U.S. tax code limits net deductible capital losses to \$3000 per year. Net capital losses in excess of \$3000 can be carried forward indefinitely. Relaxing this full loss usage assumption would increase the complexity of the problem. For a discussion of the impact from limit use of the loss and wash sale, refer to Gallmeyer and Srivastava (2011).

[2] In some countries, e.g. Canada, the weighter average tax basis is used in the tax law. Under current U.S. tax law, the investor can choose either the specific share identification method or the weighted average tax basis method.

where $\cdot$ denotes the element-wise product of two vectors. To prohibit short selling and borrowing we assume the trades at time t_k are restricted to a convex solvency set:[3]

$$\mathbb{A}_{t_k} = \left\{ \mathbf{U}_{t_k}, \mathbf{L}_{t_k} \in \mathbb{R}^n_+ : x_{t_k} + \sum_{i=1}^{n} [\frac{U_{t_k,i}}{S_{t_k,i}} b(S_{t_k,i}, B_{t_k,i}) - L_{t_k,i}] \geq 0, \mathbf{y}_{t_k} - \mathbf{U}_{t_k} \geq \mathbf{0} \right\}. \tag{3.6}$$

In addition, since investors are not barred from wash sales, they may sell the risky asset to realize a tax credit when there is a loss and then repurchase the same asset to reset its tax basis (see, e.g., Constantinides, 1983; Dammon et al., 2001). As a consequence, for the capital gain taxes problem allowing wash sales, $\mathbf{L}_{t_k}$ and $\mathbf{U}_{t_k}$ can be nonzero simultaneously, which is one critical difference from the transaction costs problem. In other words, we have to impose $\mathbf{y}_{t_k} - \mathbf{U}_{t_k} \geq \mathbf{0}$ instead of $\mathbf{y}_{t_k} + \mathbf{L}_{t_k} - \mathbf{U}_{t_k} \geq \mathbf{0}$ to prohibit short sales. The nominal wealth at time t_k is the sum of the dollar positions across risk-free and risky assets, i.e.,

$$W^n_{t_k} = x_{t_k} + \sum_{i=1}^{n} y_{t_k,i}. \tag{3.7}$$

By taking into account of the liquidation tax, the realized wealth is defined as

$$W^r_{t_k} = x_{t_k} + \sum_{i=1}^{n} \frac{y_{t_k,i}}{S_{t_k,i}} b(S_{t_k,i}, B_{t_k,i}). \tag{3.8}$$

The objective of investors is to choose a policy $(\mathbf{U}_{t_k}, \mathbf{L}_{t_k})$ at each period t_k to maximize the expected utility of the final realized wealth:

$$\max_{\substack{(\mathbf{U}_{t_k}, \mathbf{L}_{t_k}) \in \mathbb{A}_{t_k} \\ k=0,\ldots,m-1}} \mathbb{E}[\mathcal{U}(W^r_T)] \tag{3.9}$$

given the CRRA utility function:

$$\mathcal{U}(x) = \begin{cases} \dfrac{x^\gamma}{\gamma} & \gamma < 1, \gamma \neq 0 \\ \ln(x) & \gamma = 0 \end{cases}, \tag{3.10}$$

where tax forgiveness upon maturity is prohibited. Further, the portfolio optimization problem (3.9) can be formulated as a stochastic dynamic program with state variables consisting of the current positions in the risk-free asset x_{t_k} and the risky assets $\mathbf{y}_{t_k}$, the

[3]This solvency set is slightly different from the one in Garlappi et al. (2001) and Tahar et al. (2010) where the realized wealth is restricted nonnegative. It can be easily shown that their solvency set, which allows for some leverage, contains our set $\mathbb{A}_{t_k}$.

basis prices $\mathbf{B}_{t_k}$ and the risky asset prices $\mathbf{S}_{t_k}$. The terminal value function is the utility of terminal realized wealth $V_T = \mathcal{U}(W_T^r)$, and the earlier value functions V_{t_k} are given recursively by

$$V_{t_k}(x_{t_k}, \mathbf{y}_{t_k}, \mathbf{B}_{t_k}, \mathbf{S}_{t_k}) = \max_{(\mathbf{U}_{t_k}, \mathbf{L}_{t_k}) \in \mathbb{A}_{t_k}} \mathbb{E}_{t_k}[V_{t_{k+1}}(x_{t_{k+1}}(\mathbf{U}_{t_k}, \mathbf{L}_{t_k}), \mathbf{y}_{t_{k+1}}(\mathbf{U}_{t_k}, \mathbf{L}_{t_k}), \mathbf{B}_{t_{k+1}}, \mathbf{S}_{t_{k+1}})] \tag{3.11}$$

where the expectations are taken over the stochastic return of the risky assets $\mathbf{R}_{t_{k+1}}$, and $\mathbb{E}_{t_k}[\cdot]$ denotes the conditional expectation conditioned on the information up to time t_k. In the recursive relation (3.11), we explicitly write out the dependence of the value function with the basis prices and the risky asset prices to show the state space of the capital gain taxes problem is larger than that of the transaction costs problem. In the sequel, we denote the certainty equivalent of the value function $V_{t_k}(\cdot)$ as a strictly monotonic transformation:

$$C_{t_k}(\cdot) = \mathcal{U}^{-1}(V_{t_k}(\cdot)). \tag{3.12}$$

3.3 Model Properties and Approximate Dynamic Programming

In this section, we analyze the relevant properties of the portfolio optimization problem under capital gain taxes and discuss all the elements needed in the approximate dynamic programming approach to more accurately solve the dynamic program (3.11). Dynamic programs with continuous decision and state spaces have been noticed to be difficult and require careful error control in each step of approximate dynamic programming algorithms (see, e.g., Rust, 1996). To this end, we split the task into three segments. First, we derive an equivalent formulation for the problem by incorporating the optimal solution of the case with capital losses into the original formulas. Second, we further reduce the state space by the homothetic property of the problem. Third, we discuss how to obtain approximated value functions with a high accuracy in backward iteration.

Constantinides (1983), Dammon et al. (2001) and Tahar et al. (2010) have shown that if wash sales are allowed and the taxation rule is linear, it is optimal to realize all capital losses first and then buy back the corresponding assets. In other words, capital losses will act as transaction revenues. Hence after reformulating the basis price relation (3.2) and the controlled evolution equations (3.5), we only need to work on the state space representing the region for capital gains. In particular, if there is a capital loss the basis price will be reset to the current risky asset price; whereas if there is a capital gain the basis price will change as before. Thus, the basis price for the i-th risky asset can be reformulated as:

$$B_{t_{k+1},i} = \begin{cases} S_{t_k,i} & S_{t_k,i} \leq B_{t_k,i} \\ \dfrac{B_{t_k,i}(y_{t_k,i} - U_{t_k,i}) + S_{t_k,i} L_{t_k,i}}{y_{t_k,i} + L_{t_k,i} - U_{t_k,i}} & S_{t_k,i} > B_{t_k,i} \end{cases}, \tag{3.13}$$

or in a compact form

$$B_{t_{k+1},i} = S_{t_k,i} + \frac{(B_{t_k,i} - S_{t_k,i})(y_{t_k,i} - U_{t_k,i})}{y_{t_k,i} + L_{t_k,i} - U_{t_k,i}} \mathbb{1}_{S_{t_k,i} > B_{t_k,i}}. \tag{3.14}$$

where $\mathbb{1}$ is the indicator function. In addition, by liquidating the entire position if there is a capital loss and then rebalance, the i-th risky asset position evolves as

$$y_{t_{k+1},i} = \begin{cases} R_{t_{k+1},i}\left(y_{t_{k,i}} + L_{t_{k,i}} - y_{t_{k,i}}\right) & S_{t_k,i} \leq B_{t_k,i} \\ R_{t_{k+1},i}\left(y_{t_{k,i}} + L_{t_{k,i}} - U_{t_{k,i}}\right) & S_{t_k,i} > B_{t_k,i} \end{cases}, \tag{3.15}$$

and the corresponding risk-free asset position evolves as

$$x_{t_{k+1}} = \begin{cases} R_f\left(x_{t_k} + \sum_{i=1}^{n}\left[\dfrac{y_{t_k,i}}{S_{t_k,i}} b(S_{t_k,i}, B_{t_k,i}) - L_{t_k,i}\right]\right) & S_{t_k,i} \leq B_{t_k,i} \\ R_f\left(x_{t_k} + \sum_{i=1}^{n}\left[\dfrac{U_{t_k,i}}{S_{t_k,i}} b(S_{t_k,i}, B_{t_k,i}) - L_{t_k,i}\right]\right) & S_{t_k,i} > B_{t_k,i} \end{cases}. \tag{3.16}$$

In a compact form, the new controlled dynamics is:

$$\begin{pmatrix} x_{t_{k+1}} \\ \mathbf{y}_{t_{k+1}} \end{pmatrix} = \begin{pmatrix} R_f\left(W^r_{t_k} + \sum_{i=1}^{n}\left[\dfrac{U_{t_k,i} - y_{t_k,i}}{S_{t_k,i}} b(S_{t_k,i}, B_{t_k,i}) \mathbb{1}_{S_{t_k,i} > B_{t_k,i}} - L_{t_k,i}\right]\right) \\ \mathbf{R}_{t_{k+1}} \cdot \left(\mathbf{L}_{t_k} - (\mathbf{U}_{t_k} - \mathbf{y}_{t_k}) \mathbb{1}_{\mathbf{S}_{t_k} > \mathbf{B}_{t_k}}\right) \end{pmatrix}. \tag{3.17}$$

The corresponding solvency set is rewritten as

$$\mathbb{A}_{t_k} = \left\{ \mathbf{U}_{t_k}, \mathbf{L}_{t_k} \in \mathbb{R}^n_+ : W^r_{t_k} + \sum_{i=1}^{n}\left[\frac{U_{t_k,i} - y_{t_k,i}}{S_{t_k,i}} b(S_{t_k,i}, B_{t_k,i}) \mathbb{1}_{S_{t_k,i} > B_{t_k,i}} - L_{t_k,i}\right] \geq 0, \mathbf{y}_{t_k} - \mathbf{U}_{t_k} \geq \mathbf{0} \right\}. \tag{3.18}$$

Tahar et al. (2010) have theoretically proved that using the new formulas will yield the same results as the original. Garlappi et al. (2001) have noticed the value function of the taxes problem has a "kink" when it goes from the region in the state space for capital losses to that for capital gains. The new formulas automatically take the optimal decision when there is a capital loss. Hence the state space is reduced to the region representing capital gains and the difficulty of approximating the value function with a kink has been resolved. The new formulations will be applied in lower bound strategies. On the other hand, Wang (2008) and Tahar et al. (2010) rigorously show only the relative value $S_{t_k,i}/B_{t_k,i}$ matters for the optimal solution. Therefore, let us define the relative basis price for the i-th risky asset by

$$c_{t_k,i} = \ln \frac{S_{t_k,i}}{B_{t_k,i}}, \tag{3.19}$$

as the risky asset returns follow a geometric Brownian motion. We denote the column vector $\mathbf{c}_{t_k} = (c_{t_k,1}, ..., c_{t_k,n})'$. Thus, we can consider the state space $(x_{t_k}, \mathbf{y}_{t_k}, \mathbf{c}_{t_k})$ rather than $(x_{t_k}, \mathbf{y}_{t_k}, \mathbf{B}_{t_k}, \mathbf{S}_{t_k})$.

For CRRA investors, the homothetic property of value functions from the portfolio optimization problem with taxes has been proved and applied in many studies (see, e.g., Dammon et al., 2001; Wang, 2008; Tahar et al., 2010; Dai et al., 2012). We restate the property without proof as follows:

Proposition 3. *Suppose $\mathcal{U}(x) = x^\gamma/\gamma$ or $\mathcal{U}(x) = \ln(x)$. Then the certainty equivalent C_{t_k} of the value function V_{t_k} at time t_k defined in the equation* (3.12) *has the homothetic property: for $\theta > 0$*

$$C_{t_k}(\theta x_{t_k}, \theta \mathbf{y}_{t_k}, \mathbf{c}_{t_k}) = \theta C_{t_k}(x_{t_k}, \mathbf{y}_{t_k}, \mathbf{c}_{t_k}). \tag{3.20}$$

The homothetic property (3.20) states that the certainty equivalent of the value function of the taxes problem is linear with respect to portfolio positions. Correspondingly, to compute the certainty equivalent for a portfolio position, we can always normalize the position with its realized wealth, compute the certainty equivalent for the position with unit realized wealth, and then scale it by the true realized wealth level. Namely, we choose $\theta = 1/W^r_{t_k}$ and compute the certainty equivalent as

$$C_{t_k}(x_{t_k}, \mathbf{y}_{t_k}, \mathbf{c}_{t_k}) = W^r_{t_k} C_{t_k}\left(\frac{x_{t_k}}{W^r_{t_k}}, \frac{\mathbf{y}_{t_k}}{W^r_{t_k}}, \mathbf{c}_{t_k}\right) = W^r_{t_k} \mathcal{C}_{t_k}(x_{t_k}, \mathbf{y}_{t_k}, \mathbf{c}_{t_k}), \tag{3.21}$$

where the reduced certainty equivalent $\mathcal{C}_{t_k}(x_{t_k}, \mathbf{y}_{t_k}, \mathbf{c}_{t_k})$ is defined as the certainty equivalent with unit realized wealth. By combining (3.19) and (3.21), we rewrite the recursive relation

(3.11) as

$$\mathcal{U}(W^r_{t_k}\mathcal{C}_{t_k}(x_{t_k},\mathbf{y}_{t_k},\mathbf{c}_{t_k})) = \max_{(\mathbf{U}_{t_k},\mathbf{L}_{t_k})\in\mathbb{A}_{t_k}} \mathbb{E}_{t_k}\left[\mathcal{U}\left(W^r_{t_{k+1}}\mathcal{C}_{t_{k+1}}(x_{t_{k+1}}(\mathbf{U}_{t_k},\mathbf{L}_{t_k}),\mathbf{y}_{t_{k+1}}(\mathbf{U}_{t_k},\mathbf{L}_{t_k}),\mathbf{c}_{t_{k+1}}\right)\right]. \tag{3.22}$$

Further, we can thereby focus on the case of pre-trade positions unit realized wealth, i.e., $W^r_{t_k} = 1$, which builds a relation between risk-free and risky assets. Let us define the realized i-th risky asset portfolio $v_{t_k,i}$ as

$$v_{t_k,i} = \frac{y_{t_k,i}}{S_{t_k,i}}\frac{b(S_{t_k,i},B_{t_k,i})}{W^r_{t_k}}, \tag{3.23}$$

where $v_{t_k,i}$ represents the portfolio weight of liquidating the i-th risky asset in the realized wealth. We now take the realized risky asset portfolio $v_{t_k,i}$ and the relative basis price $c_{t_k,i}$ as the new set of state variables, and therefore write each grid point in the state space as

$$(v_{t_k,i},c_{t_k,i}) = \left(\frac{y_{t_k,i}b(1,e^{-c_{t_k,i}})}{W^r_{t_k}}, c_{t_k,i}\right), \quad i=1,...,n. \tag{3.24}$$

Denote the vector $\mathbf{v}_{t_k} = (v_{t_k,1},...,v_{t_k,n})'$. By the choice of $W^r_{t_k} = 1$, the expression (3.24) simplifies to

$$(v_{t_k,i},c_{t_k,i}) = \left(y_{t_k,i}b(1,e^{-c_{t_k,i}}), c_{t_k,i}\right). \tag{3.25}$$

The above analysis indicates there are $2n$ coordinates for each grid point in the state space when investors have access to n risky assets. Given n pairs of $(v_{t_k,i},c_{t_k,i})$ and $W^r_{t_k} = 1$, the asset positions $(x_{t_k},\mathbf{y}'_{t_k})$ are uniquely determined by

$$x_{t_k} = 1 - \sum_{i=1}^n v_{t_k,i}, \quad y_{t_k,i} = \frac{v_{t_k,i}}{b(1,e^{-c_{t_k,i}})}, \quad i=1,...,n. \tag{3.26}$$

Therefore, the state space can then be denoted by:

$$\mathbb{S}_{t_k} = \left\{\mathbf{v}_{t_k},\mathbf{c}_{t_k}\in\mathbb{R}^n_+ : \sum_{i=1}^n v_{t_k,i}\le 1, \mathbf{c}_{t_k}\le\bar{\mathbf{c}}_{t_k}\right\} \tag{3.27}$$

where $\bar{\mathbf{c}}_{t_k}$ is the upper bound vector as the truncation of the unbounded state space. We choose $\bar{\mathbf{c}}_{t_k} = (\boldsymbol{\mu}-\frac{1}{2}\boldsymbol{\sigma}^2)t_k + 2.6\boldsymbol{\sigma}\sqrt{t_k}$, and linearly extrapolate the values on the grid points outside the region in our computation. At time t_k we sample the state variables according to a uniform distribution using low-discrepancy sequences. In particular, we use 2^{12} Sobol points.

Next, to control numerical errors in the optimization problem (3.22), we take the certainty equivalent of the expected value function as a monotone transformation that reduces the nonlinearity of the objective function, i.e.

$$\mathcal{C}_{t_k}(\mathbf{v}_{t_k}, \mathbf{c}_{t_k}) = \max_{(\mathbf{U}_{t_k}, \mathbf{L}_{t_k}) \in \mathbb{A}_{t_k}} \mathcal{U}^{-1}\Big\{\mathbb{E}_{t_k}[\mathcal{U}(W^r_{t_{k+1}} \mathcal{C}_{t_{k+1}}(\mathbf{v}_{t_{k+1}}(\mathbf{U}_{t_k}, \mathbf{L}_{t_k}), \mathbf{c}_{t_{k+1}})]\Big\} \tag{3.28}$$

where the transformed state variables serve as the arguments of the reduced certainty equivalent $\mathcal{C}_{t_k}$ for simplicity. At each time step, given optimal reduced certainty equivalent values on the grid from (3.28), we approximate the reduced certainty equivalent function by a set of K real-valued functions $\boldsymbol{\phi}_{t_k} = (\phi_{t_k,1}(\cdot), \ldots, \phi_{t_k,K}(\cdot))'$ on the state space $\mathbb{S}_{t_k}$ as

$$\mathcal{C}_{t_k}(\mathbf{v}_{t_k}, \mathbf{c}_{t_k}) \approx \sum_{l=1}^{K} \phi_{t_k,l}(\mathbf{v}_{t_k}, \mathbf{c}_{t_k}) \kappa_{t_k,l} \tag{3.29}$$

where the coefficient $\boldsymbol{\kappa}_{t_k} = (\kappa_{t_k,1}, ..., \kappa_{t_k,K})'$ is a column vector and can be computed by ordinary linear regression. It has been highlighted in Garlappi and Skoulakis (2009), Broadie and Shen (2013a) and Broadie and Shen (2013b) that compared to approximating V_{t_k} directly, approximating its less nonlinear transformation $\mathcal{C}_{t_k}$ is easier and yields higher accurate results. Besides the general advantages mentioned therein, we emphasize the necessity of choosing the normalization level $\theta = 1/W^r_{t_k}$ rather than $\theta = 1/W^n_{t_k}$. On the one hand, choosing $\theta = 1/W^n_{t_k}$ indicates each grid point is sampled with unit nominal wealth. Thereupon, the realized wealth and optimal solutions on grid points change substantially in different regions of the state space. This change further leads to the difficulty of approximating certainty equivalents with unit nominal wealth in a high accuracy. On the other hand, sampling grid points with unit realized wealth $\theta = 1/W^r_{t_k}$ mitigates the impact from embedded capital gains on optimal values so that the corresponding reduced certainty equivalent function is easier to approximate. We illustrate the certainty equivalent for a single risky asset case in the state space $(c_{t_k,1}, v_{t_k,1})$ that is normalized by the two different levels in Figure 3.10 and Figure 3.11, respectively. The certainty equivalent function from $\theta = 1/W^r_{t_k}$ in Figure 3.10 has smaller scale than the one from $\theta = 1/W^n_{t_k}$ in Figure 3.11. More importantly, the former is close to concave whereas the latter is apparently neither concave nor convex. We use the complete set of polynomials class introduced in Section 2.3 to approximate the reduced certainty equivalent functions. All the computation employs the complete set of polynomials of total order 7 with the new set of state variables $(\mathbf{c}_{t_k}, \mathbf{v}_{t_k})$.

Figure 3.1: Illustration of the optimal certainty equivalent of the last period when the pre-trade positions are sampled with unit realized wealth.

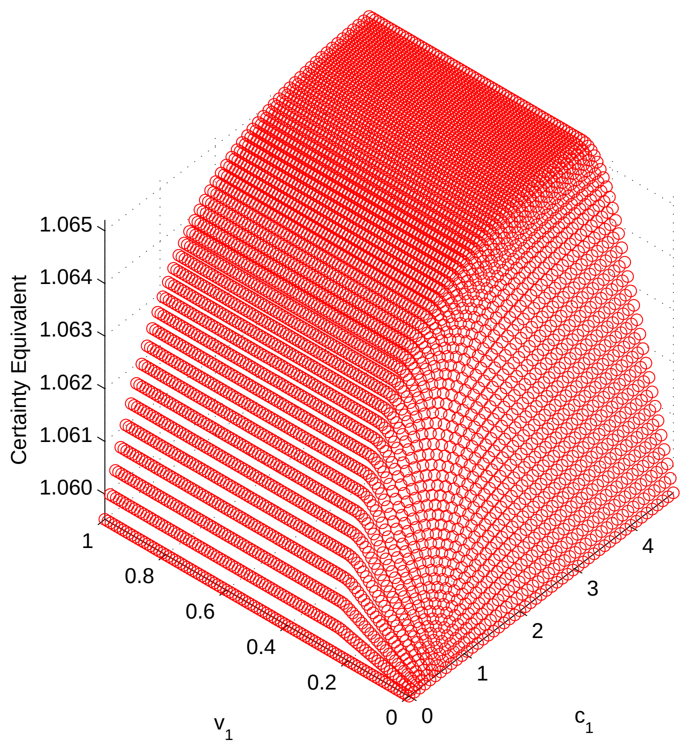

Note: The parameters are $r_f = 5.5\%$, $\mu_1 = 11\%$, $\sigma_1 = 30\%$, $\gamma = -1$, $\tau_1 = 30\%$, $T = 20$ year, $\Delta t = 1$ year. Its shape is close to concave.

Figure 3.2: Illustration of the optimal certainty equivalent of the last period when the pre-trade positions are sampled with unit nominal wealth.

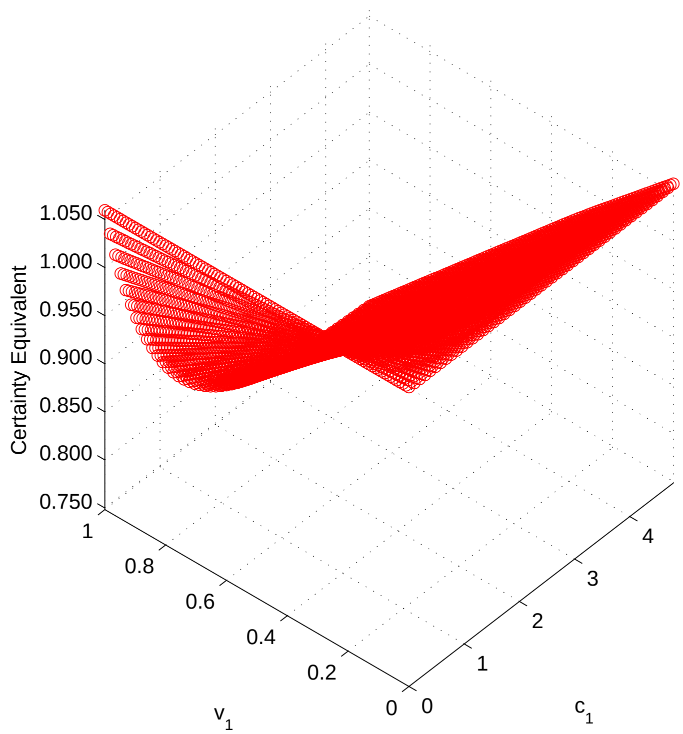

Note: The parameters are $r_f = 5.5\%$, $\mu_1 = 11\%$, $\sigma_1 = 30\%$, $\gamma = -1$, $\tau_1 = 30\%$, $T = 20$ year, $\Delta t = 1$ year. Its shape is neither concave nor convex.

To sum up, at each time step from t_m to t_0, our approximate dynamic programming algorithm involves the following steps:

1. Construct state space grid points by uniform randomly sampling over $\mathbb{S}_{t_k}$ (3.27).

2. Perform the optimization as the equation (3.28) and obtain optimal values on grid points over the state space.

3. Approximate the reduced certainty equivalent function over the entire state space $\mathcal{C}_{t_k}(\mathbf{v}_{t_k}, \mathbf{c}_{t_k})$ with optimal values on grid points by using polynomial regression (3.29).

The crucial ingredients include: (1) by the reformulated system (3.14) and (3.17), we only need to focus on the state space representing capital gains; (2) via the state variable transformation (3.25), we further reduce the size of the state space; (3) by the homothetic property (3.21), we can work on much less nonlinear transformed value functions, certainty equivalent functions; (4) by choosing the normalization level $\theta = 1/W^r_{t_k}$, we approximate functions that are close to concave; (5) by taking certainty equivalent transformation in optimization, we reduce numerical errors; (6) by applying the Sobol points and complete set of polynomials, to some extent we work around the curse of dimensionality. Relying upon those elements, in each step the relative numerical error in (3.29) measured by the l_∞ norm is about 10^{-5} and by the l_2 norm is about 10^{-10}. The similar study of the approximation error for the transaction costs problem can be found in Broadie and Shen (2013b). The results of our forward trading strategy using this approximation in Section 3.7 also prove its effectiveness.

3.4 No-Trading Region

In this section, we comprehensively investigate the no-trading region of the portfolio choice problem with capital gain taxes. It has been noticed that the portfolio choice problem with capital gain taxes also has a no-trading region (see, e.g., Garlappi et al., 2001; Wang, 2008). We first introduce the tax-adjusted Merton's solution. We then focus on the no-trading regions from single or two risky asset cases. In the single risky asset case, we emphasize the quantitative characterization of the no-trading region boundary and thereby provide insight to the cause of the no-trading region shape. In the two risky asset cases, we explain the associated optimal trades through the no-trading region and reveal a similar no-trading region shape and parameter sensitivity to that of the transaction costs problem.

3.4.1 Tax-adjusted Merton's Solution

For the transaction costs problem, the optimal solution is called Merton's solution when the transaction costs are zero. For the capital gain taxes problem, we introduce so-called the "tax-adjusted Merton's solution". Wang (2008) and Tahar et al. (2010) show that in continuous time, after realizing embedded capital losses the final portfolio is optimal for the situation where the mean return and volatility of risky assets are adjusted by a coefficient of $1 -$ tax rate in the fictitious trading environment with no tax and no transaction cost, i.e., the Merton's problem. On the other hand, in discrete time, Dammon et al. (2001) and DeMiguel and Uppal (2005) consider a relevant suboptimal strategy to realize all capital gains or losses in each rebalance time first and then rebalance back to the continuous time tax-adjusted solution. In Appendix A.3, we show that the case of forcing realizing all capital gains or losses in discrete time can also be linked to a fictitious discrete time trading environment with a tax-adjusted risky return. In the sequel, we call it the "tax-adjusted Merton's solution". In discrete time, the effective closed form solution for the tax-adjusted Merton's solution can be easily attained through a myopic optimization problem.

3.4.2 One Risky Asset

Dammon et al. (2001) have an extensive discussion of optimal investment decisions for one risky asset cases when taxes are reset upon maturity. Wang (2008) has researched the shape of no-trading region generated by one taxable and one nontaxable asset. We elucidate the quantitative characterization of the no-trading region boundary to provide insight to the cause of the shape.

Figure 3.3 displays the no-trading region in the state space $(c_{t_k,1}, v_{t_k,1})$ for a single risky asset. The red dots form the no-trading region. When the initial relative risky portfolio is outside the no-trading region, the optimal trades will bring it back to the boundary of the no-trading region. The arrows show the trading trajectories. The blue arrows represent the selling trades. As the selling trades do not change the basis prices, the trajectories are straight. The black purchasing lines are curved due to the change of the basis prices with the transaction. In the case of having a large capital gain and under-diversification, investors will buy more risky asset to reach the no-trading region. In this situation, a larger embedded capital gain results in a more dramatic reduction of the basis price. Namely, the relative basis price $c_{t_k,1}$ of the head and end of the curved trajectories reduces dramatically. The cross point of the two branches of the boundary represents the tax-adjusted Merton's solution. In Appendix A.5, we derive the solutions of the models that characterize the two boundaries for the no-trading region. Both models can be solved to optimality as they are linked to the Merton's problems with two effective risky returns, respectively. Accordingly, the selling boundary can be constructed by a Merton's problem with the effective risky return $\hat{R}_{t_{k+1},1}$, where

$$\hat{R}_{t_{k+1},1} = \frac{b(S_{t_k,1}R_{t_{k+1},1}, B_{t_k,1})}{b(S_{t_k,1}, B_{t_k,1})}. \tag{3.30}$$

As tax forgiveness is prohibited and sales do not change the basis price, the effective return (3.30) is the ratio of liquidating one share of risky asset one step ahead and liquidating that immediately. The purchasing boundary can be approximately constructed by a Merton's problem with $\tilde{R}_{t_{k+1},1}$, where

$$\tilde{R}_{t_{k+1},1} = b(R_{t_{k+1},1}, 1). \tag{3.31}$$

The purchasing trajectories in Figure 3.3 show the relative basis price will decrease drastically when investors purchase more risky asset. Also, purchases do not incur tax. The effective return (3.31) embodies this observation by simply subtracting the tax from the net return, as tax forgiveness is disallowed. Also, note that the optimal portfolio solved in the selling boundary problem represents the fraction in realized wealth, whereas the one solved in the purchasing boundary problem represents the fraction in nominal wealth. Figure 3.4 illustrates the no-trading region and the two branches of the boundary solved by the above two effective models. We observe they match closely with the numerical solutions for the original problem.

Indicated by (3.30) and (3.31), the shape of the boundary is determined by the trade-off between embedded capital gains and risky returns. On the one hand, as the effective return $\hat{R}_{t_{k+1},1}$ is increasing with the relative basis price $c_{t_k,1} = \ln(S_{t_k,1}/B_{t_k,1})$, the optimal deci-

Figure 3.3: Illustration of the no-trading region and the optimal trades.

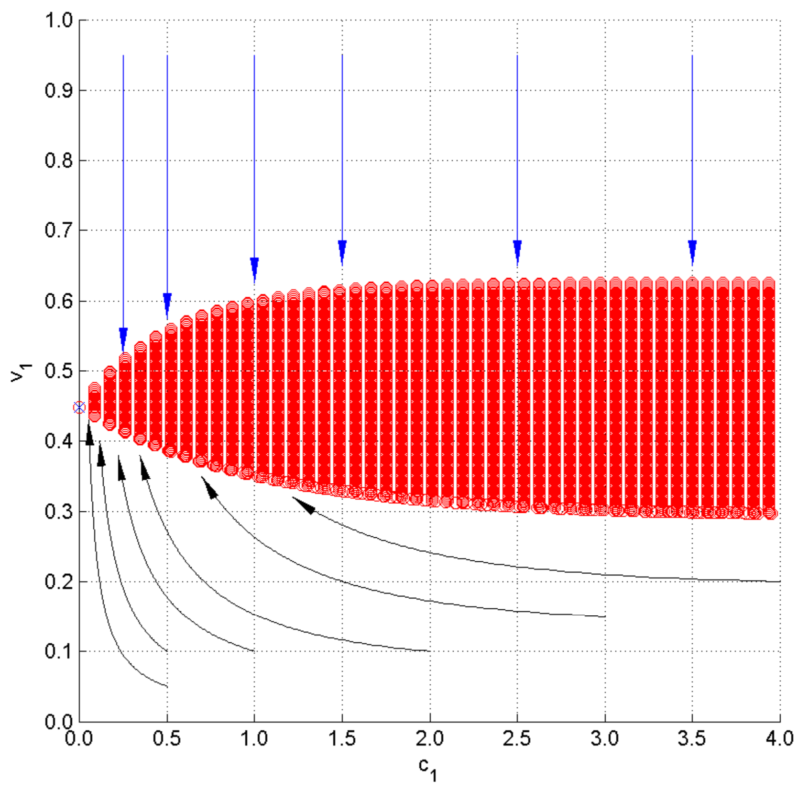

Note: The red dots form the no-trading region. The blue cross is the tax-adjusted Merton's solution. The black lines represent the purchasing trajectories. The blue lines represent the selling trajectories. The parameters are $r_f = 5\%$, $\mu_1 = 10\%$, $\sigma_1 = 20\%$, $\gamma = -1$, $\tau_1 = 35\%$.

sion will suggest investing more in the risky asset when the capital gain increases. In the limit of $c_{t_k,1} \to \infty$, $\hat{R}_{t_{k+1},1} \to R_{t_{k+1},1}$, where the corresponding optimal solutions from the limit return value represent the upper bound of the selling boundary. Intuitively, when the embedded capital gain is large, almost no difference exists between liquidating immediately and liquidating one step ahead. Hence, the first effective risky return $\hat{R}_{t_{k+1},1}$ becomes the original risk return $R_{t_{k+1},1}$. In the limit of $c_{t_k,1} \to 0$, $\hat{R}_{t_{k+1},1} \to (1-\tau_1)R_{t_{k+1},1} + \tau_1$, which yields the forcing realization solution. On the other hand, although the effective return $\tilde{R}_{t_{k+1},1}$ does not depend upon $c_{t_k,1}$, the corresponding optimal portfolio $\tilde{y}_{t_k^+,1}$ represents the optimal fraction of the nominal wealth. Hence, the optimal realized risky asset portfolio $\tilde{v}_{t_k^+,1}$ is decreasing with respect to $c_{t_k,1}$. In the limit of $c_{t_k,1} \to \infty$, $\tilde{v}_{t_k^+,1} \to (1-\tau_1)\tilde{y}_{t_k,1}/W^r_{t_k^+}$, which gives the lower bound of the purchasing boundary. Intuitively, when investors are underexposed to the risky asset, purchase generally reduces the relative basis price considerably. The trade-off as (3.30) is relatively small compared with this dramatic reduction of the basis price. The limit is simply the consequence of large relative basis price in the realized risky portfolio expression. In the limit of $c_{t_k,1} \to 0$, $\tilde{v}_{t_k^+,1} \to \tilde{y}_{t_k,1}/W^r_{t_k^+}$, which is the forcing realization solution. As a summary, both selling and purchasing boundaries need to balance tax payments with diversification. In particular, the selling boundary focuses on the benefit of deferring tax gains from the interval $[t_k, t_k^+]$ to the interval $[t_k^+, t_{k+1}]$, whereas the purchasing boundary mainly focuses on the impact from changing the relative basis price in the interval $[t_k, t_k^+]$. Those analyses are consistent with the limits of the two boundaries in Figure 3.4.

3.4.3 Two Risky Assets

For the two risky asset case, the most relevant research on the no-trading region is by Garlappi et al. (2001). In a lattice model, they present a discussion of the no-trading region. However, the no-trading region therein have not shown a clear analogy to that of the transaction costs problem presented in Muthuraman and Kumar (2006) and Lynch and Tan (2010). Two risky assets generate a four dimensional state space. Hence, we focus on visualizing its projections. The no-trading region on $(v_{t_k,1}, c_{t_k,1})$ or $(v_{t_k,2}, c_{t_k,2})$ by fixing the other two variables is similar to the pattern for the single risky asset shown in Figure 3.3.

Figure 3.4: Illustration of the no-trading region and the optimal solution from two effective models.

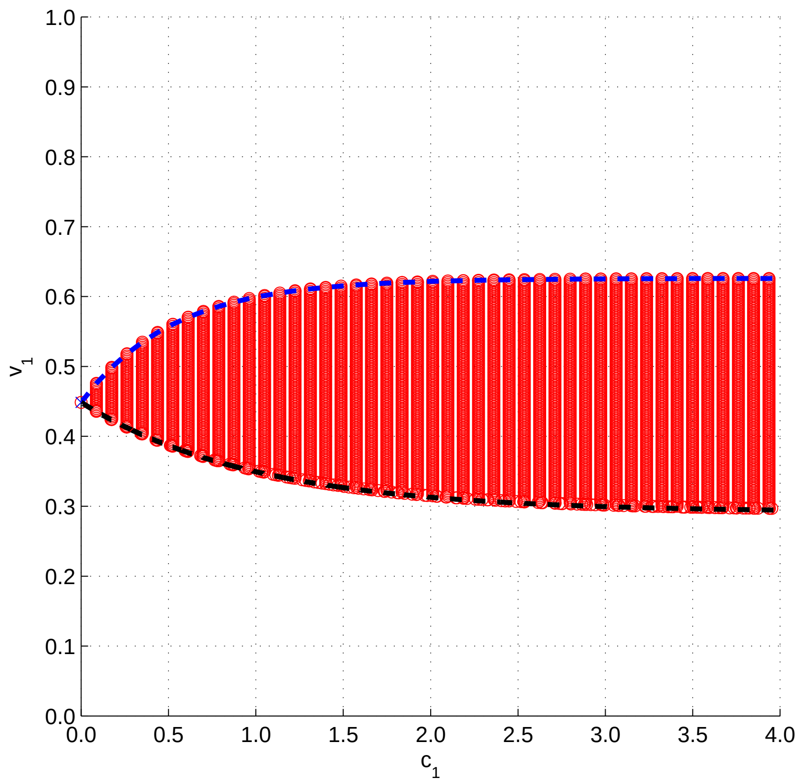

Note: The red dots form the no-trading region. The black and blue dash lines represent the two optimal solutions calculated by the corresponding effective models. The parameters are $r_f = 5\%$, $\mu_1 = 10\%$, $\sigma_1 = 20\%$, $\gamma = -1$, $\tau_1 = 35\%$.

Therefore, in the sequel we primarily present no-trading regions in $(v_{t_k,1}, v_{t_k,2})$ as the cutting planes by constant $c_{t_k,1}$ and $c_{t_k,2}$ of the four dimensional space $(v_{t_k,1}, v_{t_k,2}, c_{t_k,1}, c_{t_k,2})$.

Figure 3.5 illustrates the no-trading region with the optimal trades for different pre-trade positions. The shape of the no-trading region is close to a parallelogram. The outside region falls into two categories. Its east, south, west and north represent the trades involving one asset to bring the position to the no-trading region. In the rest domain, it is impossible to transact only one asset to reach the no-trading region. Hence, two assets are traded to reach a corner. These features are similar to those of the transaction costs problem in Muthuraman and Kumar (2006) and Lynch and Tan (2010). The unique traits for the taxes problem exhibit in three aspects. First, it is the tax-adjusted Merton's solution rather than the classic Merton's solution that lies within the no-trading region. Second, the trades involving purchases are disparate from those only involving sales. After following optimal trades, post-trade positions will reach the no-trading region in the four dimensional state space. The post-trade positions involving purchases are however reaching different cutting planes in the four dimensional space. In Figure 3.5, the dash arrows represent those trades involving purchases and thereby their post-trade positions are not lying on the same $(v_{t_k,2}, v_{t_k,2})$ plane. Specifically, we choose four of those typified pre-trade positions, labeled by a, b, c and d, to demonstrate this salient difference. Figure 3.6 shows the four no-trading regions for the post-trade positions of a, b, c and d, respectively. a represents the case of purchasing both risky assets. b and c both represent the case of only purchasing one risky asset but for different purchasing amount. d represents the case of purchasing one risky asset and selling another. The four no-trading regions are distinct from the one in Figure 3.5, as the no-trading regions on which post-trade positions stay are cut by different $c_{t_k,1}$ and $c_{t_k,2}$. In particular, the sub-figures for c and d are the same. This is because the optimal purchase trade for d is the same as that for c and meanwhile the optimal sale trade for d does not change the relative basis price. Third, Figure 3.7 illustrates the no-trading regions on $(v_{t_k,1}, v_{t_k,2})$ with different relative basis prices $c_{t_k,1}$ and $c_{t_k,2}$. Similar to the change of the no-trading region discussed in Section 3.4.2, the no-trading region shrinks in size when the relative basis price decreases. In the following, we conduct the parameter sensitivity analysis of the no-trading region.

Figure 3.5: Illustration of shape the no-trading region and the optimal trades in the last period.

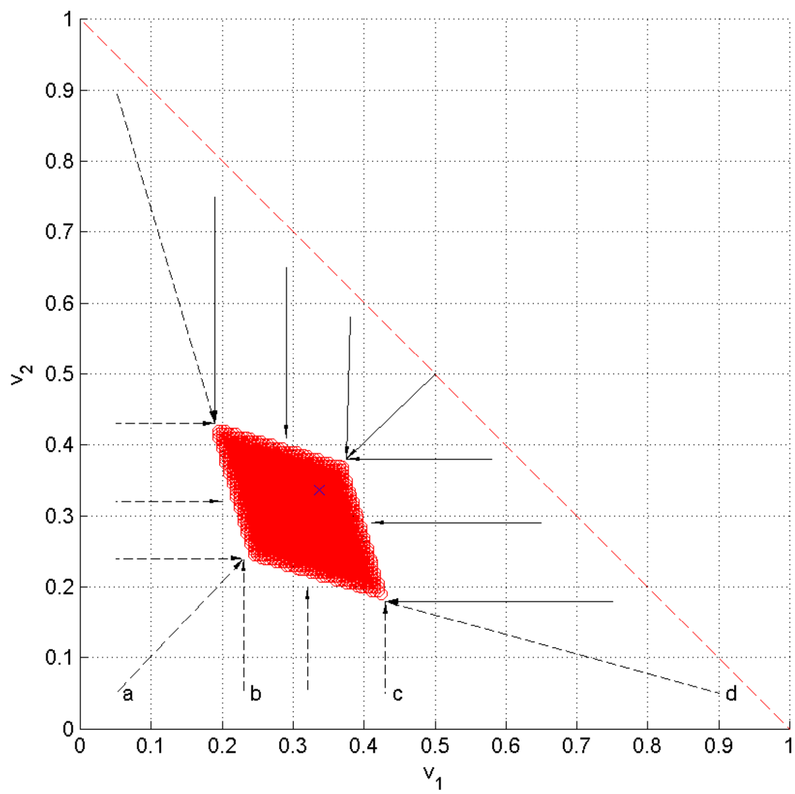

Note: The (v_1, v_2) plane is the cutting plane of $c_1 = c_2 = 2.84$ for a four dimensional space (v_1, v_2, c_1, c_2). The red dots form the no-trading region. The blue cross is the tax-adjusted Merton's solution. The black solid line arrows represent the optimal trades with post-trade positions on the same (v_1, v_2) cutting plane. The black dash line arrows represent the optimal trades with post-trade positions on other cutting planes. Four pre-trade positions, a, d, c and d are chosen to illustrate the no-trading regions to which their post-trade positions belong in Figure 3.6. Their coordinates are $(0.05, 0.05)$, $(0.25, 0.05)$, $(0.42, 0.05)$ and $(0.90, 0.05)$, respectively. The other parameters are $\gamma = -1$, $r_f = 5\%$, $\mu_1 = \mu_2 = 11\%$, $\sigma_1 = \sigma_2 = 25\%$, $\rho = 0.3$, $\tau_1 = \tau_2 = 30\%$, $\Delta t = 1$ year, $m = 10$.

Figure 3.6: Illustration of the no-trading regions for different post-trade positions.

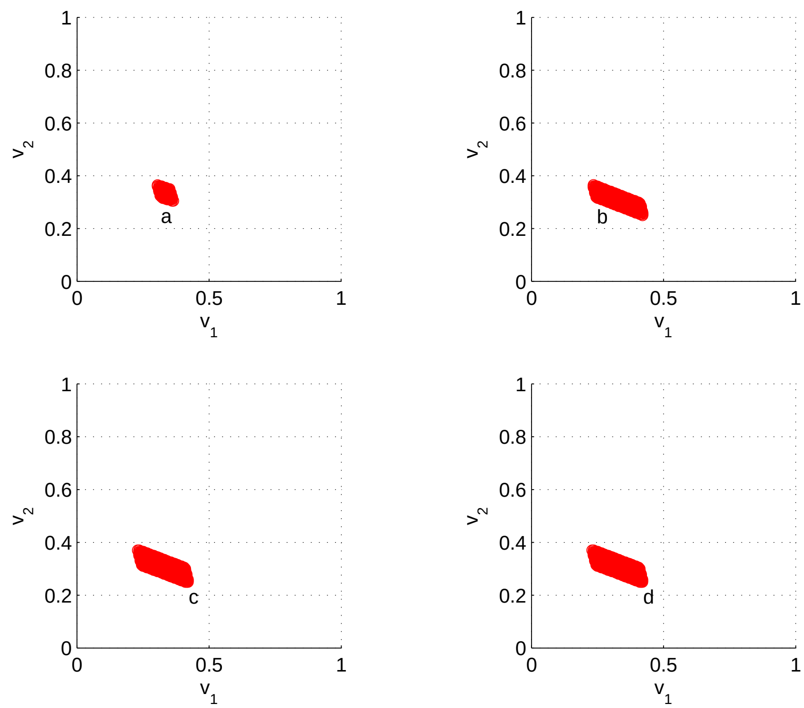

Note: The red dots form the no-trading region. From upper left to lower right, the (v_1, v_2) planes are the cutting planes of $c_1 = c_2 = 0.22$, $c_1 = 2.84$ and $c_2 = 0.22$, $c_1 = 2.84$ and $c_2 = 0.28$, $c_1 = 2.84$ and $c_2 = 0.28$, respectively. The coordinates of the four post-trade positions a, d, c and d are $(0.32, 0.32)$, $(0.25, 0.32)$, $(0.42, 0.25)$ and $(0.42, 0.25)$, respectively. The other parameters are the same as those in Figure 3.5.

Figure 3.7: Illustration of change the no-trading region with respect to the *relative basis price*.

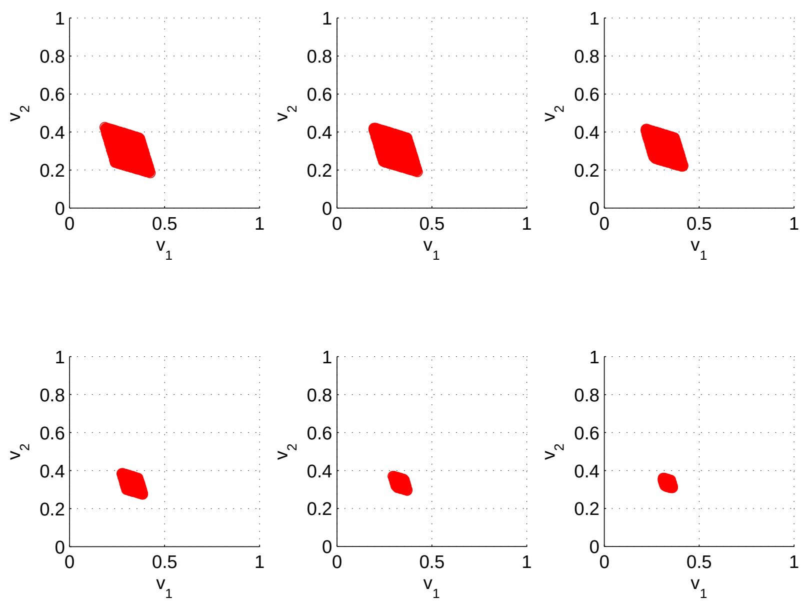

Note: The red dots form the no-trading region. From upper left to lower right, $c_1 = c_2 = 4.26$, 2.84, 1.42, 0.47, 0.28 and 0.20. The other parameters are $\gamma = -1$, $r_f = 5\%$, $\mu_1 = \mu_2 = 11\%$, $\sigma_1 = \sigma_2 = 25\%$, $\rho = 0.3$, $\tau_1 = \tau_2 = 30\%$, $\Delta t = 1$ year, $m = 10$.

Figure 3.8 shows the no-trading region at different time steps. We analyze the observation from three aspects. First, it reveals that the no-trading region becomes smaller when the investment approaches maturity, which is opposite to the results in the transaction costs problem (see, e.g., Lynch and Tan, 2010). Dammon et al. (2001) find that with mandatory realization of capital gains or losses at maturity the benefit of deferring capital gains is limited to the time value of the capital gain tax, which is small for elderly investors. Hence, elderly investors become more concerned about maintaining an optimally diversified portfolio, which leads to a smaller no-trading region. Also, the change of its size is not linear. The size is almost fixed when investors are several time steps away from maturity, as young investors are relatively insensitive to the treatment of embedded capital gains at maturity. Thus, in early stages the no-trading region mainly represents a steady balance between diversification and tax payment such that it does not vary considerably in different time steps. Second, as we have shown in the appendix, the tax-adjusted Merton's solution is fixed, but this result does not hold if tax forgiveness is allowed upon maturity. To illustrate the consistency of the analysis for the tax forgiveness cases with those in Dammon et al. (2001) and Garlappi et al. (2001), Figure 3.9 displays the no-trading region at different time steps with tax forgiveness upon maturity. The model uses the same parameters as those in Figure 3.8. Early papers highlighting tax forgiveness at maturity have documented the fact that the size of the no-trading region of the capital gain taxes problem expands when it approaches maturity. This is because the closer investors are to the time of tax forgiveness the stronger the incentive to defer is.[4] Besides, the no-trading regions in the tax forgiveness case are larger than those without tax forgiveness. This is because if investors are eligible to tax forgiveness, especially when they confront a short investment horizon, the diversification benefits cannot exceed the tax losses if they trade much. This effect can propagate back to the trading decisions in early stages of investment. In contrast, if investors are not eligible to tax forgiveness, diversification benefits are dominant given they cannot obtain the benefits of deferring tax gains. Further, the size of the no-trading regions indicates the

[4]Note the upper left and right sub-figures have been cut by the short sale constraint of the risky-free asset, which indicates the no-trading region will distort when the no borrowing constraint is binding. When we reduce the tax rate, we have seen the shape of the no-trading regions are still close to a parallelogram. That is similar to the results presented in Broadie and Shen (2013b) for the transaction costs problem.

benefits of tax forgiveness upon maturity can impact more time steps back than that without. Third, the change of the tax-adjusted Merton's solution along the time steps echoes the discussion for the one risky asset case in Dammon et al. (2001). In Dammon et al. (2001), because of allowing tax forgiveness upon maturity, the "forced realization solution" is disparate from the "unconstrained optimum".[5] When tax forgiveness is prohibited, these two solutions become identical. The "forced realization solution" is called the tax-adjusted Merton's solution in this paper, which is represented by the blue cross in Figure 3.8, whereas the unconstrained optimum in Figure 3.9 is different from the tax-adjusted Merton's solution in Figure 3.8. The unconstrained optimum is increasing with age until a few years prior to maturity. This is because young investors typically realize more to achieve better diversification, but for the deferred capital gains, they have the risk of being overexposed to the risky assets in the later stages. To balance these two parts, they limit the risky asset exposure in the early ages. The observation that the optimal holdings of risky assets decline in the last period shown in the upper left sub-figure of Figure 3.9 comes from that fact of having no chance to realize capital losses upon maturity.

Figure 3.10 displays the no-trading region for various values of tax rates. First observe that the no-trading regions are approximately squares, as we choose the same expected returns and volatilities for the two risky assets. When the tax rate increases investors would prefer to trade less. This indicates a trading policy that has a larger no-trading region. The figure shows this enlarging trend of the no-trading region. More importantly, it demonstrates the change of the location of the no-trading region. This is different from the transaction costs problem, where the center of the no-trading region is always the Merton's solution. As we illustrate in the previous section, although the tax-adjusted Merton's solution lies inside the no-trading region, it does not represent the center either. As we show in Appendix A.3 about the tax-adjusted Merton's solution, a larger tax rate results in a smaller effective risky return, which suggests investing less in the risky asset. This is consistent with the trend in Figure 3.10. In general, we have not found a particular meaning for the center of the no-trading region.

[5]The unconstrained optimum in Dammon et al. (2001) is defined as the optimal portfolio for the risky assets when there are no capital gains or losses.

Figure 3.8: Illustration of change the no-trading region with respect to the *time step*.

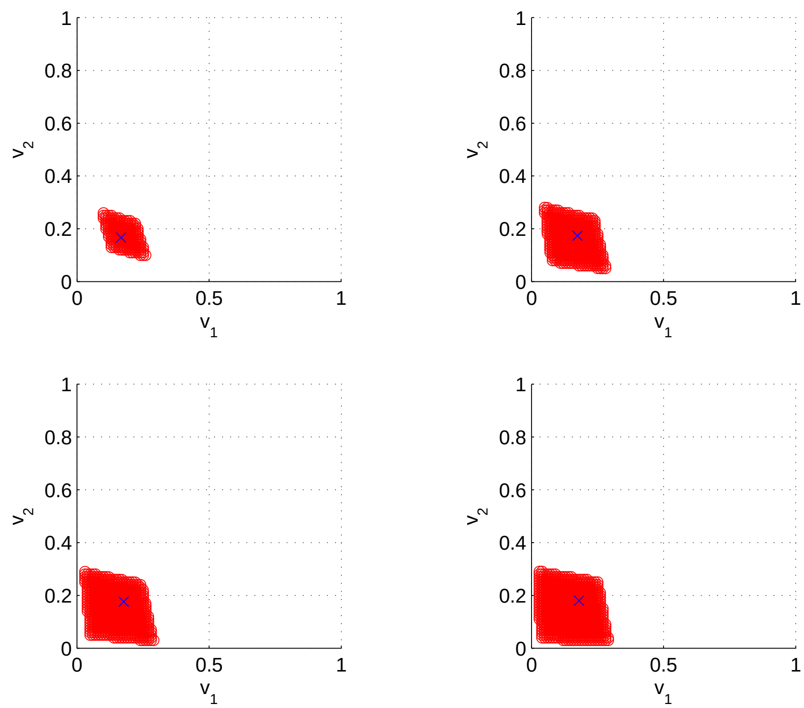

Note: The red dots form the no-trading region. The blue cross represents the tax-adjusted Merton's solution. From upper left to lower right, the time step is $k = 10$, 8, 6 and 1. The other parameters are $\gamma = -1$, $r_f = 5.55\%$, $\mu_1 = \mu_2 = 11\%$, $\sigma_1 = \sigma_2 = 30\%$, $\rho = 0.3$, $\tau_1 = \tau_2 = 35\%$, $\Delta t = 1$ year, $m = 10$. With mandatory realization of capital gains at maturity the benefit of deferring capital gains is limited to the time value of the capital gain tax, which is small for elderly investors. Hence, elderly investors become more concerned about maintaining an optimally diversified portfolio, which leads to a smaller no-trading region.

Figure 3.9: Illustration of change the no-trading region with respect to the *time step* for the tax forgiveness case.

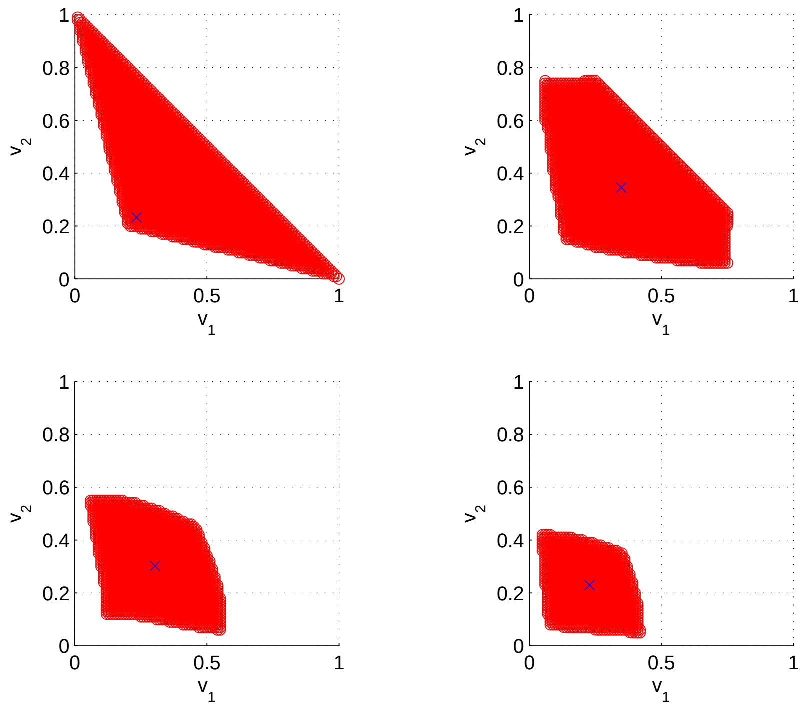

Note: The red dots form the no-trading region. The blue cross represents the unconstrained optimum. From upper left to lower right, the time step is k = 10, 8, 6 and 1. The other parameters are $\gamma = -1$, $r_f = 5.55\%$, $\mu_1 = \mu_2 = 11\%$, $\sigma_1 = \sigma_2 = 30\%$, $\rho = 0.3$, $\tau_1 = \tau_2 = 35\%$, $\Delta t = 1$ year, $m = 10$. The region expands when it approaches maturity. It is because the closer the investor is to the time of tax forgiveness the stronger incentive to defer is, i.e. the shorter the investment horizon.

Figure 3.10: Illustration of change the no-trading region with respect to the *tax rate* in the last period.

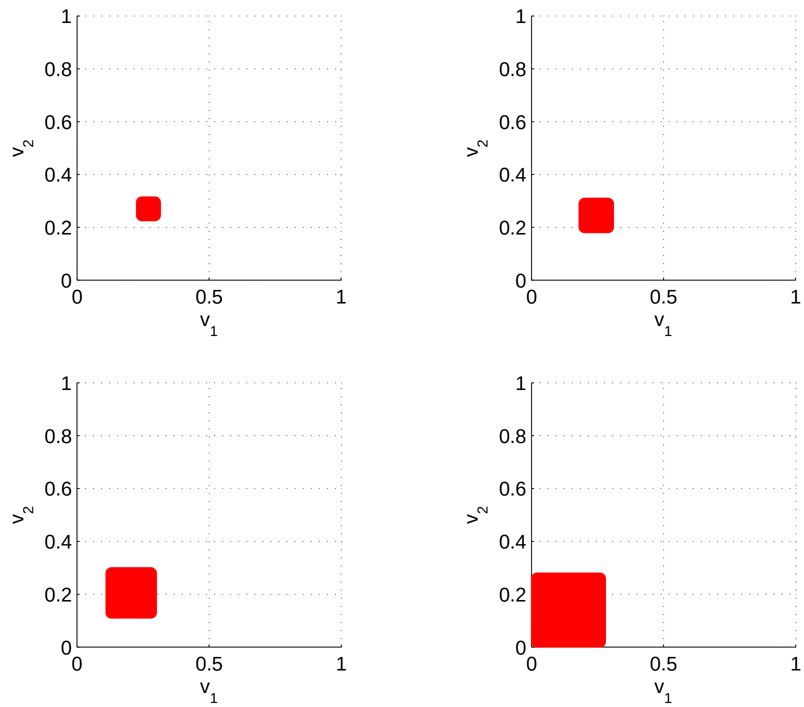

Note: The red dots form the no-trading region. From upper left to lower right, the tax rate is $\tau_1 = \tau_2 = 20\%$, 30%, 40% and 50%. The other parameters are $\gamma = -1$, $r_f = 5.5\%$, $\mu_1 = \mu_2 = 11\%$, $\sigma_1 = \sigma_2 = 30\%$, $\rho = 0$, $\Delta t = 1$ year, $m = 10$. The higher tax rate causes investors to trade less as a result of the trade-off between better diversification and more tax cost. Hence, the no-trading region enlarges with the increase of the tax rate.

Figure 3.11: Illustration of the change no-trading region with respect to the *risk aversion coefficient* in the last period.

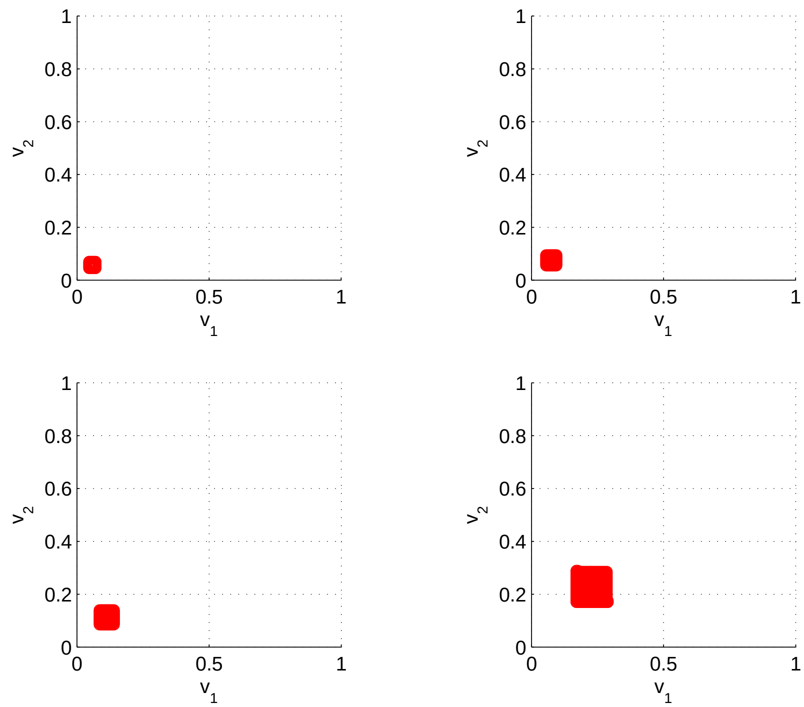

Note: The red dots form the no-trading region. From upper left to lower right, the risk aversion coefficient is $\gamma = -7$, -5, -3 and -1. The other parameters are $\tau_1 = \tau_2 = 35\%$, $r_f = 5.5\%$, $\mu_1 = \mu_2 = 11\%$, $\sigma_1 = \sigma_2 = 30\%$, $\rho = 0$, $\Delta t = 1$ year, $m = 10$. As investors becomes more risk averse they would invest less in risky assets, and trade more to keep the positions around the no-trading region.

Figure 3.11 shows the no-trading region for various values of risk aversion coefficients. As investors becomes more risk averse they would invest less in risky assets, and trade more to keep the positions around the no-trading region. Hence, the no-trading region moves towards to the origin and shrink in size. Figure 3.12 illustrates the no-trading region for various values of volatilities. As investors are risk averse they would invest less in risky assets when the volatility increases, and trade more to keep the positions around the no-trading region. Hence, the trend is similar to Figure 3.11.

Figure 3.12: Illustration of the change no-trading region with respect to the *volatility* in the last period.

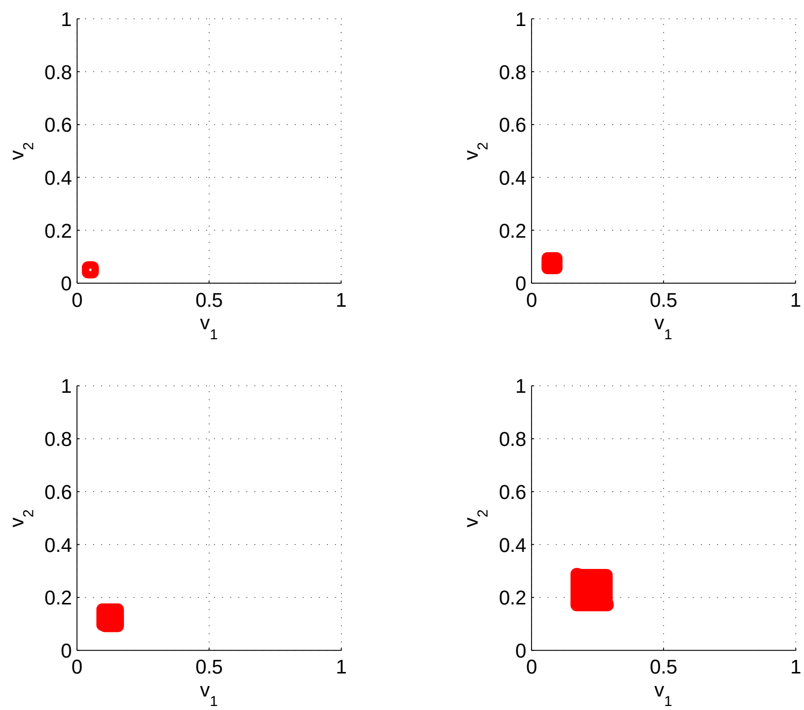

Note: The red dots form the no-trading region. From upper left to lower right, the volatility is $\sigma_1 = \sigma_2 = 60\%$, 50%, 40% and 30%. The other parameters are $\tau_1 = \tau_2 = 35\%$, $r_f = 5.5\%$, $\mu_1 = \mu_2 = 11\%$, $\rho = 0$, $\gamma = -1$, $\Delta t = 1$ year, $m = 10$. As investors are risk averse they would invest less in risky assets when the volatility increases, and trade more to keep the positions around the no-trading region.

Figures 3.13 and 3.14 display the no-trading region for various negative and positive values of correlation coefficients, respectively. In the negative correlation cases, the no-trading region shrink along $(1, -1)$ direction and enlarge along $(1, 1)$ with the increase in negative correlation. When the correlation is negative, investors would be able to tolerant more deviation along the $(1, 1)$ direction, since one risky asset serves a good hedge to the another. In the positive correlation cases, investors would take opposite trading decision as a hedge to the another.

Figure 3.13: Illustration of the change no-trading region with respect to the *negative correlation* in the last period.

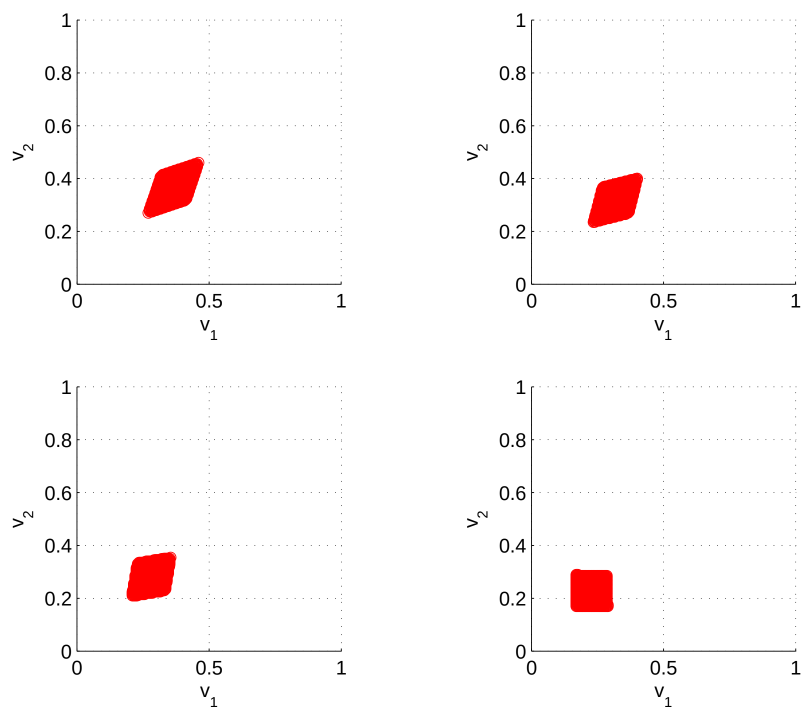

Note: The red dots form the no-trading region. From upper left to lower right, the correlation coefficient is $\rho = -0.4$, -0.3, -0.2 and 0. The other parameters are $\tau_1 = \tau_2 = 35\%$, $r_f = 5.5\%$, $\mu_1 = \mu_2 = 11\%$, $\sigma_1 = \sigma_2 = 30\%$, $\gamma = -1$, $\Delta t = 1$ year, $m = 10$. When the correlation is negative, investors would be able to tolerant more deviation along the $(1, 1)$ direction, since one risky asset serves a good hedge to the another.

Figure 3.14: Illustration of the change no-trading region with respect to the *positive correlation* in the last period.

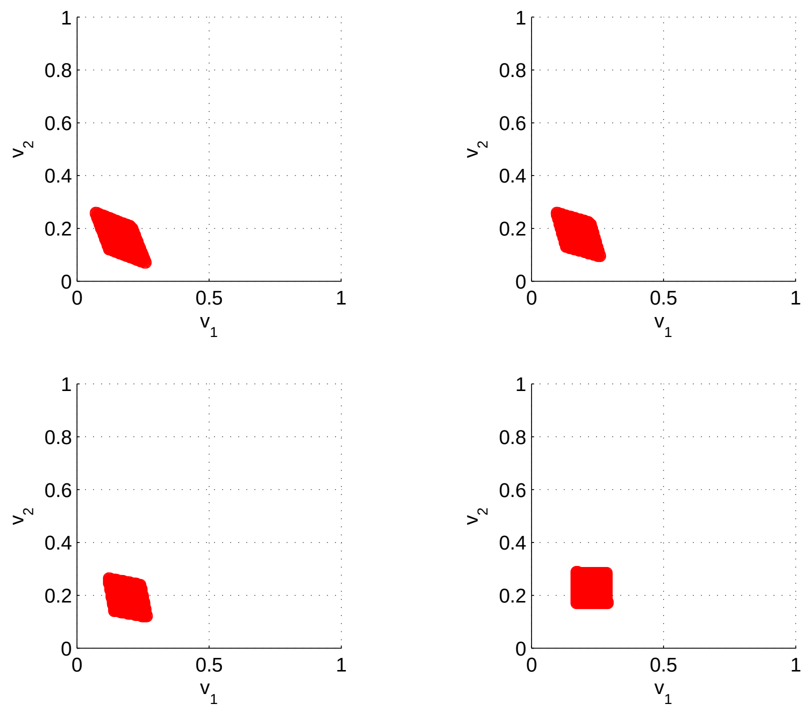

Note: The red dots form the no-trading region. From upper left to lower right, the correlation coefficient is $\rho = 0.4$, 0.3, 0.2 and 0. The other parameters are $\tau_1 = \tau_2 = 35\%$, $r_f = 5.5\%$, $\mu_1 = \mu_2 = 11\%$, $\sigma_1 = \sigma_2 = 30\%$, $\gamma = -1$, $\Delta t = 1$ year, $m = 10$. In the positive correlation cases, investors would take opposite trading decision as a hedge to the another.

3.5 Forward Trading Strategies for Lower Bounds

For portfolio optimization problems, as there are typically no closed form solutions, the focus is on searching for the near-optimal forward trading strategies. In order to get high performance trading strategies, we can approximate value functions through dynamic programming, consider heuristic strategies that embody sound intuition, or parametrize the policy motivated from solution structures. To illustrate those ideas, we will propose five novel forward trading strategies in the section. The first strategy VF in Section 3.5.1, is based on the approximate dynamic programming method discussed in Section 3.3. The RBH and MO strategies in Sections 3.5.2 and 3.5.3 are heuristic and easy to implement. The last two strategies RM and HC in Sections 3.5.4 and 3.5.5, are based on policy approximation. They characterize the optimal trading policy and are computationally economic.

3.5.1 Value Function Optimization (VF)

Approximated value functions given by backward iteration can serve as the continuation functions in forward simulation as an unbiased estimate of performance. If the approximation has a high accuracy, we should expect this trading rule generates a tight lower bound. In each period t_k for each trial VF chooses the trades $\mathbf{U}_{t_k}, \mathbf{L}_{t_k}$ that solve:

$$\max_{(\mathbf{U}_{t_k}, \mathbf{L}_{t_k}) \in \mathbb{A}_{t_k}} \mathcal{U}^{-1} \left\{ \mathbb{E}_{t_k} [\mathcal{U}(W^r_{t_{k+1}} \mathcal{C}_{t_{k+1}}(\mathbf{v}_{t_{k+1}}(\mathbf{U}_{t_k}, \mathbf{L}_{t_k}), \mathbf{c}_{t_{k+1}})] \right\}. \tag{3.32}$$

After following the recommended trades for the current portfolio positions, random returns for risky assets are generated to calculate the portfolio positions in the next period. Although it is expensive, this strategy yields near-optimal solutions if value functions has been approximated in a high accuracy. Also, the complexity of the problem grows linearly instead of exponentially with dimensions.

3.5.2 Rolling Buy-and-Hold Optimization (RBH)

For the rolling buy-and-hold strategy, in each rebalance time investors will follow the strategy obtained by an optimization problem. The optimization problem incorporates tax impact into the current period, imposes no control on the portfolio in future periods until maturity, and therefore maximizes the CRRA utility of final realized wealth. In each period t_k for each trial RBH chooses the trades $\mathbf{U}_{t_k}, \mathbf{L}_{t_k}$ that solve:

$$\max_{(\mathbf{U}_{t_k}, \mathbf{L}_{t_k}) \in \mathbb{A}_{t_k}} \mathcal{U}^{-1} \Big\{ \mathbb{E}_{t_k} \left[\mathcal{U}(W_T^r(x_T(\mathbf{U}_{t_k}, \mathbf{L}_{t_k}), \mathbf{y}_T(\mathbf{U}_{t_k}, \mathbf{L}_{t_k}), \mathbf{B}_T, \mathbf{S}_T)) \right] \Big\}, \tag{3.33}$$

where the basis price will only change with the current trading. It serves as a robust and close to optimal strategy for the transaction costs problem (see, e.g., Broadie and Shen, 2013b).

3.5.3 Myopic Optimization (MO)

The myopic optimization strategy treats each period as the last time period thus optimizing over the expected realized wealth in CRRA utility. When the no-trading region does not change dramatically in different periods, the approximation works well. Wang (2008) shows the myopic solution in a single risky asset case is near-optimal when trading intervals are small. In each period t_k for each trial MO chooses the trades $\mathbf{U}_{t_k}, \mathbf{L}_{t_k}$ that solve:

$$\max_{(\mathbf{U}_{t_k}, \mathbf{L}_{t_k}) \in \mathbb{A}_{t_k}} \mathcal{U}^{-1} \Big\{ \mathbb{E}_{t_k} \left[\mathcal{U}(W_{t_{k+1}}^r(x_{t_{k+1}}(\mathbf{U}_{t_k}, \mathbf{L}_{t_k}), \mathbf{y}_{t_{k+1}}(\mathbf{U}_{t_k}, \mathbf{L}_{t_k}), \mathbf{B}_{t_{k+1}}, \mathbf{S}_{t_{k+1}})) \right] \Big\}. \tag{3.34}$$

3.5.4 Realized Merton's Strategy (RM)

The realized Merton's strategy (RM) introduced in this section aims to improve the "forced realization" approach in Dammon et al. (2001) and DeMiguel and Uppal (2005). In the sequel, let us denote the "tax-adjusted Merton's solution" by $\mathbf{y}_{t_k}^{c,\text{tax}} = (y_{t_k,1}^{c,\text{tax}}, y_{t_k,2}^{c,\text{tax}}, ..., y_{t_k,n}^{c,\text{tax}})'$. RM chooses the known optimal strategy when there exists capital losses, and rebalances the portfolio such that the post-trade realized risky asset portfolio $\mathbf{v}_{t_k^+}$ equals to the tax-adjusted Merton's solution $\mathbf{y}_{t_k}^{c,\text{tax}}$. In discrete time, the effective closed form solution for the tax-adjusted Merton's solution can be easily attained through a myopic optimization problem.

In each period, given the pre-trade position of the risky assets as $\mathbf{y}_{t_k}$ and their tax basis prices $\mathbf{B}_{t_k}$, in which the positions with capital losses have already been liquidated and included in the risk-free asset position x_{t_k}, we first calculate the realized risky asset portfolio $\mathbf{v}_{t_k}$, and then rebalance to the tax-adjusted Merton's solution $\mathbf{y}_{t_k}^{c,\text{tax}}$. At time t_k, for the i-th risky asset the post-trade position:

$$y_{t_k^+,i} = \begin{cases} W_{t_k}^r\left(y_{t_k,i}^{c,\text{tax}} + \dfrac{y_{t_k,i}}{W_{t_k}^r} - v_{t_k,i}\right) & v_{t_k,i} < y_{t_k,i}^{c,\text{tax}} \\ \dfrac{y_{t_k,i}^{c,\text{tax}} y_{t_k,i}}{v_{t_k,i}} & v_{t_k,i} \geq y_{t_k,i}^{c,\text{tax}} \end{cases} \tag{3.35}$$

and the tax basis price:

$$B_{t_{k+1},i} = \begin{cases} \dfrac{B_{t_k,i} y_{t_k,i} + S_{t_k,i} W_{t_k}^r \left[y_{t_k,i}^{c,\text{tax}} - v_{t_k,i} \right]}{W_{t_k}^r\left(y_{t_k,i}^{c,\text{tax}} + \dfrac{y_{t_k,i}}{W_{t_k}^r} - v_{t_k,i}\right)} & v_{t_k,i} < y_{t_k,i}^{c,\text{tax}} \\ B_{t_k,i} & v_{t_k,i} \geq y_{t_k,i}^{c,\text{tax}} \end{cases}. \tag{3.36}$$

To get the post-trade risk-free asset position, we note the post-trade position of the i-th risky asset can also be calculated by

$$y_{t_k^+,i} = y_{t_k,i} + L_{t_k,i} - U_{t_k,i}. \tag{3.37}$$

which implies

$$L_{t_k,i} = \max(y_{t_k^+,i} - y_{t_k,i}, 0),\ U_{t_k,i} = \max(y_{t_k,i} - y_{t_k^+,i}, 0). \tag{3.38}$$

Relying on the above relation, we can get the post-trade risk-free asset position $x_{t_k^+}$ from $y_{t_k^+,i}$ through

$$x_{t_k^+} = x_{t_k} + \sum_{i=1}^{n} \left(\frac{U_{t_k,i}}{S_{t_k,i}} b(S_{t_k,i}, B_{t_k,i}) - L_{t_k,i} \right). \tag{3.39}$$

The above results depend upon the fact that in general the pre-trade and post-trade realized wealth is equal in each period, i.e., $W_{t_k^+}^r = W_{t_k}^r$. Refer to Appendices A.3 and A.4 for the detailed derivation of the formulas.

3.5.5 Hyper-cube Strategy (HC)

As we show in Section 3.4, the portfolio optimization under capital gain taxes has the similar feature of existing a no-trading region to the problem under transaction costs.

The hyper-cube strategy introduced in this section follows the known optimal strategy when there exists capital losses and rebalances the portfolio according to the current position in state space. In each period, if the current realized risky asset portfolio $\mathbf{v}_{t_k}$ lies inside a hyper-cube $\Omega_{t_k} = \{\mathbf{z}_{t_k} : \|\mathbf{z}_{t_k} - \mathbf{y}^{c,\mathrm{tax}}_{t_k}\|_\infty \le r_{t_k}\}$ centered at the tax-adjusted Merton's solution $\mathbf{y}^{c,\mathrm{tax}}_{t_k}$ with r_{t_k} the half of its side length,[6] HC suggests no trade. If it is outside the region, HC suggests making the trades such that the post-trade realized risky asset positions touches the boundary. The radius r_{t_k} is determined by the algorithm in the end of this section.

In each period, given the pre-trade position in the risky assets as $\mathbf{y}_{t_k}$ and the tax basis prices $\mathbf{B}_{t_k}$, we calculate the realized risky asset portfolio, and then rebalance according to rule we discussed above. The post-trade position of the i-th risky asset at time t_k is given by

$$y_{t_k^+,i} = \begin{cases} W^r_{t_k}(y^{c,\mathrm{tax}}_{t_k,i} - r_{t_k} + \dfrac{y_{t_k,i}}{W^r_{t_k}} - v_{t_k,i}) & v_{t_k,i} \le y^{c,\mathrm{tax}}_{t_k,i} - r_{t_k} \\ y_{t_k,i} & y^{c,\mathrm{tax}}_{t_k,i} - r_{t_k} < v_{t_k,i} < y^{c,\mathrm{tax}}_{t_k,i} + r_{t_k} \\ \dfrac{(y^{c,\mathrm{tax}}_{t_k,i} + r_{t_k})y_{t_k,i}}{v_{t_k,i}} & v_{t_k,i} \ge y^{c,\mathrm{tax}}_{t_k,i} + r_{t_k} \end{cases} \tag{3.40}$$

and the tax basis price can be computed by

$$B_{t_{k+1},i} = \begin{cases} \dfrac{B_{t_k,i}y_{t_k,i} + S_{t_k,i}W^r_{t_k}\left[y^{c,\mathrm{tax}}_{t_k,i} - r_{t_k} - v_{t_k,i}\right]}{W^r_{t_k}(y^{c,\mathrm{tax}}_{t_k,i} - r_{t_k} + \dfrac{y_{t_k,i}}{W^r_{t_k}} - v_{t_k,i})} & v_{t_k,i} < y^{c,\mathrm{tax}}_{t_k,i} - r_{t_k} \\ B_{t_k,i} & v_{t_k,i} \ge y^{c,\mathrm{tax}}_{t_k,i} - r_{t_k} \end{cases}. \tag{3.41}$$

We can get the post-trade risk-free asset position $x_{t_k^+}$ from the post-trade risky asset positions $y_{t_k^+,i}$ by the same method in RM. Refer to Appendix A.4 for the derivation of the formulas.

To determine a series of optimal radius r_{t_k} required in the trading strategy, we implement a two track policy approximation algorithm. First, by following a predetermined naive strategy to simulate the controlled dynamics step by step, we get the controlled scenarios distribution in each step. By using backward iteration, we determine the best radius of the hyper-cube that maximizes the expected final utility from the last step to the initial step. For instance, in the last step we find the best radius for the one period problem following the trading rule given in (3.40) and (3.41), and in the step before the last step we carry out

[6] We call it radius for simplicity in the sequel.

the same search for the best radius for that period but we will use the radius found in the last step when we simulate one step forward to reach the last period. To summarize, the algorithm can be described as

1. Decide a naive strategy to simulate to the step before the last step. The controlled asset positions at time $t_{(m-1)\Delta t}$ serve as the distribution of the starting positions for the last period. The realized Merton's strategy serves as the naive strategy.

2. Search for the optimal radius at time $t_{(m-1)\Delta t}$. We set up the search bound of the radius from the realized Merton's solution to to the furthest vertices of $\mathbb{S}_{t_k}$. This is a nonsmooth optimization with only one decision variable. Thus, we can perform a brute-force search, which is similar to the policy search for Bermudan swaption by Andersen (2000).

3. Go back to $t_{(m-2)\Delta t}$. Given the simulated paths in step 1 to $t_{(m-2)\Delta t}$, find the best radius at time $t_{(m-2)\Delta t}$ that maximizes the final expected utility function by following the policy given by step 2.

4. Iterate until reaching the first time step t_0.

5. Forward simulate according to the series of radius found in the previous steps.

Figure 3.15 displays the no-trading region with the trading polices obtained from RM and HC for a one period problem. It shows the RM strategy typically trades too much, but it ensures the post-trade relative risky asset portfolio is in the no-trading region. In high dimensions, when constraints are binding, the shape of the no-trading region will not be so regular, and our numerical results show RM performs well. The HC strategy suggests trading less than the optimal. Since the no-trading region is not so symmetric in general, its performance is not ensured better than RM.

3.5.6 Handle Borrowing

We need to formulate a rule when a forward trading strategy needs to finance purchase by borrowing cash from the risk-free account. Mathematically, we have to ensure the post-trade risk-free position $x^*_{t_k}$ nonnegative. Since HC which is derived by the corresponding

Figure 3.15: Illustration of the no-trading region and trading policy from RM and HC.

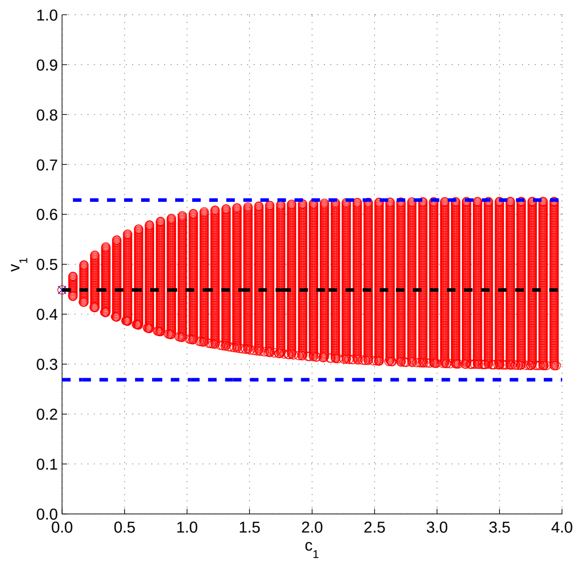

Note: The red dots form the no-trading region. The black dash line represents the policy of RM. The blue dash line represents the policy of HC. The parameters are $r_f = 5\%$, $\mu_1 = 10\%$, $\sigma_1 = 20\%$, $\gamma = -1$, $\tau_1 = 35\%$ $\Delta t = 1$ year.

geometric properties does not implicitly prohibit borrowing, we have to explicitly set up the rule to meet the borrowing constraint. Heuristically, we can either sell more or buy less risky assets. More precisely, purchase-less rule means that investors will buy λ percentage of the original suggested purchase $\mathbf{L}_{t_k}$ to guarantee exhausting the new post-trade risk-free asset position, i.e.

$$0 = x_{t_k^+} = x_{t_k} + \sum_{i=1}^{n} \left[\frac{U_{t_k,i}}{S_{t_k,i}} b(S_{t_k,i}, B_{t_k,i}) - \lambda L_{t_k,i} \right] \tag{3.42}$$

which yields the scaling factor

$$\lambda = \frac{x_{t_k} + \sum_{i=1}^{n} \frac{U_{t_k,i}}{S_{t_k,i}} b(S_{t_k,i}, B_{t_k,i})}{\sum_{i=1}^{n} L_{t_k,i}} \tag{3.43}$$

and the corresponding post-trade i-th risky asset position

$$y_{t_k^+,i} = y_{t_k,i} - U_{t_k,i} + \lambda L_{t_k,i} = y_{t_k,i} - U_{t_k,i} + \frac{x_{t_k} + \sum_{i=1}^{n} \frac{U_{t_k,i}}{S_{t_k,i}} b(S_{t_k,i}, B_{t_k,i})}{\sum_{i=1}^{n} L_{t_k,i}} L_{t_k,i}. \tag{3.44}$$

3.6 Duality Methods for Upper Bounds

After implementing a lower bound strategy, to evaluate how much better we could possibly reach, we need an upper bound, which is given by the duality methods in Brown et al. (2009) and Brown and Smith (2011). We follow the same outline and theorem used in Section 2.5, and we will not repeat here. We will discuss two upper bound methods in this section. One is the gradient-based upper bound method (termed GUB) and another is the value function-based upper bound method (termed VUB).

We compute two types of gradient-based penalty dual method. One is based on the frictionless model, and the other is based on the forcing realization model. The latter has been proved in Appendix A.3 that it is equivalent to a fictitious frictionless model with tax-adjusted returns and can be solved to optimality as well. We need to calculate the controlled positions of risk-free and risky assets at each time period. In the case of the Merton's model, the risk-free and risky asset positions are x_{t_k} and $\mathbf{y}_{t_k}$ at time t_k respectively

$$x_{t_k} = R_f^k x_0 + \sum_{j=0}^{k-1} R_f^{k-j}[\mathbf{1}'(\mathbf{U}_{t_j} - \mathbf{L}_{t_j})] \tag{3.45}$$

and

$$\mathbf{y}_{t_k} = (\mathbf{R}_{t_k} \cdot \dots \cdot \mathbf{R}_1) \cdot \mathbf{y}_0 + \sum_{j=0}^{k-1} \mathbf{R}_{t_k} \cdot \dots \cdot \mathbf{R}_{t_{j+1}}(\mathbf{L}_{t_j} - \mathbf{U}_{t_j}). \tag{3.46}$$

In the case of the forcing realization model, we only need to change the risky return $R_{t_k,i}$ above to be $(1-\tau_i)R_{t_k,i} + \tau_i$.

To compute the derivatives from the Merton's or the forcing realization model, we calculate the following gradient

$$\nabla_a W_T^n = \nabla_a \left(\sum_{j=0}^{m-1} [R_f^{m-j}[\mathbf{1}'(\mathbf{U}_{t_j} - \mathbf{L}_{t_j}) + \mathbf{L}_{t_j})] + \mathbf{R}_T \cdot \dots \cdot \mathbf{R}_{t_{j+1}} \mathbf{1}'(\mathbf{L}_{t_j} - \mathbf{U}_{t_j})] \right). \tag{3.47}$$

To get the explicitly form of this penalty, we need

$$\begin{aligned} \nabla_{\mathbf{L}_{t_k}} W_T^n =& - R_f^{m-k}\mathbf{1}' + \mathbf{R}_T \cdot \dots \cdot \mathbf{R}_{t_{k+1}}\mathbf{1}', \quad 0 \le k \le m-1 \\ \nabla_{\mathbf{U}_{t_k}} W_T^n =& R_f^{m-k}\mathbf{1}' - \mathbf{R}_T \cdot \dots \cdot \mathbf{R}_{t_{k+1}}\mathbf{1}', \quad 0 \le k \le m-1. \end{aligned} \tag{3.48}$$

On the other hand, the value function-based penalty function is written as

$$\pi = \sum_{k=0}^{m-1} (V_{t_{k+1}} - \mathbb{E}_{t_k}[V_{t_{k+1}}]). \tag{3.49}$$

Typically, value functions of primal problems are unknown and require a proxy at each time period that approximates the difference $V_{t_{k+1}} - \mathbb{E}_{t_k}[V_{t_{k+1}}]$ to characterize benefits from future information. Our implementation is based on the value function from the frictionless model or from the forcing realization model as the proxy. Both of them can be effectively solved to optimality. We apply the Gauss-Hermit quadrature method to compute the expectations numerically. For all the computation, we use 19 nodes in each dimension. Since the optimization problem is more difficult to solve after incorporating the value function-based penalty function, we only implement it for single and two risky asset cases. For GUB, the frictionless model without the constraint on the cash position have a larger feasible set than the taxes problem in general. The forcing realization model that is actually based on a heuristic trading strategy uses the original tax model, so its feasible set is the same as the original primal problem. For VUB, the dual feasibility of the value function-based penalty has been shown in Brown et al. (2009).

Garlappi et al. (2001), Wang (2008), and Tahar et al. (2010) have shown the value function for this model is non-convex. Therefore, the constructed upper bound optimization problem is non-convex. Haugh et al. (2014) propose a convex relaxation for this issue and point out that besides this convex relaxation extra reformulations and relaxations are still needed to attain a tractable solution method. In this work, first, we run global search optimization starting from 20 different initial points for the upper bounds in single or two risky asset cases. Second, we take the solution from RM as the initial point for the optimization in twenty risky asset cases. As Wang (2008) proves the primal problem of a one risky asset case is convex provided investors only take a one way trade, i.e., no simultaneous purchase or sale, the non-convex issue roots in the fact that investors may take a two way trade of realizing their loss first and then repurchasing. Intuitively the RM solution should not lie far away from the true optimal and it always realizes losses first. We compare testing results in twenty risky asset cases from running global optimizations and those from local optimizations given initial solutions from RM in Appendix A.2. We find the solutions are close. For high dimensions, we leave the investigation for a full solution such as convex-relaxation in future work.

3.7 Numerical Results

In this section, we assess the quality of the lower and upper bounds by (i) computing solutions of the basis examples in DeMiguel and Uppal (2005) for single and two risky asset cases; (ii) illustrating solutions for more parameter sets; (iii) providing solutions for twenty risky asset examples. All the results are converted to annualized certainty equivalent rates of return.

For the CRRA utility and a T year long horizon, the annualized certainty equivalent rate is defined by

$$\text{CER} = \left(\frac{\mathcal{U}^{-1}(\mathbb{E}[\mathcal{U}(W_T^r)])}{W_{t_0}^r}\right)^{1/T} - 1, \tag{3.50}$$

as the risk-free rate that makes investors indifferent between holding the optimal portfolio and earning the annual certainty equivalent rate over the next T years.

All the results are reported in a 95% confidence interval. All the simulations use the control variate from the frictionless model. All the computations start with one unit of wealth in risk-free asset. The duality gap is computed by "$(\text{CER}_{\text{upper}} - \text{CER}_{\text{lower}})/\text{CER}_{\text{lower}}$", where $\text{CER}_{\text{upper}}$ represents the annualized certainty equivalent rate computed for an upper bound and $\text{CER}_{\text{lower}}$ represents for a lower bound. In examples, we adopt the same tax rate for all the risky assets; denote CER to represent annualized certainty equivalent rates of portfolio return, CI to represent 95% confidence intervals of annualized certainty equivalent rates, and NT to represent results obtained from the frictionless model with corresponding parameters. For upper bounds that are based on the frictionless or forcing realization model, we only report the better results.[7] For comparison, we normalize the average CPU time of different methods according to that of RM. As a benchmark, RM takes less than a minutes to compute. The results for lower and upper bounds are computed by 2^9 to 2^{16} numbers of trials to reach a comparable accuracy, whereas the results for the CPU time comparison are according to 2^6 trails. All the computations are based on a Matlab implementation.

3.7.1 Model with One Risky Asset

For the one risky asset cases, we apply our new methods to the basis examples in DeMiguel and Uppal (2005) in Table 3.1 and include more challenging parameter sets to fully test the performance in Table 3.2. According to the results, the VF, MO, HC and RBH lower bound methods are comparable and near-optimal, whereas VUB always represents the best upper bound method. Among the lower bound methods, VF offers the best results in most of the cases. RM gives lower CERs than the others when the tax rate is higher than 10%, but it is computationally cheap, about two orders of magnitude faster than VF, MO and RBH. As HC has to implement a two track algorithm, it takes more time than RM, but it is still one order of magnitude faster than the previous three methods. In the case of a short horizon, as the cases in Table 3.1, the duality gaps are almost negligible. In the case

[7] We have not found any guidance of which model to choose. The results based on the frictionless model are better in most of time. The forcing realization model improves the results in several cases.

of a long horizon, especially for shorter rebalancing intervals, as the examples of $m = 30$ in Table 3.2, the gaps are a little wider. In Table 3.1 and Table 3.2 all the cases have the duality gaps smaller than 3%.

3.7.2 Model with Two Risky Assets

For the two risky asset cases, we apply our new methods to the basis examples in DeMiguel and Uppal (2005) in Table 3.3 and use more challenging parameter sets to fully test the performance in Table 3.4. Accordingly, the VF, MO, HC and RBH lower bound methods are comparable and near-optimal and VUB gives tight upper bounds. Among the lower bound methods, RBH gives the best results in most of the cases. Its dominance is a result of considering the effect from multiple periods. As is shown in Section 3.4, the no-trading regions vary with time steps. Similar to the results of the one risky asset, RM is computationally cheap, about two orders of magnitude faster than VF, MO and RBH; and HC is about one order of magnitude faster than them. Table 3.3 shows the impact of the correlation and the length of the investment horizon on the performance. The negative correlation and long horizon case represents the most difficult condition in terms of the width of the duality gaps. The largest gap is about 10%. The rest are all smaller than 5%. Table 3.4 illustrates the impact from asymmetric returns. Therein, MO works the best, indicating even in large trading intervals the limit solution proposed in Wang (2008) is near-optimal. The gaps on average are wider than those in Table 3.3.

3.7.3 Model with Twenty Risky Assets

In the twenty asset cases, we assume annual adjustment of the portfolio and give two examples based on twenty stocks in a 10-year-long and a 30-year-long horizon, respectively. We use the model parameters of the twenty stocks as transaction costs problem.

According to Table 3.5 and Table 3.6, MO exhibits robustness and produces the best lower bounds in many examples. Both HC and RM are much faster than the rest and do not sacrifice CER much. Typically, RM does not take more than a couple of minutes to compute to achieve the precision shown in the tables. Since the nonnegativity constraints will bind in those cases, similar to the transaction costs problem the shape of the no-trading region of the capital gain taxes problem will distort (see Broadie and Shen, 2013b). Hence, the performance of HC may not be better than RM in general. The same reason can be applied to the observation that it is different from the one and two risky asset cases where RBH works better than MO. In some cases of the 10-year-long example, GUB gives looser upper bounds than NT. That is reasonable because given the linear taxation rule and a particular path of return, the problem with capital gain taxes could produce higher wealth than the frictionless model. Brown and Smith (2011) show this situation leads to a looser upper bound than NT. In the 30-year-long horizon examples, GUB provides better upper bounds than NT. This comes from the fact that the problem with a longer horizon and the same length of rebalancing intervals has lower CER than the Merton's model for almost all the returns trials. In the 30-year-long horizon example all the duality gaps are smaller than 3%.

Table 3.1: Results of the one risky asset model for a seven-year-long horizon.

Parameters				Forward Strategies					Dual Bounds		Best Performance		
μ_1	σ_1	γ		VF	MO	HC	RM	RBH	VUB	NT	Strategy	Dual Bound	Gap
0.10	0.20	-1	CER(%)	6.37	6.35	6.36	6.24	6.36	6.37	7.25	6.37	6.37	0.0%
			CI(%)	±0.01	±0.01	±0.00	±0.00	±0.01	±0.01		VF	VUB	
0.10	0.20	-3	CER(%)	6.28	6.27	6.27	6.20	6.27	6.28	6.71	6.28	6.28	0.0%
			CI(%)	±0.01	±0.00	±0.00	±0.01	±0.01	±0.00		VF	VUB	
0.10	0.20	-7	CER(%)	6.23	6.22	6.23	6.19	6.23	6.23	6.45	6.23	6.23	0.0%
			CI(%)	±0.00	±0.00	±0.00	±0.00	±0.00	±0.00		HC	VUB	
0.12	0.25	-1	CER(%)	6.76	6.76	6.76	6.74	6.76	6.76	7.71	6.76	6.76	0.0%
			CI(%)	±0.01	±0.01	±0.01	±0.01	±0.01	±0.00		HC	VUB	
0.12	0.25	-3	CER(%)	6.46	6.46	6.46	6.44	6.46	6.47	6.94	6.47	6.47	0.1%
			CI(%)	±0.01	±0.01	±0.01	±0.00	±0.01	±0.00		HC	VUB	
0.12	0.25	-7	CER(%)	6.32	6.32	6.32	6.31	6.32	6.32	6.56	6.32	6.32	0.0%
			CI(%)	±0.00	±0.01	±0.00	±0.00	±0.00	±0.00		HC	VUB	
Average CPU Time				120	17	2	1	14	1501				

Note: The other parameters are: $r_f = 6\%$, $\tau_1 = 35\%$, $\Delta t = 1$ year, $m = 7$.

Those parameters are taken from DeMiguel and Uppal (2005).

Table 3.2: Results of the one risky asset model.

Parameters				Forward Strategies					Dual Bounds		Best Performance		
m	τ_1	γ		VF	MO	HC	RM	RBH	VUB	NT	Strategy	Dual Bound	Gap
10	10%	-1	CER(%)	7.00	7.00	7.00	7.00	7.00	7.01	7.17	7.00	7.01	0.1%
			CI(%)	±0.01	±0.01	±0.00	±0.00	±0.01	±0.01		VF	VUB	
10	30%	-1	CER(%)	6.62	6.61	6.61	6.58	6.61	6.65	7.17	6.62	6.65	0.5%
			CI(%)	±0.01	±0.01	±0.01	±0.00	±0.01	±0.01		VF	VUB	
10	50%	-1	CER(%)	6.14	6.12	6.14	6.05	6.14	6.24	7.17	6.14	6.24	1.6%
			CI(%)	±0.01	±0.01	±0.01	±0.01	±0.01	±0.01		HC	VUB	
30	50%	-1	CER(%)	6.17	6.16	6.18	6.04	6.19	6.33	7.20	6.19	6.33	2.3%
			CI(%)	±0.01	±0.01	±0.01	±0.01	±0.01	±0.01		RBH	VUB	
10	10%	-3	CER(%)	6.03	6.02	6.02	6.02	6.02	6.04	6.12	6.03	6.04	0.2%
			CI(%)	±0.00	±0.00	±0.00	±0.00	±0.00	±0.01		VF	VUB	
10	30%	-3	CER(%)	5.82	5.82	5.81	5.81	5.81	5.86	6.12	5.82	5.86	0.7%
			CI(%)	±0.01	±0.00	±0.01	±0.00	±0.01	±0.00		HC	VUB	
10	50%	-3	CER(%)	5.59	5.58	5.59	5.53	5.58	5.67	6.12	5.59	5.67	1.4%
			CI(%)	±0.01	±0.01	±0.01	±0.01	±0.01	±0.01		HC	VUB	
30	50%	-3	CER(%)	5.61	5.61	5.61	5.52	5.60	5.72	6.15	5.61	5.72	2.0%
			CI(%)	±0.01	±0.01	±0.01	±0.01	±0.01	±0.01		HC	VUB	
10	10%	-7	CER(%)	5.57	5.57	5.56	5.56	5.56	5.59	5.61	5.57	5.59	0.4%
			CI(%)	±0.00	±0.01	±0.00	±0.00	±0.00	±0.00		VF	VUB	
10	30%	-7	CER(%)	5.46	5.46	5.46	5.45	5.45	5.50	5.61	5.46	5.50	0.7%
			CI(%)	±0.01	±0.00	±0.00	±0.00	±0.01	±0.00		VF	VUB	
10	50%	-7	CER(%)	5.35	5.34	5.34	5.32	5.34	5.42	5.61	5.35	5.42	1.3%
			CI(%)	±0.01	±0.01	±0.01	±0.00	±0.01	±0.01		VF	VUB	
30	50%	-7	CER(%)	5.36	5.36	5.36	5.31	5.35	5.40	5.63	5.36	5.40	0.7%
			CI(%)	±0.01	±0.01	±0.01	±0.00	±0.01	±0.01		HC	VUB	
			Average CPU Time	150	20	3	1	18	2102				

Note: The other parameters are: $\mu_1 = 12\%$, $\sigma_1 = 25\%$, $r_f = 5\%$. $\Delta t = 3$ year for $m = 10$ and $\Delta t = 1$ year for $m = 30$.

Table 3.3: Results of the two risky asset model with annual rebalance.

Parameters			Forward Strategies					Dual Bounds		Best Performance		
ρ	m		VF	MO	HC	RM	RBH	VUB	NT	Strategy	Dual Bound	Gap
0.5	7	CER(%)	6.35	6.33	6.33	6.22	6.35	6.35	7.13	6.35	6.35	0.0%
		CI(%)	±0.01	±0.01	±0.01	±0.01	±0.01	±0.01		RBH	VUB	
0.5	10	CER(%)	6.39	6.37	6.38	6.28	6.39	6.40	7.13	6.39	6.40	0.2%
		CI(%)	±0.01	±0.01	±0.01	±0.00	±0.01	±0.00		RBH	VUB	
0.5	30	CER(%)	6.60	6.55	6.59	6.44	6.61	6.67	7.13	6.61	6.67	0.9%
		CI(%)	±0.01	±0.01	±0.01	±0.00	±0.01	±0.01		RBH	VUB	
0.0	7	CER(%)	6.42	6.41	6.41	6.24	6.42	6.43	7.59	6.42	6.43	0.2%
		CI(%)	±0.01	±0.01	±0.01	±0.01	±0.01	±0.00		RBH	VUB	
0.0	10	CER(%)	6.48	6.46	6.48	6.32	6.50	6.51	7.59	6.50	6.51	0.2%
		CI(%)	±0.01	±0.01	±0.01	±0.01	±0.01	±0.01		RBH	VUB	
0.0	30	CER(%)	6.78	6.73	6.76	6.57	6.79	7.03	7.59	6.79	7.03	3.5%
		CI(%)	±0.01	±0.01	±0.01	±0.01	±0.01	±0.01		RBH	VUB	
-0.5	7	CER(%)	6.61	6.61	6.60	6.52	6.64	6.65	8.80	6.64	6.65	0.2%
		CI(%)	±0.01	±0.01	±0.01	±0.01	±0.01	±0.01		RBH	VUB	
-0.5	10	CER(%)	6.73	6.73	6.71	6.65	6.76	6.83	8.80	6.76	6.83	1.0%
		CI(%)	±0.01	±0.01	±0.01	±0.01	±0.01	±0.01		RBH	VUB	
-0.5	30	CER(%)	7.24	7.22	7.26	7.06	7.25	7.95	8.80	7.26	7.95	9.5%
		CI(%)	±0.01	±0.01	±0.01	±0.01	±0.01	±0.01		RBH	VUB	
Average CPU Time			567	19	2	1	17	4087				

Note: The other parameters are: $\mu_1 = \mu_2 = 10\%$, $\sigma_1 = \sigma_2 = 20\%$, $\tau_1 = \tau_2 = 35\%$, $r_f = 6\%$, $\gamma = -2$, $\Delta t = 1$ year. Those parameters are taken from DeMiguel and Uppal (2005).

Table 3.4: Results of the two risky asset model with asymmetric returns.

Parameters				Forward Strategies					Dual Bounds		Best Performance		
m	τ_1	γ		VF	MO	HC	RM	RBH	VUB	NT	Strategy	Dual Bound	Gap
10	10%	-1	CER(%)	8.70	8.70	8.69	8.69	8.70	8.73	8.97	8.70	8.73	0.3%
			CI(%)	±0.01	±0.00	±0.01	±0.01	±0.01	±0.00		MO	VUB	
10	30%	-1	CER(%)	8.09	8.08	8.06	8.03	8.75	8.23	8.97	8.09	8.23	1.7%
			CI(%)	±0.01	±0.01	±0.01	±0.01	±0.01	±0.01		VF	VUB	
10	50%	-1	CER(%)	7.32	7.30	7.30	7.18	8.45	7.69	8.97	7.34	7.69	4.8%
			CI(%)	±0.01	±0.01	±0.01	±0.01	±0.01	±0.01		RBH	VUB	
10	10%	-3	CER(%)	6.84	6.84	6.84	6.84	6.84	6.87	6.99	6.84	6.87	0.4%
			CI(%)	±0.01	±0.01	±0.01	±0.00	±0.01	±0.01		MO	VUB	
10	30%	-3	CER(%)	6.51	6.52	6.50	6.50	6.50	6.68	6.99	6.52	6.68	2.5%
			CI(%)	±0.01	±0.01	±0.01	±0.01	±0.01	±0.01		MO	VUB	
10	50%	-3	CER(%)	6.11	6.13	6.12	6.06	6.13	6.42	6.99	6.13	6.42	4.7%
			CI(%)	±0.01	±0.01	±0.01	±0.01	±0.01	±0.01		MO	VUB	
10	10%	-7	CER(%)	5.96	5.96	5.96	5.96	5.95	5.98	6.04	5.96	5.98	0.3%
			CI(%)	±0.01	±0.01	±0.01	±0.00	±0.01	±0.01		HC	VUB	
10	30%	-7	CER(%)	5.79	5.80	5.79	5.79	5.78	5.87	6.04	5.80	5.87	1.2%
			CI(%)	±0.01	±0.01	±0.01	±0.01	±0.01	±0.01		MO	VUB	
10	50%	-7	CER(%)	5.59	5.60	5.60	5.57	5.60	5.76	6.04	5.60	5.76	2.9%
			CI(%)	±0.01	±0.01	±0.01	±0.01	±0.01	±0.01		MO	VUB	
Average CPU Time				650	27	3	1	32	6574				

Note: The other parameters are: $\tau_2 = \tau_1$, $\mu_1 = 15\%$, $\mu_2 = 12\%$, $\sigma_1 = 30\%$, $\sigma_2 = 25\%$, $\rho = 30\%$, $r_f = 5\%$, $\Delta t = 3$ year.

Table 3.5: Results of the twenty risky asset model for a 10-year-long horizon.

Parameters				Forward Strategies				Dual Bounds		Best Performance		
m	τ	γ		MO	HC	MR	RBH	GUB	NT	Strategy	Dual Bound	Gap
10	10%	-1	CER(%)	3.84	3.84	3.84	3.84	3.84	4.03	3.84	3.84	0.0%
			CI(%)	±0.01	±0.01	±0.01	±0.01	±0.01		HC	GUB	
10	30%	-1	CER(%)	3.42	3.41	3.41	3.42	3.61	4.03	3.42	3.61	5.6%
			CI(%)	±0.01	±0.01	±0.01	±0.01	±0.01		HC	GUB	
10	50%	-1	CER(%)	2.87	2.85	2.85	2.87	3.70	4.03	2.87	3.70	28.9%
			CI(%)	±0.01	±0.01	±0.01	±0.01	±0.02		RBH	GUB	
10	10%	-3	CER(%)	2.41	2.41	2.41	2.40	2.43	2.42	2.41	2.42	0.4%
			CI(%)	±0.01	±0.00	±0.00	±0.01	±0.01		HC	NT	
10	30%	-3	CER(%)	2.34	2.33	2.33	2.33	2.57	2.42	2.34	2.42	3.4%
			CI(%)	±0.02	±0.01	±0.01	±0.01	±0.02		HC	NT	
10	50%	-3	CER(%)	2.09	2.09	2.09	2.09	2.70	2.42	2.09	2.42	15.7%
			CI(%)	±0.01	±0.01	±0.01	±0.01	±0.01		HC	NT	
10	10%	-7	CER(%)	1.20	1.20	1.20	1.19	1.20	1.20	1.20	1.20	0.0%
			CI(%)	±0.00	±0.00	±0.00	±0.01	±0.01		HC	GUB	
10	30%	-7	CER(%)	1.19	1.19	1.19	1.19	1.28	1.20	1.19	1.20	0.1%
			CI(%)	±0.00	±0.00	±0.00	±0.01	±0.02		HC	GUB	
10	50%	-7	CER(%)	1.18	1.18	1.18	1.19	1.34	1.20	1.18	1.20	0.2%
			CI(%)	±0.00	±0.00	±0.01	±0.01	±0.01		HC	GUB	
Average CPU Time				1311	5	1	746	1523				

Table 3.6: Results of the twenty risky asset model for a 30-year-long horizon.

Parameters				Forward Strategies				Dual Bounds		Best Performance		
m	τ	γ		MO	HC	MR	RBH	GUB	NT	Strategy	Dual Bound	Gap
30	10%	-1	CER(%)	3.87	3.87	3.87	3.87	3.87	4.03	3.87	3.87	0.0%
			CI(%)	±0.01	±0.00	±0.00	±0.00	±0.01		MR	GUB	
30	30%	-1	CER(%)	3.52	3.48	3.48	3.51	3.52	4.03	3.52	3.52	0.0%
			CI(%)	±0.01	±0.01	±0.01	±0.01	±0.01		MO	GUB	
30	50%	-1	CER(%)	3.06	2.99	2.95	3.06	3.07	4.03	3.06	3.07	0.1%
			CI(%)	±0.01	±0.01	±0.01	±0.01	±0.01		MO	GUB	
30	10%	-3	CER(%)	2.41	2.39	2.41	2.38	2.42	2.42	2.41	2.42	0.4%
			CI(%)	±0.00	±0.01	±0.00	±0.01	±0.01		MO	GUB	
30	30%	-3	CER(%)	2.35	2.33	2.34	2.33	2.37	2.42	2.35	2.37	0.9%
			CI(%)	±0.02	±0.01	±0.02	±0.01	±0.01		MO	GUB	
30	50%	-3	CER(%)	2.15	2.14	2.13	2.14	2.19	2.42	2.15	2.19	2.3%
			CI(%)	±0.02	±0.01	±0.01	±0.02	±0.01		MO	GUB	
30	10%	-7	CER(%)	1.20	1.18	1.20	1.17	1.21	1.20	1.20	1.20	0.0%
			CI(%)	±0.00	±0.01	±0.01	±0.01	±0.01		MO	NT	
30	30%	-7	CER(%)	1.19	1.17	1.19	1.17	1.19	1.20	1.19	1.19	0.0%
			CI(%)	±0.00	±0.01	±0.01	±0.01	±0.01		MO	GUB	
30	50%	-7	CER(%)	1.18	1.16	1.16	1.17	1.18	1.20	1.18	1.18	0.0%
			CI(%)	±0.00	±0.01	±0.01	±0.01	±0.00		MO	GUB	
			Average CPU Time	2433	22	1	11133	2217				

3.8 Concluding Remarks

In this thesis we carry out a computational study of optimal investment decisions with taxes over multiple periods to maximize the expected utility of terminal realized wealth. Our general model considers risk aversion, nonnegativity constraints on portfolio positions, and capital gain taxes. The tax model is similar to the one in Dammon et al. (2001). We allow wash sales, rule out "shorting against the box", and prohibit tax forgiveness at maturity.

After formulating the problem as a dynamic programming problem with continuous decision space, we sample returns from the continuous distribution directly, which leaves us a dynamic program with continuous decision and state spaces. We provide detailed ingredients of effective error control in each part of the approximate dynamic programming backward iteration algorithm. Accordingly, in each step of the iteration the relative numerical error in approximating the value function by a polynomial basis function measured by the l_∞ norm is about 10^{-5} and by the l_2 norm is about 10^{-10}.

Relying on the highly accurate numerical solution and choosing relative basis prices and realized risky asset portfolio as a set of two new state variables, we visualize and understand the no-trading region better and find very close relation to the transaction costs problem. Specifically, for the single risky asset case, besides illustrating the optimal trading, we quantitatively characterize the selling and purchasing boundaries by using two Merton's problems with effective risky returns. For the two risky asset case, we numerically show the no-trading region that has similar shape and parameter sensitivity to that of the transaction costs problem.

We also propose five lower bound strategies and assess their quality by comparing with upper bounds. In most of our numerical examples, the duality gaps are smaller than 5%. We are able to solve problems for both lower and upper bounds up to 20 risky assets and 30 periods.

The future research direction includes refining the tax model to embody tax rules that are closer to the reality such as limited use of capital losses, enriching the return model as we mentioned in Section 2.7, and exploiting proper optimization reformulation that converts the non-convex problem to a convex one.

Bibliography

M. Akian, J. L. Menaldi, and A. Sulem. On an investment-consumption model with transaction costs. *SIAM Journal on Control and Optimization*, 34(1):329–364, 1996.

L. Andersen. A simple approach to the pricing of Bermudan swaptions in the multi-factor market model. *Journal of Computational Finance*, 3(1):5–32, 2000.

L. Andersen and M. Broadie. Primal-dual simulation algorithm for pricing multidimensional American options. *Management Science*, 50(9):1222–1234, 2004.

C. Atkinson and P. Ingpochai. The influence of correlation on multi-asset portfolio optimization with transaction costs. *Journal of Computational Finance*, 10:53–96, 2006.

C. Atkinson and S. Mokkhavesa. Multi-asset portfolio optimization with transaction cost. *Applied Mathematical Finance*, 11:95–123, 2004.

C. Atkinson, S. R. Pliska, and P. Wilmott. Portfolio management with transaction costs. *Proceedings of the Royal Society of London. Series A: Mathematical, Physical and Engineering Sciences*, 453(1958):551–562, 1997.

P. Balduzzi and A. W. Lynch. Transaction costs and predictability: Some utility cost calculations. *Journal of Financial Economics*, 52(1):47–78, 1999.

F. Black and R. Litterman. Global portfolio optimization. *Financial Analysts Journal*, 48: 28–43, 1992.

P. Boyle, M. Broadie, and P. Glasserman. Monte Carlo methods for security pricing. *Journal of Economic Dynamics and Control*, 21:31267–1322, 1997.

M. W. Brandt. Portfolio choice problems. In Y. Ait-Sahalia and L. P. Hansen, editors, *Handbooks of Financial Econometrics*, pages 269–336. Elsevier, 2010.

M. W. Brandt, A. Goyal, P. Santa-Clara, and J. R. Stroud. A simulation approach to dynamic portfolio choice with an application to learning about return predictability. *Review of Financial Studies*, 18(3):831–873, 2005.

M. Broadie. Computing efficient frontiers using estimated parameters. *Annals of Operations Research*, 45(1):21–58, 1993.

M. Broadie and W. Shen. Numerical solutions to dynamic portfolio problems with upper bounds. Working Paper, Columbia University, 2013a.

M. Broadie and W. Shen. High dimensional portfolio optimization with transaction costs. Working Paper, Columbia University, 2013b.

M. Broadie, Y. Du, and C. C. Moallemi. Risk estimation via regression. Working Paper, Columbia University, 2011.

D. B. Brown and J. Smith. Dynamic portfolio optimiztion with transaction costs: Heuristics and dual bounds. *Management Science*, 57:1110–1377, 2011.

D. B. Brown, J. Smith, and P. Sun. Information relaxations and duality in stochastic dynamic programs. *Operations Research*, 58:785–801, 2009.

J. Y. Campbell, J. Cocco, F. Gomes, P. J. Maenhout, and L. M. Viceira. Stock market mean reversion and the optimal equity allocation of a long-lived investor. *European Finance Review*, 5(3):269–292, 2001.

J. Choi, M. Sirbu, and G. Zitkovic. Shadow prices and well-posedness in the problem of optimal investment and consumption with transaction costs. *arXiv preprint arXiv:1204.0305*, 2013.

G. M. Constantinides. Multiperiod consumption and investment behavior with convex transactions costs. *Management Science*, 25:1127–1137, 1979.

G. M. Constantinides. Capital market equilibrium with personal tax. *Econometrica: Journal of the Econometric Society*, pages 611–636, 1983.

G. M. Constantinides. Optimal stock trading with personal taxes: Implications for prices and the abnormal January returns. *Journal of Financial Economics*, 13(1):65–89, 1984.

G. M. Constantinides. Capital market equilibrium with transactions costs. *Journal of Political Economy*, 94:842–862, 1986.

J. Cox and C. Huang. Optimum consumption and portfolio policies when asset prices follow a diffusion process. *Journal of Economic Theory*, 49:33–83, 1989.

J. Cvitanic. Theory of portfolio optimization in markets with frictions. In E. Jouini, J. Cvitanic, and M. Musiela, editors, *Handbooks in Mathematical Finance*. Cambridge University Press, 2001.

M. Dai and Y. Zhong. Penalty methods for continuous-time portfolio selection with proportional transaction costs. *The Journal of Computational Finance*, 13(3):1–31, 2010.

M. Dai, H. Liu, and Y. Zhong. Optimal consumption and investment with asymmetric long-term/short-term capital gains taxes. Working Paper, Washington University, 2012.

R. Dammon and C. Spatt. The optimal trading and pricing of securities with asymmetric capital gains taxes and transaction costs. *Review of Financial Studies*, 9(3):921–952, 1996.

R. Dammon and C. Spatt. Taxes and investment choice. *The Annual Review of Financial Economics*, 4(1):411–429, 2012.

R. Dammon, K. Dunn, and C. Spatt. A reexamination of the value of tax options. *Review of Financial Studies*, 2(3):341–372, 1989.

R. Dammon, C. Spatt, and H. Zhang. Optimal consumption and investment with capital gains taxes. *Review of Financial Studies*, 14(3):583–616, 2001.

R. Dammon, H. Zhang, and C. Spatt. Diversification and capital gains taxes with multiple risky assets. Working Paper, Tepper School of Business, 2002.

R. Dammon, C. Spatt, and H. Zhang. Optimal asset location and allocation with taxable and tax-deferred investing. *The Journal of Finance*, 59(3):999–1037, 2004.

M. H. A. Davis and I. Karatzas. A deterministic approach to optimal stopping. In F.P. Kelly, editor, *Probability, Statistics and Optimization: A Tribute to Peter Whittle*, pages 455–466. Chichester, 1994.

M. H. A. Davis and A. R. Norman. Portfolio selection with transaction costs. *Mathematics of Operations Research*, 15:676–713, 1990.

V. DeMiguel and R. Uppal. Portfolio investment with the exact tax basis via nonlinear programming. *Management Science*, 51(2):277–290, 2005.

V. V. Desai, V. F. Farias, and C. C. Moallemi. Pathwise optimization for optimal stopping problems. *Management Science*, 58(12):2292–2308, 2012.

B. Dumas and E. Luciano. An exact solution to a dynamic portfolio choice problem under transactions costs. *The Journal of Finance*, 46:577–595, 1991.

P. Dybvig and H. K. Koo. Investment with taxes. Working Paper, Washington University, 1996.

J. Fan, Y. Fan, and J. Lv. High dimensional covariance matrix estimation using a factor model. *Journal of Econometrics*, 147(1):186–197, 2008.

M. F. Gallmeyer and S. Srivastava. Arbitrage and the tax code. *Mathematics and Financial Economics*, 4(3):183–221, 2011.

M. F. Gallmeyer, R. Kaniel, and S. Tompaidis. Tax management strategies with multiple risky assets. *Journal of Financial Economics*, 80(2):243–291, 2006.

L. Garlappi and G. Skoulakis. Numerical solutions to dynamic portfolio problems: The case for value function iteration using Taylor approximation. *Computational Economics*, 33:193–207, 2009.

L. Garlappi and G. Skoulakis. Solving consumption and portfolio choice problems: The state variable decomposition method. *The Review of Financial Study*, 23:3346–3400, 2010.

L. Garlappi, V. Naik, and J. Slive. Portfolio selection with multiple assets and capital gains taxes. Working Paper, The University of British Columbia, 2001.

J. Gaspar and K. L. Judd. Solving large-scale rational-expectations models. *Macroeconomic Dynamics*, 1:45–75, 1997.

S. Gerhold, J. Muhle-Karbe, and W. Schachermayer. The dual optimizer for the growth-optimal portfolio under transaction costs. *Finance and Stochastics*, pages 1–30, 2011.

S. Gerhold, P. Guasoni, J. Muhle-Karbe, and W. Schachermayer. Transaction costs, trading volume, and the liquidity premium. *Finance and Stochastics*, pages 1–37, 2013.

J. Goodman and D. N. Ostrov. Balancing small transaction costs with loss of optimal allocation in dynamic stock trading strategies. *SIAM Journal on Applied Mathematics*, 70(6):1977–1998, 2010.

M. B. Haugh and L. Kogan. Pricing American options: A duality approach. *Operations Research*, 52(2):258–270, 2004.

M. B. Haugh, G. Iyengar, and C. Wang. Tax-aware dynamic asset allocation. Working Paper, Columbia University, 2014.

S. L. Heston. A closed-form solution for options with stochastic volatility with applications to bond and currency options. *Review of financial studies*, 6(2):327–343, 1993.

K. Janecek and S. Shreve. Asymptotic analysis for optimal investment and consumption with transaction costs. *Finance and Stochastics*, 8:181–206, 2004.

K. L. Judd. *Numerical Methods in Economics*. MIT Press, 1998.

K. L. Judd and A. Solnick. Numerical dynamic programming with shape-preserving splines. Working Paper, Stanford University, 1994.

J. Kallsen and J. Muhle-Karbe. On using shadow prices in portfolio optimization with transaction costs. *Annals of Applied Probability*, 20:1341–1358, 2010.

M. S. Kimball, C. R. Sahm, and M. D. Shapiro. Imputing risk tolerance from survey responses. *Journal of the American Statistical Association*, 103(483):1028–1038, 2008.

G. Lai, F. Margot, and N. Secomandi. An approximate dynamic programming approach to benchmark practice-based heuristics for natural gas storage valuation. *Operations Research*, 58(3):564–582, 2010.

G. Lai, M. Wang, S. Kekre, A. Scheller-Wolf, and N. Secomandi. Valuation of storage at a liquefied natural gas terminal. *Operations Research*, 59(3):602–616, 2011.

H. E. Leland. Optimal portfolio implementation with transactions costs and capital gains taxes. Working Paper, Haas School of Business, 2000.

H. Liu. Optimal consumption and investment with transaction costs and multiple risky assets. *The Journal of Finance*, 6:289–338, 2004.

H. Liu and M. Loewenstein. Optimal portfolio selection with transaction costs and finite horizons. *The Review of Financial Study*, 15:805–835, 2002.

F. A. Longstaff and E. S. Schwartz. Valuing American options by simulation: A simple least-squares approach. *The Review of Financial Studies*, 14:113–147, 2001.

A. W. Lynch and P. Balduzzi. Predictability and transaction costs: The impact on rebalancing rules and behavior. *The Journal of Finance*, 55(5):2285–2309, 2000.

A. W. Lynch and S. Tan. Multiple risky assets, transaction costs and return predictability: Allocation rules and implications for U.S. investors. *Journal of Financial and Quantitative Analysis*, 45:1015–1053, 2010.

M. Magill and G. M. Constantinides. Portfolio selection with transaction costs. *Journal of Economic Theory*, 13(2):245–263, 1976.

R. C. Merton. Lifetime portfolio selection under uncertainty: The continuous time model. *Review of Economics and Statistics*, 51:247–257, 1969.

R. C. Merton. Optimum consumption and portfolio rules in a continuous time model. *The Journal of Economic Theory*, 3:373–413, 1971.

R. C. Merton. Option pricing when underlying stock returns are discontinuous. *Journal of financial economics*, 3(1):125–144, 1976.

R. C. Merton. On estimating the expected return on the market: An exploratory investigation. *Journal of Financial Economics*, 8:323–361, 1980.

A. Metrick. A natural experiment in "jeopardy!". *American Economic Review*, 85(1):240–53, 1995.

A. J. Morton and S. R. Pliska. Optimal portfolio management with fixed transaction costs. *Mathematical Finance*, 5(4):337–356, 1995.

J. M. Mulvey and H. Vladimirou. Stochastic network programming for financial planning problems. *Management Science*, 38:1642–1664, 1992.

K. Muthuraman and S. Kumar. Multidimensional portfolio optimization with proportional transaction costs. *Mathematical Finance*, 16:301–335, 2006.

K. Muthuraman and H. Zha. Simulation based portfolio optimization for large portfolios with transaction costs. *Mathematical Finance*, 18:115–134, 2008.

B. Oksendal and A. Sulem. Optimal consumption and portfolio with both fixed and proportional transaction costs. *Society for Industrial and Applied Mathematics*, 6:1765–1790, 2002.

S. R. Pliska. A stochastic calculus model of continuous trading: Optimal portfolios. *Mathematics of Operations Research*, 11(2):371–382, 1986.

L. C. G. Rogers. Monte Carlo valuation of American options. *Mathematical Finance*, 12 (3):271–286, 2002.

L. C. G. Rogers. Pathwise stochastic optimal control. *SIAM Journal on Control and Optimization*, 46(3):1116–1132, 2007.

J. Rust. Numerical dynamic programming in economics. In *Handbook of Computational Economics*, volume 1, pages 619–729. Elsevier, 1996.

M. Schroder. Optimal portfolio selection with fixed transaction costs: Numerical solutions. Working Paper, Michigan State University, 1995.

W. F. Sharpe. Imputing expected security returns from portfolio composition. *Journal of Financial and Quantitative Analysis*, 9:463–472, 1974.

S. E. Shreve and H. M. Soner. Optimal investment and consumption with transactions costs. *The Annals of Applied Probability*, 4:609–692, 1994.

A. H. Stroud. *Approximate Calculation of Multiple Integrals*. Prentice-Hall, 1971.

I. B. Tahar, H. M. Soner, and N. Touzi. The dynamic programming equation for the problem of optimal investment under capital gains taxes. *SIAM Journal on Control and Optimization*, 46(5):1779–1801, 2007.

I. B. Tahar, H. M. Soner, and N. Touzi. Merton problem with taxes: characterization, computation, and approximation. *SIAM Journal on Financial Mathematics*, 1(1):366–395, 2010.

J. H. van Binsbergen and M. Brandt. Solving dynamic portfolio choice problems by recursing on optimized portfolio weights or on the value function? *Computational Economics*, 29: 355–368, 2007.

Z. Wang. *Optimal Dynamic Allocation Between Taxable and Nontaxable Assets*. PhD thesis, Columbia University, 2008.

Appendix A

Appendix

A.1 Homotheticity and Scaling

Proposition 4. *Suppose $\mathcal{U}(x) = x^\gamma/\gamma$ or $\mathcal{U}(x) = \ln(x)$. Then the certainty equivalent C_{t_k} of the value function V_{t_k} at time t_k has the homothetic property: for $\theta > 0$*

$$C_{t_k}(\theta x_{t_k}, \theta \mathbf{y}_{t_k}) = \theta C_{t_k}(x_{t_k}, \mathbf{y}_{t_k}) \tag{A.1}$$

Proof. Recall the feasible set $\mathbb{A}_{t_k}$ of the equation (2.3). Denote $\mathbb{A}_{t_k}(x_{t_k}, \mathbf{y}_{t_k})$ the feasible set for the pre-trade positions $(x_{t_k}, \mathbf{y}'_{t_k})$.

From the equation (2.2), for any $\theta > 0$ and t_k we have

$$\mathbb{A}_{t_k}(\theta x_{t_k}, \theta \mathbf{y}_{t_k}) = \{(\theta \mathbf{L}_{t_k}, \theta \mathbf{U}_{t_k}) : (\mathbf{L}_{t_k}, \mathbf{U}_{t_k}) \in \mathbb{A}_{t_k}(x_{t_k}, \mathbf{y}_{t_k})\} \tag{A.2}$$

Thus, in the last time step the value function is

$$\begin{aligned}
&V_{T-\Delta t}(\theta x_{T-\Delta t}, \theta \mathbf{y}_{T-\Delta t}) \\
=& \max_{\mathbb{A}_{T-\Delta t}(\theta x_{T-\Delta t}, \theta \mathbf{y}_{T-\Delta t})} \mathbb{E}_{T-\Delta t}[\mathcal{U}(\theta x_T + \theta 1' \mathbf{y}_T)] \\
=& \begin{cases} \theta^\gamma \max_{\mathbb{A}_{T-\Delta t}(x_{T-\Delta t}, \mathbf{y}_{T-\Delta t})} \mathbb{E}_{T-\Delta t}[\mathcal{U}(x_T + 1' \mathbf{y}_T)] & \gamma \leq 1, \gamma \neq 0 \\ \ln \theta + \max_{\mathbb{A}_{T-\Delta t}(x_{T-\Delta t}, \mathbf{y}_{T-\Delta t})} \mathbb{E}_{T-\Delta t}[\mathcal{U}(x_T + 1' \mathbf{y}_T)] & \gamma = 0 \end{cases}
\end{aligned} \tag{A.3}$$

Using the relation (A.2) and the Bellman principle gives

$$
\begin{aligned}
V_{t_k}(\theta x_{t_k}, \theta \mathbf{y}_{t_k}) &= \max_{\{(\mathbf{L}_{t_s}, \mathbf{U}_{t_s})\}_{t_s=t_k}^{T-\Delta t}} \mathbb{E}_{t_k}\{\mathcal{U}(\theta x_T + \theta 1' \mathbf{y}_T)\}, \quad k = 0, ..., m-1 \\
&= \max_{(\mathbf{L}_{t_k}, \mathbf{U}_{t_k})} \mathbb{E}_{t_k}\left[\max_{\{(\mathbf{L}_{t_s}, \mathbf{U}_{t_s})\}_{t_s=t_{k+1}}^{T-\Delta t}} \mathbb{E}_{t_{k+1}}\{\mathcal{U}(\theta x_T + \theta 1' \mathbf{y}_T)\} \right] \\
&= \max_{(\mathbf{L}_{t_k}, \mathbf{U}_{t_k})} \mathbb{E}_{t_k}\left[\max_{(\mathbf{L}_{t_{k+1}}, \mathbf{U}_{t_{k+1}})} \mathbb{E}_{t_{k+1}}\Big[\max_{\{(\mathbf{L}_{t_s}, \mathbf{U}_{t_s})\}_{t_s=t_{k+2}}^{T-\Delta t}} \mathbb{E}_{t_{k+2}}\{\mathcal{U}(\theta x_T + \theta 1' \mathbf{y}_T)\}\Big] \right] \\
&= \begin{cases} \theta^{\gamma} V_{t_k}(x_{t_k}, \mathbf{y}_{t_k}) & \gamma \le 1, \gamma \ne 0 \\ \ln \theta + V_{t_k}(x_{t_k}, \mathbf{y}_{t_k}) & \gamma = 0 \end{cases}.
\end{aligned}
$$

Recall $C_{t_k}(x_{t_k}, \mathbf{y}_{t_k}) = \mathcal{U}^{-1}(V_{t_k}(x_{t_k}, \mathbf{y}_{t_k}))$. Hence $C_{t_k}(\theta x_{t_k}, \theta \mathbf{y}_{t_k}) = \theta C_{t_k}(x_{t_k}, \mathbf{y}_{t_k})$.

We prove the homothetic property for the last period in the equation (A.3) and by backward induction we obtain the conclusion. A similar proof can be found in many relevant papers (see, e.g., Constantinides, 1986; Davis and Norman, 1990; Shreve and Soner, 1994). □

A.2 Approximation Accuracy with and without CE Transformation

To illustrate the approximation accuracy of different types of polynomials and the benefit of using certainty equivalents, Table A.1 investigates the approximation accuracy calculated by different methods. Refer to the caption of Table A.1 for the relevant definition. Approximating certainty equivalent functions is better than approximating value functions directly in terms of prediction errors. The level of the risk aversion coefficients γ determines how well approximating certainty equivalent functions perform. In upper panel $\gamma = -2$. For CS(3), using the transformation cuts the mean squared relative predicting error by a factor of 4 and cuts the maximum relative predicting error by a factor of 2. The middle panel is based on $\gamma = -7$. For PS(4), using the transformation cuts the mean squared relative predicting error by a factor of 45 and cuts the maximum relative predicting error by a factor of 6. In bottom panel $\gamma = -13$. For CS(3), using the transformation cuts the mean squared relative predicting error by a factor of 4727 and cuts the maximum relative predicting error by a factor of 30. On the other hand, by comparing prediction errors yield by various polynomials in left panel, it is hard to conclude the general winner. However, when the risk averse coefficient γ is large, CS(3) works the best; and PS(4) and PS(5) methods beat CS(3).

A.3 Extra Properties and Forcing Realization Model

In Section 3.5.4 and 3.5.5, the derivation rests on the fact that the pre-trade and post-trade realized wealth is equal regardless of what the trades are, i.e., $W^r_{t_k} = W^r_{t_k^+}$. Intuitively, it must be true by virtue of the self-financing feature of the model. Let us prove it explicitly in the section. To this end, recall the controlled dynamics is

$$\begin{pmatrix} x_{t_k^+} \\ y_{t_k^+,i} \end{pmatrix} = \begin{pmatrix} x_{t_k} + \sum_{i=1}^{n} \left[\frac{U_{t_k,i}}{S_{t_k,i}} b(S_{t_k,i}, B_{t_k,i}) - L_{t_k,i} \right] \\ y_{t_k,i} + L_{t_k,i} - U_{t_k,i} \end{pmatrix}. \tag{A.4}$$

The realized wealth before trading is

$$W^r_{t_k} = x_{t_k} + \sum_{i=1}^{n} \frac{y_{t_k,i}}{S_{t_k,i}} b(S_{t_k,i}, B_{t_k,i}). \tag{A.5}$$

If we immediately liquidate the entire position after any trading, the post-trade realized wealth can be calculated as

$$W^r_{t_k^+} = x_{t_k^+} + \sum_{i=1}^{n} \frac{y_{t_k^+,i}}{S_{t_k,i}} b(S_{t_k,i}, B_{t_k^+,i}) \tag{A.6}$$

where

$$B_{t_k^+,i} = \frac{B_{t_k,i}(y_{t_k,i} - U_{t_k,i}) + S_{t_k,i} L_{t_k,i}}{y_{t_k,i} + L_{t_k,i} - U_{t_k,i}}. \tag{A.7}$$

Simplifying the expression for the post-trade realized wealth gives

$$W^r_{t_k^+} = x_{t_k} + \sum_{i=1}^{n} \left[\frac{U_{t_k,i}}{S_{t_k,i}} b(S_{t_k,i}, B_{t_k,i}) - L_{t_k,i} \right] + \sum_{i=1}^{n} \left[\frac{y_{t_k,i} + L_{t_k,i} - U_{t_k,i}}{S_{t_k,i}} b(S_{t_k,i}, B_{t_k^+,i}) \right] \tag{A.8}$$

Table A.1: Fitting and predicting errors for different basis functions with or without CE transformation.

		CE Transform				Value Function			
	γ	CS(2)	CS(3)	PS(4)	PS(5)	CS(2)	CS(3)	PS(4)	PS(5)
MSRPE	-2	2.1e-07	4.0e-08	9.3e-08	8.8e-08	3.9	4.0	4.0	4.0
MaxRPE		4.1e-03	1.1e-03	2.0e-03	1.6e-03	2.0	2.1	2.0	2.0
MSRPE	-7	1.3e-06	5.0e-07	1.1e-07	1.3e-06	19.2	48.0	45.5	4.7
MaxRPE		5.3e-03	3.3e-03	5.1e-03	4.8e-03	5.8	7.9	6.3	5.4
MSRPE	-13	8.5e-12	1.1e-12	6.2e-08	6.2e-08	1529.4	4727.3	177.4	177.4
MaxRPE		4.6e-05	2.7e-05	1.2e-03	1.3e-03	13.3	30.4	13.1	12.9

Note: We use the same transaction costs factor $\beta = 2\%$ for all the risky assets in all the three cases. The first two cases use the return parameters in the twenty stock example, the last one use the return parameters in the ten risky asset example. The left panel labeled as "CE Transform" denotes the results by approximating the certainty equivalent transformation of the value function; the right panel labeled as "Value Function" represents the factor of error increased by approximating the value function without taking the transformation. MSRPE represents the mean squared relative predicting error. MaxRPE represents the maximum relative predicting error. PS represents "Principal Set" and CS represents "Complete Set" from Section 2.3. CS(2) means using the basis functions from the complete polynomial set up to the second order. CS(3) represents using the basis functions from the complete polynomial set to the second order and plus the third order principal terms. PS(4) denotes using the basis functions from the complete polynomial set up to the fourth order without any cross terms. PS(5) represents using the basis functions from the complete polynomial set up to the fifth order without any cross terms. We use 2^{10} training data and 2^{10} predicting data to compute the error.

where

$$\begin{aligned}
&\frac{y_{t_k,i}+L_{t_k,i}-U_{t_k,i}}{S_{t_k,i}}b(S_{t_k,i},B_{t_k^+,i})\\
&=b(y_{t_k,i}+L_{t_k,i}-U_{t_k,i},\frac{B_{t_k,i}}{S_{t_k,i}}(y_{t_k,i}-U_{t_k,i})+L_{t_k,i})\\
&=(y_{t_k,i}-U_{t_k,i})b(1,\frac{B_{t_k,i}}{S_{t_k,i}})+L_{t_k,i}\\
&=\frac{y_{t_k,i}-U_{t_k,i}}{S_{t_k,i}}b(S_{t_k,i},B_{t_k,i})+L_{t_k,i}.
\end{aligned} \tag{A.9}$$

Hence

$$W^r_{t_k^+}=x_{t_k}+\sum_{i=1}^{n}\left[\frac{U_{t_k,i}}{S_{t_k,i}}b(S_{t_k,i},B_{t_k,i})-L_{t_k,i}\right]+\sum_{i=1}^{n}\left[\frac{y_{t_k,i}-U_{t_k,i}}{S_{t_k,i}}b(S_{t_k,i},B_{t_k,i})+L_{t_k,i}\right]=W^r_{t_k}. \tag{A.10}$$

In discrete time, the forcing realization model as a common heuristic strategy has been implemented for comparison in many papers (see, e.g., Dammon et al., 2001; Garlappi et al., 2001; DeMiguel and Uppal, 2005). This strategy realizes all capital gains or losses in each rebalance time first and then rebalance back to a continuous time tax-adjusted solution. In the following, we will show that this model is linked to a fictitious frictionless discrete time trading environment with tax-adjusted risky returns. To this end, as the initial position will be converted to risk-free asset by realizing all the capital gains or losses, the controlled dynamics can be written as

$$\begin{pmatrix} x_{t_k^+} \\ y_{t_k^+,i} \end{pmatrix}=\begin{pmatrix} W^r_{t_k}-\sum_{i=1}^{n}L_{t_k,i} \\ L_{t_k,i} \end{pmatrix}. \tag{A.11}$$

By introducing the portfolio weight of the risky asset for the realized wealth as $\boldsymbol{\omega}_{t_k}=(\omega_{t_k,1},\cdots\omega_{t_k,n})'$, we rewrite the above system as

$$\begin{pmatrix} x_{t_k^+} \\ y_{t_k^+,i} \end{pmatrix}=\begin{pmatrix} W^r_{t_k}(1-\sum_{i=1}^{n}\omega_{t_k,i}) \\ W^r_{t_k}\omega_{t_k,i} \end{pmatrix}, \tag{A.12}$$

and notice the basis price $B_{t_{k+1},i} = B_{t_k^+,i} = S_{t_k,i}$. Hence the realized wealth at time t_{k+1} is

$$\begin{aligned} W^r_{t_{k+1}} &= x_{t_{k+1}} + \sum_{i=1}^{n} \frac{y_{t_{k+1},i}}{S_{t_{k+1},i}} b(S_{t_{k+1},i}, B_{t_{k+1},i}) \\ &= R_f W^r_{t_k}(1 - \sum_{i=1}^{n} \omega_{t_k,i}) + \sum_{i=1}^{n} W^r_{t_k} \omega_{t_k,i} b(R_{t_k,i}, 1) \\ &= W^r_{t_k}[R_f + \sum_{i=1}^{n} \omega_{t_k,i}((1-\tau_i)R_{t_k,i} + \tau_i - R_f)]. \end{aligned} \tag{A.13}$$

By defining the tax-adjusted risky excess return $R^{\text{tax}}_{t_k,i} = (1-\tau_i)R_{t_k,i} + \tau_i - R_f$, we end up with the expression for the final realized wealth as

$$W^r_T = W^r_0 \prod_{k=0}^{m-1} (R_f + \boldsymbol{\omega}'_{t_k} \mathbf{R}^{\text{tax}}_{t_{k+1}}). \tag{A.14}$$

The feasible set in this case is just to keep the portfolio weight $\omega_{t_k,i} \in [0,1]$. As the formula above is equivalent to the classic Merton's portfolio optimization problem with the tax-adjusted return, the problem can be solved to optimality.

A.4 Derivation of RM and HC Strategies

In this section, we derive the formulas in Section 3.5.4 and 3.5.5. For RM, given the pre-trade positions, we first compute the realized risky asset portfolio $v_{t_k,i} = \frac{y_{t_k,i}}{S_{t_k,i}} \frac{b(S_{t_k,i}, B_{t_k,i})}{W^r_{t_k}}$. If $v_{t_k,i} \geq y^{c,\text{tax}}_{t_k,i}$, investors will sell to reach $y^{c,\text{tax}}_{t_k,i}$, i.e.,

$$\frac{y_{t_k^+,i}}{S_{t_k,i}} \frac{b(S_{t_k,i}, B_{t_k,i})}{W^r_{t_k}} = y^{c,\text{tax}}_{t_k,i} \tag{A.15}$$

or the post-trade position is

$$y_{t_k^+,i} = \frac{y^{c,\text{tax}}_{t_k,i} y_{t_k,i}}{v_{t_k,i}}. \tag{A.16}$$

If $v_{t_k,i} < y^{c,\text{tax}}_{t_k,i}$, investors will buy more risky asset to reach $y^{c,\text{tax}}_{t_k,i}$, i.e.,

$$\frac{y_{t_k^+,i}}{S_{t_k,i}} \frac{b(S_{t_k,i}, B_{t_k^+,i})}{W^r_{t_k}} = y^{c,\text{tax}}_{t_k,i} \tag{A.17}$$

and therefore this trade will change the basis price as well, i.e.,

$$B_{t_k^+,i} = \frac{B_{t_k,i} y_{t_k,i} + S_{t_k,i}(y_{t_k^+,i} - y_{t_k,i})}{y_{t_k^+,i}} = S_{t_k,i} + \frac{(B_{t_k,i} - S_{t_k,i}) y_{t_k,i}}{y_{t_k^+,i}}. \tag{A.18}$$

Plugging it into (A.17) and simplifying yields

$$y_{t_k^+,i} - \tau_i(1 - \frac{B_{t_k,i}}{S_{t_k,i}}) = y_{t_k,i}^{c,\text{tax}} W_{t_k}^r \tag{A.19}$$

or the post-trade position is

$$y_{t_k^+,i} = W_{t_k}^r (y_{t_k,i}^{c,\text{tax}} + \frac{y_{t_k,i}}{W_{t_k}^r} - v_{t_k,i}). \tag{A.20}$$

In the purchasing case, the basis price is computed by

$$B_{t_k^+,i} = \frac{B_{t_k,i} y_{t_k,i} + S_{t_k,i}(y_{t_k^+,i} - y_{t_k,i})}{y_{t_k^+,i}} = \frac{B_{t_k,i} y_{t_k,i} + S_{t_k,i} W_{t_k}^r \left[y_{t_k,i}^{c,\text{tax}} - v_{t_k,i} \right]}{W_{t_k}^r (y_{t_k,i}^{c,\text{tax}} + \frac{y_{t_k,i}}{W_{t_k}^r} - v_{t_k,i})}. \tag{A.21}$$

The similar derivation applies for HC except that the selling and buying boundaries are $y_{t_k,i}^{c,\text{tax}} + r_{t_k}$ and $y_{t_k,i}^{c,\text{tax}} - r_{t_k}$, respectively. Since selling does not change the basis price, the basis price will only be split into two regions by $y_{t_k,i}^{c,\text{tax}} - r_{t_k}$.

A.5 Derivation for Two Effective Merton's Models

In the section, we will give the derivation of the formulas in Section 3.4. The solutions of the two models represent the buying and selling boundaries of the no-trading region for a single risky asset case. Assume the optimal trade is to buy certain amount of risky asset. The system of the dynamics is

$$\begin{pmatrix} x_{t_{k+1}} \\ y_{t_{k+1},1} \end{pmatrix} = \begin{pmatrix} R_f \left(x_{t_k} + \frac{U_{t_k,1}}{S_{t_k,1}} b(S_{t_k,1}, B_{t_k,1}) \right) \\ R_{t_{k+1},1} \left(y_{t_k,1} - U_{t_k,1} \right) \end{pmatrix} \tag{A.22}$$

and the basis price keeps unchanged. Hence the realized wealth at time t_{k+1} is calculated as

$$W_{t_{k+1}}^r = x_{t_{k+1}} + \frac{y_{t_{k+1},1}}{S_{t_{k+1},1}} b(S_{t_{k+1},1}, B_{t_k,1}). \tag{A.23}$$

Recall the post-trade positions are denoted by $x_{t_k^+}$ and $y_{t_k^+,1}$, respectively. The realized wealth can be simplified by

$$\begin{aligned} W_{t_{k+1}}^r &= R_f x_{t_k^+} + y_{t_k^+,1} b(R_{t_{k+1},1}, B_{t_k,1}/S_{t_k,1}) \\ &= R_f x_{t_k^+} + y_{t_k^+,1} b(1, B_{t_k,1}/S_{t_k,1}) \frac{b(R_{t_{k+1},1}, B_{t_k,1}/S_{t_k,1})}{b(1, B_{t_k,1}/S_{t_k,1})}. \end{aligned} \tag{A.24}$$

Note there is a relation:

$$x_{t_k^+}+y_{t_k^+,1}b(1,B_{t_k,1}/S_{t_k,1}) = x_{t_k}+\frac{U_{t_k,1}}{S_{t_k,1}}b(S_{t_k,1},B_{t_k,1})+(y_{t_k,1}-U_{t_k,1})\,b(1,B_{t_k,1}/S_{t_k,1}) = W^r_{t_k}. \tag{A.25}$$

Similar to the method in Appendix A.3, if we introduce the new decision variable, portfolio weight of the risky asset $\omega_{t_k,1}\in[0,1]$, i.e., $x_{t_k^+}=(1-\omega_{t_k,1})W^r_{t_k}$ and $y_{t_k^+,1}b(1,B_{t_k,1}/S_{t_k,1}) = \omega_{t_k,1}W^r_{t_k}$, we end up with the dynamics of the realized wealth:

$$W^r_{t_{k+1}} = W^r_{t_k}\Big[R_f(1-\omega_{t_k,1})+\omega_{t_k,1}\hat{R}_{t_{k+1},1}\Big] \tag{A.26}$$

where we denote the first effective risky return as

$$\hat{R}_{t_{k+1},1} = \frac{b(S_{t_k,1}R_{t_{k+1},1},B_{t_k,1})}{b(S_{t_k,1},B_{t_k,1})}. \tag{A.27}$$

Comparing it with the Merton's problem, the only difference is the risky return and therefore the above problem can be solved to optimality. On the other hand, if we only buy certain amount of risky asset to reach the no-trading region, the system of the dynamics is

$$\begin{pmatrix} x_{t_{k+1}} \\ y_{t_{k+1},1} \end{pmatrix} = \begin{pmatrix} R_f\,(x_{t_k}-L_{t_k,1}) \\ R_{t_{k+1},1}\,(y_{t_k,1}+L_{t_k,1}) \end{pmatrix} \tag{A.28}$$

and the basis price in this case changes as

$$B_{t_{k+1},1} = \frac{B_{t_k,1}y_{t_k,1}+S_{t_k,1}L_{t_k,1}}{y_{t_k,1}+L_{t_k,1}}. \tag{A.29}$$

We need to maximize the expectation of the realized wealth

$$\begin{aligned} W^r_{t_{k+1}} &= R_f x_{t_k^+} + y_{t_k^+,1}b(R_{t_{k+1},1},B_{t_{k+1},1}/S_{t_k,1}) \\ &= R_f x_{t_k^+} + y_{t_k^+,1}(R_{t_{k+1},1}(1-\tau_1)+\tau_1)+\tau_1(\frac{B_{t_k,1}}{S_{t_k,1}}-1)y_{t_k,1}. \end{aligned} \tag{A.30}$$

Note there is a relation:

$$x_{t_k^+}+y_{t_k^+,1} = W^n_{t_k}. \tag{A.31}$$

Having the third term in the realized wealth expression (A.30), the model cannot be linked to the classic Merton's solution. Hence, we drop the last term and denote the second effective risky return as

$$\tilde{R}_{t_{k+1},1} = R_{t_{k+1},1}(1-\tau_1)+\tau_1 = b(R_{t_{k+1},1},1), \tag{A.32}$$

which implies

$$W^r_{t_{k+1}} \approx R_f x_{t_k^+} + y_{t_k^+,1} \tilde{R}_{t_{k+1},1}. \tag{A.33}$$

By following the similar approach as the selling case we realize the system is similar to the Merton's problem but with the second effective risky return $\tilde{R}_{t_{k+1},1}$. The effectiveness of the approximation depends on the size of the third term dropped. In the state space with unit realized wealth, the third term typically is not large as the purchasing rebalance will considerably reduce the basis price as we see in Figure 3.3. Note the portfolio weight in the above derivation for purchasing boundary represents the fraction of the risky asset in the nominal wealth.

A.6 Optimization Test for Twenty Asset Taxes Problem

Table A.2 indicates the difference between using global and local optimizations is small. The average relative difference of the twenty scenarios is about 0.3% when $m = 10$ and 0.1% when $m = 30$. The largest difference is about 0.07% when $m = 10$ and 0.02% when $m = 30$. For twenty assets, the optimization problem has to handle 400 decision variables when $m = 10$ and 1200 decision variables when $m = 30$. Without a good guess of the initial point, finding such a close result for a non-convex problem with this scale is difficult. Therefore, the results with small differences in the table enhance our confidence of using local optimization with RM solutions generates near-optimal solutions. We leave the investigation for a full solution such as convex-relaxation in future work.

Table A.2: Annualized return rates (%) for upper bounds by global or local optimization.

	$m = 10$		$m = 30$	
Path	Global	Local	Global	Local
1	1.01	1.01	3.07	3.07
2	**8.21**	**8.25**	3.55	3.55
3	7.58	7.58	1.07	1.07
4	0.48	0.48	5.50	5.50
5	7.06	7.06	3.40	3.40
6	**0.91**	**0.98**	2.37	2.37
7	2.17	2.17	2.54	2.54
8	2.76	2.76	**4.39**	**4.40**
9	2.76	2.76	**1.85**	**1.88**
10	**1.18**	**1.23**	**3.92**	**3.94**
11	5.35	5.35	4.24	4.24
12	2.89	2.89	4.55	4.55
13	5.51	5.51	5.14	5.14
14	**2.60**	**2.62**	2.79	2.79
15	2.16	2.16	2.30	2.30
16	4.52	4.54	**1.52**	**1.53**
17	**3.74**	**3.75**	5.27	5.27
18	3.82	3.82	**2.57**	**2.58**
19	0.17	0.17	2.45	2.45
20	6.21	6.21	2.80	2.80

Note: The results represent the annualized return rates in twenty different scenarios for the twenty risky asset model in a 10-year-long horizon or in a 30-year-long horizon. "Global" means the results in the column underneath are computed by multi-start global optimization with 200 different starting points. "Local" means the results in the column underneath are computed by a local optimization with the solution from RM as the initial point. The values in bold show the cases that global and local optimization generate different results. $\gamma = -3$, $\tau_i = 30\%$, $\Delta t = 1$ year, and the return parameters are from Table A.4.

A.7 Return and Covariance Model for Ten Asset Problem

We use the ten assets return model with no predictability given in Brown and Smith (2011). See Table A.3. These parameters were estimated as the means and covariances of historical returns for these indices using monthly return data from 1981 − 2006. The indices are, from left to right, 5 stock indices: the S&P 500, the Russell 1000 Value Index, Russell MidCap Index, Russell 2000 Value, and MSCI World Gross index; Lehman Brothers' US government and corporate bond indices; Lehman Brothers' Fixed Rate Mortgage Backed Securities Index, a real estate index trust (NAREIT), and a composite index of 1 − 5 Year US Treasuries.

A.8 Return and Covariance Model for Twenty Asset Problem

We adopt the Fama-French three factor model for the twenty stock case and adopt implied expected returns from equilibrium for the twenty ETF case. The latter was originally introduced in Sharpe (1974) and broadly applied in Black and Litterman (1992).

The Fama-French factors are constructed by using the 6 value-weight portfolios formed on size and book-to-market.[1] The excess return of the asset in the three factor model is describes as

$$\mathbb{E}(R_{t_k,i} - R_{f,t_k}) = c_{1,i}\mathbb{E}(\mathrm{SMB}_{t_k}) + c_{2,i}\mathbb{E}(\mathrm{HML}_{t_k}) + c_{3,i}\mathbb{E}(R_{m,t_k} - R_{f,t_k}). \tag{A.34}$$

SMB (Small Minus Big) is the average return on the three small portfolios minus the average return on the three big portfolios,

$$\begin{aligned}\mathrm{SMB} = 1/3(&\text{Small Value} + \text{Small Neutral} + \text{Small Growth})\\ &-1/3(\text{Big Value} + \text{Big Neutral} + \text{Big Growth})\end{aligned}$$

HML (High Minus Low) is the average return on the two value portfolios minus the average

[1] One can find three factor data and details of how to construct the three factors from Kenneth R. French's website:
`http://mba.tuck.dartmouth.edu/pages/faculty/ken.french/Data_Library/f-f_factors.html`

	SP500	R1000V	RMidC	R2000V	MSCIW	NAREIT	LBUSGv	LBUSCp	LBMortBnd	USTreasBnd
Mean($\mathbf{a}_r$)	0.009850	0.010672	0.010868	0.011173	0.009073	0.009432	0.007239	0.008111	0.007828	0.006424
Covariance($\mathbf{\Sigma}_e$)	SP500	R1000V	RMidC	R2000V	MSCIW	NAREIT	LBUSGv	LBUSCp	LBMortBnd	USTreasBnd
SP500	0.001887	0.001659	0.001897	0.001592	0.001531	0.000742	0.000112	0.000243	0.000194	0.000054
R1000V		0.001650	0.001721	0.001549	0.001339	0.000821	0.000109	0.000233	0.000183	0.000052
RMidC			0.002199	0.001995	0.001549	0.000968	0.000097	0.000242	0.000183	0.000039
R2000V				0.002194	0.001318	0.001166	0.000048	0.000189	0.000121	0.000011
MSCIW					0.001738	0.000634	0.000083	0.000188	0.000147	0.000041
NAREIT						0.001269	0.000110	0.000206	0.000142	0.000060
LBUSGv							0.000224	0.000259	0.000231	0.000128
LBUSCp								0.000346	0.000308	0.000150
LBMortBnd									0.000336	0.000144
USTreasBnd										0.000082

Table A.3: Data for the Ten Assets Model.

return on the two growth portfolios,

$$\begin{aligned}\text{HML} &= 1/2(\text{Small Value} + \text{Big Value}) \\ &\quad -1/2(\text{Small Growth} + \text{Big Growth})\end{aligned}$$

$R_{m,t_k} - R_{f,t_k}$ the excess return on the market, is the value-weight return on all NYSE, AMEX, and NASDAQ stocks (from CRSP) minus the one-month Treasury bill rate (from Ibbotson Associates).

To estimate the coefficients $c_{1,i}$, $c_{2,i}$ and $c_{3,i}$ in the model, given the monthly three factors and risk free rates provided by the aforementioned website, we take the regression of

$$R_{t_k,i} - R_{f,t_k} = \alpha_i + c_{1,i}\text{SMB}_{t_k} + c_{2,i}\text{HML}_{t_k} + c_{3,i}(R_{m,t_k} - R_{f,t_k}) + e_{t_k,i} \tag{A.35}$$

on the monthly data for the twenty stocks from 2001 to 2011.[2] After attaining the regression coefficients, we compute the mean of different assets by (A.34), with the eight year data of three factors from 2003 to 2011 and the available risk-free rate $r_f = 0\%$ in December, 2011.

Explicitly, the mean μ in the lognormal return model is estimated by

$$\hat{\mu}_i = \frac{\ln(\hat{R}_{t,i} + 1)}{\Delta t} \tag{A.36}$$

with

$$\hat{R}_{t,i} = r_f + \frac{c_{1,i}}{m}\sum_{j=0}^{m-1}\text{SMB}_{j\Delta t} + \frac{c_{2,i}}{m}\sum_{j=0}^{m-1}\text{HML}_{j\Delta t} + \frac{c_{3,i}}{m}\sum_{j=0}^{m-1}(R_{m,j\Delta t} - R_{f,j\Delta t}). \tag{A.37}$$

In order to estimate the volatility and correlations in the return model, we compute the sample volatility and correlations by the monthly asset price data $S_{j\Delta t,i}$, $j = 0, ..., m$. Explicitly, the volatility parameter for the i-th asset is estimated by

$$\hat{\sigma}_i = \sqrt{\frac{1}{(m-1)\Delta t}\sum_{j=0}^{m-1}\left(\ln\left(\frac{S_{(j+1)\Delta t,i}}{S_{j\Delta t,i}}\right) - \bar{\mu}_i\Delta t\right)^2} \tag{A.38}$$

[2]The complete list of the Goldman Sachs VIP stocks could be found from the website:
`http://tradewithpete.com/2012/01/17/goldman-sachs-hedge-fund-vip-list-for-wednesday-33/`

and the correlation parameter between the i-th and k-th asset is estimated by

$$\hat{\rho}_{i,k} = \frac{\sum_{j=0}^{m-1}\left(\ln\left(\frac{S_{(j+1)\Delta t,i}}{S_{j\Delta t,i}}\right) - \Delta t\bar{\mu}_i\right)\left(\ln\left(\frac{S_{(j+1)\Delta t,k}}{S_{j\Delta t,k}}\right) - \Delta t\bar{\mu}_k\right)}{\sqrt{\sum_{j=0}^{m-1}\left(\ln\left(\frac{S_{(j+1)\Delta t,i}}{S_{j\Delta t,i}}\right) - \Delta t\bar{\mu}_i\right)^2 \sum_{j=0}^{m-1}\left(\ln\left(\frac{S_{(j+1)\Delta t,k}}{S_{j\Delta t,k}}\right) - \Delta t\bar{\mu}_k\right)^2}} \tag{A.39}$$

where $\bar{\mu}_i$ is the i-th asset sample mean

$$\bar{\mu}_i = \frac{1}{m\Delta t}\sum_{j=0}^{m-1}\ln\left(\frac{S_{(j+1)\Delta t,i}}{S_{j\Delta t,i}}\right). \tag{A.40}$$

In the ETF case, we use the same approach to estimate the variance and the correlations of the asset returns. However, to estimate the means of returns, we appeal to "reverse engineering". Namely, under the assumption that equilibrium defines a neutral benchmark of returns, we back out asset returns as

$$\hat{\boldsymbol{\mu}} = \frac{\ln(\hat{\mathbf{R}}^{\mathrm{EQ}} + 1)}{\Delta t}, \tag{A.41}$$

with the implied expected return

$$\hat{\mathbf{R}}^{\mathrm{EQ}} = R_f + (1 - \gamma_{\mathrm{mkt}})Vw_{\mathrm{MCAP}} \tag{A.42}$$

where γ_{mkt} is the risk aversion coefficient of the market, V is the variance-covariance matrix of the linear return of the market data and w_{MCAP} is the market capitalization weight of assets.

All the parameters are included in Table A.4. The indices of stocks are, from left to right, Apple (AAPL), EMC (EMC), Bank of America (BAC), Yahoo (YHOO), JPMorgan Chase (JPM), Microsoft (MSFT), Intel (INTC), Apache (APA), Wells Fargo (WFC), CVS Caremark (CVS), Amazon (AMZN), Hewlett Packard (HPQ), Monsanto (MON), Hess Corporation (HES), Cisco Systems (CSCO), Macy's Inc (M), Oracle (ORCL), Qualcomm (QCOM), Exxon Mobil (XOM), Ebay (EBAY).

The indices of ETFs are, from left to right, SPDR S&P 500 ETF (SPY), First Trust Dow Jones Select MicroCap ETF (FDM), S&P MidCap 400 SPDR ETF (MDY), iShares S&P Small Cap 600 Index ETF (IJR), Vauguard Total Stock Market ETF (VTI), iShares iBoxx High Yield Corporate Bond Fund (HYG), Emerging Markets Sovereign Debt Portfolio ETF (PCY), iShares S&P National Municipal (MUB), iShares Barclays TIPS Bond

Fund (TIP), Vanguard REIT ETF (VNQ), United States Oil Fund (USO), StreetTRACKS Gold Shares ETF (GLD), iShares Silver Trust Fund (SLV), ELEMENTS Rogers International Commodity-Energy Index ETN (RJN), iShares MSCI Emerging Index Fund (EEM), PowerShares QQQ Trust (QQQ), PowerShares DB Commodity Index (DBC), iShares MSCI Brazil Index Fund (EWZ), iShares FTSE China 25 Index Fund (FXI), iShares MSCI Japan Index Fund (EWJ).

	AAPL	EMC	BAC	YHOO	JPM	MSFT	INTC	APA	WFC	CVS	AMZN	HPQ	MON	HES	CSCO	M	ORCL	QCOM	XOM	EBAY
Mean(μ)	0.0536	0.0516	0.0769	0.0524	0.0593	0.0370	0.0497	0.0458	0.0471	0.0344	0.0509	0.0544	0.0349	0.0432	0.0564	0.0869	0.0349	0.0392	0.0131	0.0643
Volatility(σ)	0.1900	0.2915	0.4008	0.2782	0.3203	0.1451	0.2402	0.4048	0.1592	0.1715	0.1906	0.4047	0.2782	0.3155	0.2690	0.2902	0.2190	0.2156	0.1805	0.2583
Correlation($\boldsymbol{\Sigma}_e$)	AAPL	EMC	BAC	YHOO	JPM	MSFT	INTC	APA	WFC	CVS	AMZN	HPQ	MON	HES	CSCO	M	ORCL	QCOM	XOM	EBAY
AAPL	1.0000	0.4700	0.1911	0.3686	0.2912	0.4457	0.5967	0.3047	0.0634	0.2233	0.4021	0.4664	0.3721	0.3173	0.3066	0.3192	0.3155	0.3523	0.3093	0.4287
EMC		1.0000	0.1277	0.5918	0.4602	0.4501	0.6353	0.1084	0.0821	0.2293	0.5074	0.5390	0.2349	0.0849	0.6799	0.3305	0.6377	0.5173	0.2063	0.4575
BAC			1.0000	0.1372	0.6587	0.3738	0.2682	0.2019	0.7980	0.2223	0.1033	0.3615	0.1741	0.0663	0.2569	0.4097	0.2255	0.2672	0.1371	0.3523
YHOO				1.0000	0.3623	0.4526	0.5685	0.1960	0.0542	0.2232	0.4989	0.4753	0.1461	0.1005	0.5920	0.3721	0.4619	0.4920	0.1544	0.5601
JPM					1.0000	0.5021	0.4149	0.1905	0.5828	0.3185	0.3062	0.4760	0.3505	0.1697	0.5160	0.4818	0.3062	0.4201	0.2146	0.4406
MSFT						1.0000	0.4799	0.1898	0.2249	0.2482	0.4174	0.4557	0.2792	0.2189	0.4793	0.3996	0.4598	0.3144	0.3231	0.5783
INTC							1.0000	0.0994	0.1784	0.3130	0.5813	0.6405	0.3246	0.0777	0.6608	0.4642	0.4731	0.5074	0.1689	0.5175
APA								1.0000	0.1673	0.2958	0.1291	0.2364	0.2590	0.6510	0.1845	0.2205	0.1693	0.1023	0.5512	0.2068
WFC									1.0000	0.3038	0.0659	0.2962	0.1155	0.0368	0.1900	0.3620	0.1844	0.2025	0.1386	0.2004
CVS										1.0000	0.1713	0.3126	0.2879	0.2821	0.2140	0.3864	0.0779	0.2383	0.2947	0.1433
AMZN											1.0000	0.4713	0.1270	0.1674	0.5042	0.3559	0.4029	0.4706	0.1037	0.5637
HPQ												1.0000	0.4160	0.2181	0.5897	0.4419	0.4177	0.5332	0.2987	0.4620
MON													1.0000	0.3206	0.2893	0.2101	0.1816	0.3408	0.2636	0.2497
HES														1.0000	0.1278	0.1673	0.0575	0.1460	0.5435	0.2028
CSCO															1.0000	0.4223	0.5395	0.5421	0.1997	0.5098
M																1.0000	0.2981	0.3185	0.0725	0.4562
ORCL																	1.0000	0.3761	0.2769	0.3850
QCOM																		1.0000	0.2130	0.5301
XOM																			1.0000	0.3029
EBAY																				1.0000

Table A.4: Data for the Twenty Stocks.

	SPY	FDM	MDY	IJR	VTI	HYG	PCY	MUB	TIP	VNQ	USO	GLD	SLV	RJN	EEM	QQQ	DBC	EWZ	FXI	EWJ
Mean(μ)	0.0421	0.0563	0.0469	0.0503	0.0436	0.0257	0.0128	0.0007	0.0041	0.0586	0.0512	0.0187	0.0609	0.0449	0.0651	0.0409	0.0399	0.0707	0.0561	0.0303
Volatility(σ)	0.1888	0.2833	0.2155	0.2451	0.1954	0.1396	0.1058	0.0530	0.0577	0.3139	0.2988	0.1995	0.4326	0.2539	0.2854	0.1902	0.2071	0.3238	0.2777	0.1938
Correlation($\mathbf{\Sigma}_c$)	SPY	FDM	MDY	IJR	VTI	HYG	PCY	MUB	TIP	VNQ	USO	GLD	SLV	RJN	EEM	QQQ	DBC	EWZ	FXI	EWJ
SPY	1.0000	0.9151	0.9558	0.9363	0.9976	0.8118	0.4162	0.0114	0.1781	0.8624	0.6708	0.0405	0.2955	0.6479	0.8728	0.9176	0.6887	0.7813	0.7625	0.7782
FDM		1.0000	0.9607	0.9865	0.9331	0.8043	0.2913	-0.0360	0.0162	0.8505	0.5753	-0.0802	0.2183	0.5426	0.8111	0.8730	0.5311	0.6828	0.7136	0.6810
MDY			1.0000	0.9803	0.9722	0.8152	0.4374	0.0175	0.0367	0.8543	0.6044	0.0214	0.3146	0.5895	0.8628	0.9231	0.6099	0.7799	0.7383	0.6902
IJR				1.0000	0.9541	0.8251	0.3593	0.0107	0.0016	0.8727	0.5836	-0.0501	0.2291	0.5559	0.8222	0.8876	0.5570	0.7043	0.7119	0.7074
VTI					1.0000	0.8169	0.4209	0.0159	0.1447	0.8674	0.6584	0.0309	0.3000	0.6377	0.8769	0.9267	0.6735	0.7855	0.7593	0.7683
HYG						1.0000	0.6375	0.1394	0.0564	0.8229	0.4589	-0.0572	0.1386	0.4600	0.7473	0.7848	0.5100	0.7257	0.6426	0.5848
PCY							1.0000	0.3284	0.2317	0.4725	0.1685	0.1610	0.2699	0.1841	0.5013	0.4479	0.2864	0.6008	0.3929	0.1929
MUB								1.0000	0.1138	0.2593	-0.3208	0.1029	-0.0198	-0.2816	0.0021	0.0175	-0.1882	0.0318	-0.0660	-0.0293
TIP									1.0000	0.0889	0.2062	0.3880	0.3196	0.1578	0.2382	0.1071	0.2748	0.1134	0.2829	0.1373
VNQ										1.0000	0.4067	-0.0194	0.1778	0.3782	0.7044	0.7569	0.4518	0.6115	0.5865	0.7003
USO											1.0000	0.2293	0.4586	0.9690	0.6968	0.5630	0.8490	0.6652	0.7130	0.5182
GLD												1.0000	0.8219	0.3163	0.2124	0.0154	0.4598	0.2978	0.2204	-0.0752
SLV													1.0000	0.5539	0.4563	0.2748	0.6279	0.5037	0.3888	0.1533
RJN														1.0000	0.6930	0.5711	0.9068	0.6976	0.6959	0.4932
EEM															1.0000	0.8414	0.7373	0.9271	0.9156	0.6148
QQQ																1.0000	0.6134	0.7857	0.7194	0.6596
DBC																	1.0000	0.7353	0.7176	0.5155
EWZ																		1.0000	0.8277	0.4641
FXI																			1.0000	0.5102
EWJ																				1.0000

Table A.5: Data for the Twenty ETFs.